FAULT DIAGNOSIS OF ANALOG CIRCUITS

J.W. Bandler and A.E. Salama

SOS-84-10-R2

May 1985

© J.W. Bandler and A.E. Salama 1984, 1985

No part of this document may be copied, translated, transcribed or entered in any form into any machine without written permission. Address enquiries in this regard to Dr. J.W. Bandler. Excerpts may be quoted for scholarly purposes with full acknowledgement of source. This document may not be lent or circulated without this title page and its original cover.

FAULT DIAGNOSIS OF ANALOG CIRCUITS

John W. Bandler, Fellow, IEEE, and Aly E. Salama, Member, IEEE

Abstract

In this paper, various fault location techniques in analog networks are described and compared. The emphasis is on the more recent developments in the subject. Four main approaches for fault location are addressed, examined and illustrated using simple network examples. In particular, we consider the fault dictionary approach, the parameter identification approach, the fault verification approach and the approximation approach. Theory and algorithms that are associated with these approaches are reviewed and problems of their practical application are identified. Associated with the fault dictionary approach we consider fault dictionary construction techniques, methods of optimum measurement selection, different fault isolation criteria and efficient fault simulation techniques. Parameter identification techniques that either utilize linear or nonlinear systems of equations to identify all network elements are examined very thoroughly. Under fault verification techniques we discuss node-fault diagnosis, branch-fault diagnosis, subnetwork testability conditions as well as combinatorial techniques, failure bound technique and the network decomposition technique. For the approximation approach we consider probabilistic methods and optimization based methods. The artificial intelligence technique and the different measures of testability are also considered. The main features of the techniques considered are summarized in a comparative table. An extensive, but not exhaustive, bibliography is provided.

This work was supported by the Natural Sciences and Engineering Research Council of Canada under Grant A7239.

J.W. Bandler is with the Simulation Optimization Systems Research Laboratory and the Department of Electrical and Computer Engineering, McMaster University, Hamilton, Canada L8S 4L7. He is also with Optimization Systems Associates, 163 Watson's Lane, Dundas, Ontario, Canada L9H 6L1.

A.E. Salama was with the Simulation Optimization Systems Research Laboratory and the Department of Electrical and Computer Engineering, McMaster University, Hamilton, Canada L8S 4L7. He is now with the Department of Electronics and Electrical Communications Engineering, Faculty of Engineering, Cairo University, Giza, Egypt.

I. INTRODUCTION

For more than two decades, the subject of fault location in analog circuits has been of interest to researchers in circuits and systems. In recent years this interest has intensified and a number of promising developments has emerged.

One distinguishes three main problems that are the main concern in network testing, namely, fault detection, fault location and identification and finally fault prediction. In the fault prediction problem [1], [63], [119], [120], [167], the response of the network is continuously monitored to identify whether any of the network elements is about to fail. The main concern is to replace these elements before an actual failure occurs and with minimum loss in the lifetime of the replaced elements. Fault detection is obviously a minimum requirement for fault location and identification. We address in this paper the fault location and identification techniques for analog networks. Therefore, we assume that the network has already been identified as faulty, i.e., a fault has been detected.

The analog circuit fault location problem [32] can be an extremely difficult problem [162]. This is because of the difficulty of measuring currents in-situ (without breaking connections), the lack of good fault models for analog components similar to the stuck-at-one and stuck-at-zero fault models, which are widely accepted by the digital test community, and the nonlinear nature of the problem. If, for example, a parameter value changes by a certain factor, the responses do not change by the same factor, i.e., the relationship between the circuit responses and the component characteristics is nonlinear, even though the circuit may be linear.

By a fault we mean, in general, any change in the value of an element with respect to its nominal value which can cause the failure of the whole circuit.

The faults could be catastrophic faults (hard faults) when the faulty element produces either a short circuit or an open circuit, or deviation faults (soft faults) when the faulty element deviates from its nominal value without reaching its extreme bounds. These soft faults could result from manufacturing tolerances, aging or parasitic effects. Many fault

location techniques only address the case when just one parameter causes the fault. This is referred to as a single fault. Practically, multiple faults, simultaneous changes in several parameters, could occur and recent techniques address this difficult case.

Several criteria may be used for categorizing fault location techniques. The most popular one is categorization according to the stage in the testing process at which simulation of the tested circuit occurs [102], [121], [130]. In particular, we have the simulation-before-test approach as well as the simulation-after-test approach [5], [70]. Fig. 1 summarizes the different techniques according to this classification.

In Section II we consider the fault dictionary techniques. These techniques, as indicated in Fig. 1, fall under the simulation-before-test approach. The techniques are widely used in digital networks. We first consider the three main methods in constructing a fault dictionary of the analog circuit, namely, the dc, frequency domain and time domain approaches. We then study methods for the optimum selection of a limited number of measurements to achieve the required degree of diagnosability. Many criteria could be implemented for the on-line isolation of faulty elements using the stored entries in the dictionary. We consider heuristic as well as statistically based criteria that have been proposed for that purpose. Fault simulation plays a very important role in the fault dictionary approach. We therefore consider efficient simulation methods for simulating network faults for linear and nonlinear networks.

Parameter identification techniques are addressed in Section III. Under the assumption that enough independent measurements are available, all network parameters could be identified. These techniques fall under the simulation-after-test approach, since most of the network simulations are performed at the testing time to identify the network parameters. These techniques are classified as linear or nonlinear according to the nature of the diagnosis equations. For the nonlinear techniques we consider dc testing, time domain testing, multifrequency testing and resistive network testing. For linear techniques we consider the generalized star-delta transformation technique as well as the component

simulation techniques. The main theoretical results for the parameter identification techniques are given and illustrated using simple network examples.

Under the assumption of a limited number of measurements, all parameters of the network can not be identified. Fault verification techniques address this problem (Section IV). The basic assumption is that a few elements are faulty and the rest of the network elements are within design tolerances. Network theory, mathematical theory and graph theory are utilized to provide very promising theoretically based techniques. Fault verification techniques fall under the simulation-after-test category. We consider the substitution theorem based techniques, failure bound technique, the network decomposition approach, the symbolic function techniques and fault verification using nonlinear diagnosis equations. The techniques are explained and the theoretical bases of these techniques are examined and illustrated.

In Section V we consider the approximation techniques which utilize optimization. We also consider the inverse probability method. Being a probabilistic technique, many network simulations are performed before testing to characterize the network statistically. ℓ_2 optimization, ℓ_1 optimization and quadratic optimization techniques utilize an appropriate objective function to estimate the most likely faulty elements. On-line simulation is needed and these techniques are considered under the simulation-after-test techniques.

The artificial intelligence technique is briefly described in Section VI. We then give an overall comparison of the different techniques against the practical goals and examine in some detail the problems with the practical implementation of the techniques. Throughout the paper a number of testability measures are considered. Since design for testability is quite important, we consider different measures of testability that have been proposed in a separate subsection.

II. FAULT DICTIONARY APPROACH

The usual method of automatically testing digital networks compares failed board output levels with a set of pre-stored outputs on the Automatic Test Equipment (ATE). Similar techniques are developed for fault location of analog networks. These techniques are based upon pattern recognition methods [7], [169].

The first step in constructing the dictionary (look-up table) is fault definition, where the most likely faults are anticipated. This is a very critical aspect of the entire approach since only these faults could be identified. Large numbers of potential faults must be included. This, of course, will have an impact on the size of the dictionary and impose a limitation on the approach.

The circuit under test (CUT) is then simulated for these hypothesized faulty cases, in order to develop sets of stimuli and responses which will detect and isolate the faults. The signatures of the responses are stored in a dictionary for use in the on-line identification of faults. The optimum choice of stimuli, responses and signatures is required to store the minimum amount of data that achieves the desired degree of detection and isolation.

At the time of testing, the faulty CUT is excited by the same stimuli that are used in constructing the dictionary. The signatures obtained are compared with those stored in the dictionary. A fault isolation criterion is implemented to identify the faulty CUT to one of prestored faults or to an ambiguity set that contains a set of possible faults.

2.1 *Dictionary Construction*

The construction of the dictionary is initiated by choosing the input signals to the circuit, the domain of analysis and the responses to be measured. We classify the different methods according to the domain of analysis.

2.1.1 *DC Approach for Dictionary Construction*

A representative method of this class has been described by Hochwald and Bastian [53] and Bastian [6]. Their method utilizes SYSCAP II, a general purpose computer-aided design simulator, to compute the dc voltages at the nodes of the circuit under arbitrary dc stimulus. A block diagram of the overall dc approach is shown in Fig. 2. The approach is summarized in the following steps:

Step 0 — The test engineer provides the network description, fault definition and the input stimuli.

Comment — The input stimuli are selected to exercise the "on", "off" and "linear" states of the semiconductor devices (e.g., diodes, transistors, FETs, etc.).

Step 1 — Different fault situations (single, hard or soft faults) are inserted one at a time into the circuit simulator. The simulator computes dc nodal voltages and component overstresses resulting from the faults.

Step 2 — The effectiveness of a stimulus in detecting a fault f is evaluated using the Euclidean distance d_f defined by

$$d_f \triangleq \sum_{j \in M} (V_j^0 - V_j^f)^2 , \quad f \in F , \tag{2.1}$$

where V_j^0 is the nominal dc voltage of jth node, V_j^f is the fault dc voltage of the jth node, M is the set of measurement nodes and F is the index set of possible faults.

Comment — If $d_f < 0.5\, n_m$ (heuristic bound), where n_m is the number of measurement nodes, the fault f is not detected and another stimulus is required.

Step 3 — Form the ambiguity sets for every measurement node using the different input stimuli. Every ambiguity set has a range 1.4 V ($\pm$ 0.7 V of a specific fault voltage).

Comment — The nominal ambiguity set has a range of $\pm$ 0.7 V of the measurement node nominal voltage value.

Step 4 Manipulate the ambiguity sets to find out the level (degree) of isolation and the unnecessary measurement nodes.

Comment This is achieved using logical intersection and symmetric difference operations on the elements of the ambiguity sets, as explained in Section 2.2.1.

Step 5 Construct the fault dictionary using the reduced set of measurement nodes. Indicate the ambiguity groups and the secondary overstresses caused by faults.

For the video amplifier circuit of Fig. 3 [53] a set of 20 possible faults outlined in Table 2.1 are considered. Among the possible test node candidates 2, 5, 8, 11, 16, 18, 26, 27, 33 and 36 only five nodes, namely, nodes 2, 5, 8, 11 and 16 are utilized in constructing the dictionary using two input stimuli $\pm$ 30 V dc. A part of the fault dictionary corresponding to fault numbers 4, 10 and 14 is shown in Table 2.2, where the simulated nodal voltages are stored.

2.1.2 *Frequency Domain Approach*

Different approaches are proposed that utilize the sinusoidal excitations to linear and nonlinear networks (higher-order harmonics are included in the dictionary [88], [89]). Frequency domain approaches have the advantage that the theory employed is well understood by most test engineers [24], [157]. Also, the hardware required for their implementation is simple, basically a sinusoidal generator, voltmeters and spectrum analyzers for testing of nonlinear networks.

2.1.2.1 *Seshu and Waxman Approach* [79], [135]

This is one of the earliest techniques for constructing a fault dictionary for linear frequency dependent circuits. Using only input-output measurements and magnitude information the dictionary is constructed.

Let the input-output rational transfer function H(s) be represented by

$$H(s) = k \frac{\prod_{i=1}^{n_z} (s - z_i)}{\prod_{j=1}^{n_p} (s - p_j)}, \tag{2.2}$$

where s is the complex frequency and z_i, p_j, $i = 1, 2, \ldots n_z$ and $j = 1, 2, \ldots, n_p$ are the transfer function zeros and poles, respectively. Let the angular frequencies, ω_i, ω_j be the corresponding magnitudes of z_i, p_j. These frequencies are called the breakpoints and they could be identified from the amplitude response of H(s). The test frequencies are chosen such that there must be at least one test frequency below the lowest nonzero break frequency, one above the highest finite break frequency and one between successive breakpoints. The rationale behind this choice is that all poles and zeros of the network are functions in the network parameters. Parameter deviations cause changes in the pole and zero locations and consequently change the magnitude of the transfer function H(s). This choice of test frequencies has been widely used ever since proposed by Seshu and Waxman [46], [135], [144]. The procedure for constructing the dictionary could be summarized as follows:

Step 1 — Compute the transfer function of the given network in symbolic form as a rational function in s, with the coefficients expressed as function of the network elements.

Step 2 — Use nominal element values to compute the breakpoints. Consequently, choose the test frequencies.

Step 3 — For every fault situation (deviation in the network parameter) compute the gain signature at the different frequencies.

Comment — The gain signature is obtained by quantizing the deviation of the gain from nominal (e.g., within 0.5 dB of nominal corresponds to (0) signature, from 0.5 to 1.5 dB higher than nominal corresponds to (1) signature, and so on).

Step 4 — The fault dictionary is constructed using the gain signatures of all fault cases.

Comment Dictionary entries are codes not actual gain values.

For the passive circuit of Fig. 4 [169], the input-output relation is given by

$$\frac{V_{out}}{V_{in}} = \frac{a_0 + a_1 s}{b_0 + b_1 s + b_2 s^2 + b_3 s^3},$$

where the coefficients as functions of the network elements are given by

$$a_0 = R_2,$$

$$a_1 = R_1 R_2 C_1,$$

$$b_0 = R_1 + R_2,$$

$$b_1 = R_1 C_1 R_2 + R_2 R_4 C_3 + (C_2 + C_3)(R_2 R_3 + R_3 R_1 + R_2 R_1) + R_1 R_4 C_3,$$

$$b_2 = R_1 R_2 R_3 C_1 (C_2 + C_3) + R_1 R_2 R_4 C_3 (C_1 + C_2) + R_3 R_4 C_2 C_3 (R_1 + R_2),$$

$$b_3 = R_1 R_2 R_3 R_4 C_1 C_2 C_3.$$

The circuit has 3 poles and one zero. For the nominal values $R_1 = R_4 = 1\,M\Omega$, $R_2 = 10\,M\Omega$, $R_3 = 2\,M\Omega$, $C_1 = 0.01\,\mu F$ and $C_2 = C_3 = 0.001\,\mu F$, the break points of the network are at 100 rad/sec for the zero and 83.3, 288.6 and 2288.1 rad/sec for the network poles. Five test frequencies are chosen according to the proposed suggestion by Seshu and Waxman. The fault signature codes are given in Table 2.3. The fault dictionary using the test frequencies 10, 95, 200, 800 and 5000 rad/sec for $\pm 50\%$ deviations in the network elements is shown in Table 2.4. Note that the first column of the code corresponds to the amplitude response at 10 rad/sec. Similarly, the remaining columns correspond to test frequencies 95, 200, 800 and 5000 rad/sec, respectively. Also, note that both R_3^+ and C_3^+ as well as R_3^- and C_3^- have the same codes (see Table 2.4). As such they form ambiguity sets. The rest of the fault cases are uniquely identified.

2.1.2.2 *Bilinear Transformation Method*

The method, as presented by Martens and Dyck [81], is based on the fact that the transfer function of a linear network can be expressed as bilinear function in any network elements ϕ_i, $i \in I_\phi$, as follows

$$H(s, \phi_i) = \frac{a_{1i}(s)\,\phi_i + a_{0i}(s)}{b_{1i}(s)\,\phi_i + b_{0i}(s)}\ , \quad i \in I_\phi\ , \tag{2.3a}$$

where

$$I_\phi \triangleq \{1, 2, \ldots, n_\phi\}, \tag{2.3b}$$

is the index set of the network parameters and $a_{ji}(s)$, $b_{ji}(s)$ are polynomials in the complex frequency variable s and are evaluated at the nominal values of the remaining network elements $\phi_j, j \in I_\phi, j \neq i$. We are interested in the variation of the function given in (2.3a) with respect to the change in the network element ϕ_i (ϕ_i is to change between its bounds) at a number of test frequencies. The locus of the change in the function $H(s,\phi_i)$ with respect to ϕ_i is plotted in the complex plane. As such, both the magnitude and angle of the transfer function are taken into consideration. The locus of $H(s,\phi_i)$ is either a straight line or an arc of a circle for a given frequency $s_\ell = j\omega_\ell$. Test frequencies are chosen according to the Seshu and Waxman proposal with the assumption that the change in ϕ_i should produce appreciable change in the transfer function H(s) at the chosen frequencies. From (2.3a) it is clear that to compute the coefficients a_{ji} and b_{ji}, $j = 0, 1$, three settings of ϕ_i are needed. So for n_ω frequency points, a network of n_ϕ elements will need $3\, n_\omega\, n_\phi$ simulations to construct the different loci of the transfer function. These loci constitute the dictionary. The method is applicable to single soft or hard faults in linear networks.

The loci of the transfer function of the network of Fig. 4 is drawn in Fig. 5 at the test frequency $\omega = 200$ rad/sec. Each locus is obtained by changing a single network element from 0.1 to ten times its nominal value, as is indicated on the figure for the seven different elements of the network.

2.1.2.3 *Sparse Matrix Recognition Techniques*

A number of approaches has been proposed which use the frequency domain response in constructing a sparse recognition matrix (dictionary).

In one version of the voting technique, [141], [143], the response of the network is quantized into three levels. Let

$$d_{if}^{*} \triangleq H^{0}(\omega_i) - H^{f}(\omega_i) \tag{2.4}$$

be the deviation of the network response from nominal due to fault f = 1, 2, ..., n_f at ω_i, i = 1, 2, ..., n_ω, where $H(\omega_i)$ is a real gain or phase. The response deviation is quantized as follows

$$d_{if} = \begin{cases} 1 & \text{for } d_{if}^{*} > \psi_i, \\ 0 & \text{for } |d_{if}^{*}| \leq \psi_i, \\ -1 & \text{for } d_{if}^{*} < -\psi_i, \end{cases} \tag{2.5}$$

where ψ_i is a predetermined threshold level related to uncertainty in the network response resulting from parameter tolerances and measurement errors. The number of test frequencies n_ω is usually chosen such that $n_\omega \geq 3\, n_\phi$. These extra redundant frequencies are utilized to improve the isolation capabilities of the voting technique. The dictionary is constructed using the entries d_{if}. It is clear that a sparse dictionary will result.

A sparse fault dictionary for the network of Fig. 4 is constructed in Table 2.5, utilizing gain measurements at ω = 10, 200 and 800 rad/sec as well as phase measurements at ω = 2000 and 8000 rad/sec. We applied the quantization indicated in (2.5), with ψ_i = 0.08 for phase measurements and 0.025 for gain measurements. Only the fault cases similar to that of Table 2.4 are considered. Note that (R_1^+, R_2^-), (R_1^-, R_2^+), (C_2^+, C_3^+) and (C_2^-, C_3^-) form ambiguity sets.

Another approach for constructing a sparse recognition matrix was proposed by Varghese et al. [168]-[170]. Prior to the storage of the elements d_{if}^{*}, they are normalized to compensate for wide ranging deviations in the elements of d_{if}^{*}. If ψ_i is the threshold level defined in (2.5) the elements d_{if}^{*} are modified to

$$d_{if}' = \frac{d_{if}^{*}}{|\psi_i|}, \quad i = 1,2,\ldots, n_\omega, \quad f = 1,2,\ldots, n_f. \tag{2.6}$$

If frequency domain gain and phase measurements are used, the checkout normalization will enable these different physical quantities to become comparable. Other

normalizations are reported in [55]. Let $\|\mathbf{d}'^{f}\|$ represent the Euclidean norm of $\mathbf{d}'^{f} = [d'_{1f}\ d'_{2f} \ldots\ d'_{n_\omega f}]^T$, where T indicates the transpose. The normalized response of (2.6) is given by

$$d_{if} = \frac{d'_{if}}{\|\mathbf{d}'^{f}\|}\ ,\ i = 1,2,\ldots, n_\omega\ ,\ f = 1,2,\ldots, n_f\ . \tag{2.7}$$

Let the ℓ_1 norm of $\mathbf{d}^f = [d_{1f}\ d_{2f} \ldots\ d_{n_\omega f}]^T$ be given by

$$\sum_{i=1}^{n_\omega} |d_{if}|\ . \tag{2.8}$$

If the absolute value of any of the elements of $\mathbf{d}^f$ is less than a certain fraction of the ℓ_1 norm (2.8) (say $(1/(3n_\omega))$) it is set to zero. With these elements set to zero the renormalized stored entries of d_{if} constitute a sparse fault dictionary.

Sparse formulation of the dictionary results in the saving of dictionary memory and required computing time.

In Table 2.6 we followed the procedure described by equations (2.5) - (2.8) to construct a normalized nondimensionalized sparse fault dictionary. The threshold level ψ_i is taken as in Table 2.5. Note the similarity in the configuration between Table 2.5 and Table 2.6.

2.1.3 *Time Domain Analysis Approach*

The dynamic testing approach has been proposed for testing linear dynamic circuits. We consider here two representative techniques of this approach [129]-[132], [142], [156].

2.1.3.1 *Pseudo-Noise Signal Method* [76]-[78]

The network under test is excited by a periodic pseudo-noise signal $\eta(t)$ as shown in Fig. 6 [83], [86]. Under certain well-defined conditions [156], the input-output cross-correlation function approximates the circuit impulse response, i.e.,

$$h(i\tau) \simeq \frac{1}{T}\int_0^T \eta(t - i\tau)\, v(t)\, dt\ , \tag{2.9}$$

where $i\tau$ is a multiple of the pseudo-noise clock frequency and v(t) is the output signal. The test time T depends on the signal/noise ratio required to reduce measurement errors to

acceptable levels. If the cross-correlation function does not approximate the circuit impulse response, it can still be used as a signature describing the condition of the circuit. Let the deviation in the impulse response, for the fth fault case, from its nominal value at the ith time delay be given by

$$d_{if}^{*} \triangleq h^{0}(i\upsilon) - h^{f}(i\upsilon) \ . \tag{2.10}$$

Either the d_{if}^{*}, $i = 1, 2, ..., n_m$, $f = 1, 2, ..., n_f$, where n_m is the number of measurements, are used directly in forming the dictionary or they are first quantized as illustrated in (2.5) and then stored in a dictionary.

2.1.3.2 *Test-Signal Design Method* [129]-[132]

Schreiber proposed the test-signal design method which utilizes the modern ATE system capabilities for arbitrary signal generation [129]. A test signal is designed that first drives the linear dynamic circuit under test to a non-trivial initial state and then to a zero state in finite time. This signal, realized as a piecewise constant waveform, is called the complementary signal. It constitutes a fault signature because its step amplitudes are functions of the circuit pole locations in the complex s-plane and therefore are also functions of the circuit element values.

When zeros of transmission are present in the transfer function of the circuit the response of the system to the complementary signal could cross the zero level at a number of times less than or equal to the number of zeros of the transmission. The changes in the zero crossings in the time domain are augmented to the changes in the complementary signal levels due to all possible faulty cases and are compiled to form the fault dictionary. Or, similar to the bilinear transform method, the fault dictionary is established by drawing the loci of all single element drift failure fault signatures in the augmented signal space. A decision region is defined around each locus to uniquely identify an ambiguity group of elements. The definition of these regions takes into account the tolerance variations in the

good element components and simplifies the definition of the dictionary. For non-catastrophic failures, the dictionary takes the form of a set of mathematical inequalities.

The complementary signal is derived for the nominal as well as the faulty circuit using the circuit response to a pulse function u(t). Let

$$u(t) = \begin{cases} 1 \ , & 0 \le t \le \tau \ , \\ 0 \ , & \text{elsewhere} \ . \end{cases} \tag{2.11}$$

Then the complementary signal may be written as

$$\sum_{i=0}^{n_p} \alpha_i \, u(t - i\tau) \ , \tag{2.12}$$

where $\alpha_0 = 1$ and n_p is the number of poles. Let $v_u(t)$ be the response of the circuit to u(t). The response of the circuit to the complementary signal is given by

$$\sum_{i=0}^{n_p} \alpha_i \, v_u(t - i\tau). \tag{2.13}$$

The complementary signal $[\alpha_1 \ \alpha_2 \ \dots \ \alpha_{n_p}]^T$ is chosen such that the response must vanish for $t \ge (n_p + 1)\tau$. Let the response in (2.13) be sampled at q points, τ intervals apart, for $t \ge (n_p+1)\tau$. If $q \ge n_p+1$, a system of overdetermined equations in the parameters $\boldsymbol{\alpha}$ is constructed. The system of equations has the form

$$\begin{bmatrix} -v_u((n_p+1)\tau) \\ -v_u((n_p+2)\tau) \\ \vdots \\ -v_u((n_p+q)\tau) \end{bmatrix} = \begin{bmatrix} v_u(n_p\tau) & v_u((n_p-1)\tau) \dots & v_u(\tau) \\ v_u((n_p+1)\tau) & v_u(n_p\tau) \dots & v_u(2\tau) \\ \vdots & \vdots & \vdots \\ v_u((n_p+q-1)\tau) & v_u((n_p+q-2)\tau) \dots & v_u(q\tau) \end{bmatrix} \begin{bmatrix} \alpha_1 \\ \alpha_2 \\ \vdots \\ \alpha_{n_p} \end{bmatrix} . \tag{2.14}$$

The least-squares solution is employed to find approximate values of the parameters $\boldsymbol{\alpha}$.

The implementation of the method utilizes a programmable waveform analyzer to obtain the samples needed in (2.14) from the CUT and a programmable waveform generator to apply the complementary signal, computed in (2.14), to the CUT and observe the possible

changes in the zero crossings of the time response of the system. An example of the application of the complementary signal to a two-pole filter is given in Fig. 7.

The complementary signal approach has been utilized for go-no-go testing of a partitioned CUT [132], [175]. In [25] it has been shown that one signal is not always sufficient and a generalization of the complementary signal concept has been proposed.

2.2 *Selecting an Optimum Set of Measurements*

The objective of optimum selection of measurements is to reduce the number of measurements without affecting diagnosis capability. It should be possible to select few measurements and still retain relatively good isolation properties. Consequently, this will lead to eliminating redundant measurements and reducing the dimensionality of the fault dictionary.

2.2.1 *Binary Logical Manipulation Technique* [53]

For every measurement $i \in I_M$, where

$$I_M \triangleq \{1, 2, \ldots, n_m\} \tag{2.15}$$

is the index set of measurements, the different hypothesized faults are grouped into γ_i ambiguity sets, $F_{i1}, F_{i2}, \ldots, F_{i\gamma_i}$. Every ambiguity set contains the faults that produce almost the same value of the measurement, taking into consideration measurement errors and parameters tolerances. In Table 2.7, the ambiguity sets for the video amplifier circuit of Fig. 3 are given for a number of possible candidates of the measurement nodes. An example of forming ambiguity sets is shown in Fig. 8 [165], [166], where heuristic as well as more accurate fault groups are generated. A theoretically based method utilizing worst-case analysis could be implemented to characterize the fault bands. The problem is that exact worst-case analysis is too expensive to be performed in very large networks. Monte-Carlo simulation could be employed to identify the fault bands.

The ambiguity sets must be manipulated to determine which faults can be isolated uniquely and what measurements provide the highest degree of isolation and, consequently, should be retained. The basic procedure applies the following logical rules.

Rule 1 Any ambiguity set which has a single fault within it, identifies uniquely that fault. The measurement corresponding to this ambiguity set is retained.

Rule 2 Ambiguity sets whose intersection or symmetric difference result in a single fault, also uniquely define the fault. The measurements corresponding to these ambiguity sets are retained.

An algorithm that implements the above stated rules will proceed by selecting the two measurements that have the highest number of ambiguity sets. They are manipulated using the logical rules to obtain a list of faults which are uniquely isolated. If all faults have not been isolated uniquely, the ambiguity sets of the measurement that has the next highest number of ambiguity sets are utilized. If the ambiguity sets of a measurement do not isolate any new faults, then the measurement is discarded. The process is continued until all faults are uniquely isolated. If after going through all measurements unique identification is not achieved for single faults, the procedure is repeated to see if isolation can be obtained for two faults together, and so forth. Hochwald and Bastian [53] applied this algorithm quite successfully to reduce the number of needed measurement nodes of the video amplifier circuit to nodes 2, 5, 8, 11 and 16. As an example of the application of Rule 2, fault number 4 is uniquely identified by the symmetric difference of node 8's ambiguity set 1 with node 11's ambiguity sets 1, 2 and 3 (all at -30 V input) of Table 2.7.

2.2.2 *Heuristic Technique for Measurements Selection by Optimization*

A heuristic approach which selects the optimum set of measurements was proposed by Varghese et al. [169]. The proposed procedure selects a set of measurements without performing an exhaustive search of all subsets of possible measurements. A performance index or a confidence level is introduced as a measure of the effectiveness of a subset of

measurements. This confidence level is optimized. As such, the chosen subset of measurements could be considered optimum.

The discrimination power of the ith measurement is defined as

$$D_i \triangleq \left[\sum_{f=1}^{n_f-1} \left(d_{if} - d_{i,f+1} \right)^2 \right]^{1/2} , \; i \in I_M . \tag{2.16}$$

This is a "distance" measure computed using the entries of the dictionary matrix d_{if}. It measures the effectiveness of each measurement to discriminate between the different n_f fault cases. A measurement of very low discrimination power is of little use in fault isolation.

In many pattern recognition techniques separability measures are employed for pattern classification. It is applied here (measurements selection) to reflect the fault cases separability of a given set of measurements. The following distance measure is proposed to measure the separability of two fault cases f_1, f_2 in the set F of all possible faults using the set of I_M measurements.

$$D_{f_1 f_2} = \left[\sum_{i=1}^{n_m} \left(d_{if_1} - d_{if_2} \right)^2 \right]^{1/2} \quad \forall f_1, f_2 \in F , \; f_1 \neq f_2 . \tag{2.17}$$

For n_f fault cases we will have $n_f(n_f-1)/2$ separability measures. A low separability measure indicates close fault similarity and possibly confusion in the diagnosis. The separability measure is usually expressed as a percentage by finding

$$D^* = \text{Max } D_{f_1 f_2} \quad \forall f_1, f_2 \in F , \; f_1 \neq f_2 \tag{2.18}$$

and modifying (2.17) as follows.

$$D^*_{f_1 f_2} = \frac{D_{f_1 f_2}}{D^*} . \tag{2.19}$$

The measurement selection problem in the classical sense can be viewed as a combinatorial optimization problem requiring the setting of a criterion function such as the degree of diagnosability together with a search procedure. The ability of the measurements to discriminate between two fault cases depends upon the distance between them. The confidence level is defined as a function of the separability measure. A confidence level of

unity is assigned to combinations of fault cases with separability measure of 50% or more. Those fault case combinations with separability measures less than 50% retain the actual value of the separability measures. Let CONF1 be the number of combinations with percentage separability measure $\geq$ 50% and CONF2 be the cumulative sum of separability measure of combinations with percentage separability measure $<$ 50%. Then the confidence level is given by

$$\text{CONF} \triangleq \frac{\text{CONF1} + \text{CONF2}}{n_f\,(n_f - 1)/2} \times 100 \ . \tag{2.20}$$

The iterative procedure of measurement selection is explained in the flow diagram of Fig. 9. Optimization is carried out as follows. Let

$$D_f' \triangleq |\, d_{if} - d_{j.f} \,| \quad , f = 1,2,\ldots,n_f \quad , \ i,j \in I_M \ , \tag{2.21}$$

$$L_i \triangleq \sum_{f=1}^{n_f} |\, d_{if} \,| \quad , i = 1,2,\ldots,n_m \tag{2.22}$$

and

$$L \triangleq L_i + L_j \ . \tag{2.23}$$

If D_f', $f = 1, 2, \ldots, n_f$ is less than a fraction (say $1/\theta$) of L (2.23) the retention of both measurements i, j need not increase the discriminatory information and hence the measurement of less discriminating power is discarded. The factor "θ" is kept a variable to add or discard measurements to achieve maximum confidence level.

For the passive circuit of Fig. 4, 56 measurements (gain and phase) obtained at 28 different test frequencies are considered as candidates of the diagnostic measurements. The selection procedure of Fig. 9 is applied. In Table 2.8, the list of the sets of measurements that are selected during the heuristic optimization process together with their confidence levels are given [169]. Note that a few measurements achieve a high confidence level and increasing the number of measurements increases this level slightly. We have investigated different implementations of the heuristic technique, applying them to the circuit of Fig. 4. The results obtained were quite similar to those of Table 2.8.

2.2.3 *Probabilistic Theoretic Approach for Optimum Features Selection*

The actual value of a voltage measurement due to the departure of the component values from nominal and to measurement errors could be given by [39], [43]

$$V_i^m = V_i^0 + \sum_{j \in I_\phi} \frac{\partial V_i^0}{\partial \Phi_j} \Delta\Phi_j + \delta_i , \quad i \in I_M , \tag{2.24}$$

where $\Delta\Phi_j$ represents the deviation of the jth component value from nominal, δ_i represents the error in measurement, V_i^0 is the nominal value of voltage at the ith node (non-catastrophic faults are assumed) and the partial derivatives are evaluated at $\boldsymbol{\Phi} = \boldsymbol{\Phi}^0$.

Given that $\Delta\Phi_j$, $j \in I_\phi$, and δ_i, $i \in I_M$, are independent normal random variables, their probability distributions are fully specified by their means and standard deviations. Let us assume that the means are zeros and the standard deviations of $\Delta\Phi_j$ and δ_i are ε_j and ξ_i, respectively. As such, the probability of measuring $\mathbf{V}^m$ is given by

$$\text{Prob}(\mathbf{V}^m) = \frac{\exp\{-\frac{1}{2}(\mathbf{V}^m - \mathbf{V}^0)^T \boldsymbol{\Lambda}_{mm}^{-1} (\mathbf{V}^m - \mathbf{V}^0)\}}{(2\pi)^{1/2} |\boldsymbol{\Lambda}_{mm}|^{1/2}} , \tag{2.25}$$

where exp is the exponential function and $|\boldsymbol{\Lambda}_{mm}|$ is the determinant of the matrix $\boldsymbol{\Lambda}_{mm}$ whose (i,j) element is given by

$$\sum_{k \in I_\phi} \left(\frac{\partial V_i^0}{\partial \Phi_k} \right) \left(\frac{\partial V_j^0}{\partial \Phi_k} \right) \varepsilon_k^2 , \tag{2.26a}$$

if $i \neq j$ and by

$$\xi_i^2 + \sum_{k \in I_\phi} \left(\frac{\partial V_i^0}{\partial \Phi_k} \right)^2 \varepsilon_k^2 , \tag{2.26b}$$

when $i = j$.

Similarly, we can write the probability of the changes in the parameter values $\Delta\boldsymbol{\Phi}$ conditional on the observed measurements, namely, Prob $(\Delta\boldsymbol{\Phi}|\mathbf{V}^m)$. The conditional distribution is normal with the mean vector given by

$$\boldsymbol{\Lambda}_{\phi m} \boldsymbol{\Lambda}_{mm}^{-1} (\mathbf{V}^m - \mathbf{V}^0) \tag{2.27a}$$

and covariance matrix

$$\Lambda'_{\phi\phi} \triangleq \Lambda_{\phi\phi} - \Lambda_{\phi m}\, \Lambda_{mm}^{-1}\, \Lambda_{\phi m}^{T} \ , \tag{2.27b}$$

where

$$\Lambda_{\phi\phi} \triangleq \text{diag}\,\{\varepsilon_1^2, \varepsilon_2^2, \ldots, \varepsilon_{n_\phi}^2\} \tag{2.28a}$$

and the (i,j) element of the matrix $\Lambda_{\phi m}$ is given by

$$\left(\frac{\partial V_j^0}{\partial \Phi_i}\right) \varepsilon_i^2 \ , \tag{2.28b}$$

with the derivatives in (2.26) and (2.28b) are evaluated at nominal values.

An information theoretic measure of the expected information deficit (compared with perfect certainty) when we have performed a set of measurements $\mathbf{V}^m$ is given by [39]

$$J(\mathbf{V}^m) \triangleq -\int \text{Prob}\,(\Delta\boldsymbol{\phi} \mid \mathbf{V}^m) \log_e [\text{Prob}(\Delta\boldsymbol{\phi} \mid \mathbf{V}^m)]\, d(\Delta\boldsymbol{\phi}) \,, \tag{2.29}$$

where $\log_e$ is the natural logarithm function.

The information deficit expected in advance of actually performing the tests is obtained by integrating over all possible outcomes of $\mathbf{V}^m$ each weighted by its respective probability, Prob($\mathbf{V}^m$):

$$J \triangleq -\int \text{Prob}\,(\mathbf{V}^m) \left[\int \text{Prob}\,(\Delta\boldsymbol{\phi} \mid \mathbf{V}^m) \log_e [\text{Prob}(\Delta\boldsymbol{\phi} \mid \mathbf{V}^m)]\, d\Delta\boldsymbol{\phi} \right] d\mathbf{V}^m. \tag{2.30}$$

Since Prob ($\Delta\boldsymbol{\phi}|\mathbf{V}^m$) is given by (2.27) and (2.28) the second integral can be evaluated and (2.30) could be expressed as

$$J = \text{constant} + \frac{1}{2} \log_e |\Lambda'_{\phi\phi}| \ . \tag{2.31}$$

To minimize J (information deficit), i.e., maximizing the information from a set of measurements I_M, we minimize the determinant of $\Lambda'_{\phi\phi}$. Freeman [39] has shown that the determinant of $\Lambda'_{\phi\phi}$ will be proportional to the determinant of Λ_{mm}^{-1} under certain reasonable conditions. Then the selection criterion is to

$$\text{maximize } |\Lambda_{mm}| \ . \tag{2.32}$$

Criterion (2.32) is quite useful for screening possible measurements to obtain a small efficient set. The application of this criterion requires simulation only of the normal circuit. The criterion is similar to the D-optimal design criterion in the design of experiments problem

[101], [104]. It is clear that the selection of measurements could be viewed as an exercise in designing the optimum experiments for reducing the uncertainties in the parameter estimates.

Other statistical techniques for the best choice of response measurements are given in [54], [55].

Due to the nature of the D-optimal experiment design problems, complex optimization calculations are required. Nevertheless, the concept could be illustrated analytically on simple examples. Consider the passive circuit of Fig. 10a. Assume that R is the only element that could be faulty and changes from its nominal value of 1.0. Both L and C are assumed fixed at their nominal values of 1.0 each. Using $|V_{out1}/V_{in}|$ as the measured output we get

$$\left| \frac{V_{out1}}{V_{in}} \right| = \frac{1-\omega^2 LC}{[(1-\omega^2 LC)^2 + (\omega CR)^2]^{1/2}} .$$

Therefore, using (2.26b) the matrix Λ_{mm} is just a scalar value, which is given by

$$\xi_1^2 + \frac{[(\omega C)^2 (1-\omega^2 LC)R]^2}{[(1-\omega^2 LC)^2 + (\omega CR)^2]^3} \varepsilon_R^2 ,$$

where ε_R^2 is the variance of the element R. The frequency dependent part is plotted in Fig. 10b as the dashed curve with R = L = C = 1.0. It shows that the determinant of Λ_{mm} is strongly dependent upon the test frequencies. Specifically, the points $\omega = 0$ and $\omega = 1.0$ are to be avoided because they are noninformative. The region $\omega >> 1.0$ is unacceptable for the same reason. Using $|V_{out2}/V_{in}|$ instead as the measured output, the frequency dependency of $|\Lambda_{mm}|$ is plotted in Fig. 10b as the solid curve. Note that, using statistical interpretation, $|V_{out2}|$ provides more information than $|V_{out1}|$.

2.3 *Fault Isolation Techniques*

A fault tree approach [153] is usually followed during the diagnosis process. First the CUT is diagnosed to be either sick or healthy. If the CUT appears faulty, the fault is first

assigned to a certain ambiguity set F_i. Then, the fault is isolated to a component of this ambiguity set, $\phi_{i_j} \in F_i$. It is possible that a component be a member of more than one subset.

We consider a statistically based criterion, a fuzzy concept criterion and other heuristic techniques for isolating faults.

2.3.1 *Maximum Likelihood Measure* [39]

Freeman [39] has utilized the theory of statistics to develop a fault isolation criterion. For n_f fault cases (2.24) is given by

$$V_i^m = V_i^f + \sum_{j \in I_\phi} \frac{\partial V_i^f}{\partial \phi_j} \Delta\phi_j + \delta_i, \; i \in I_M, \tag{2.33}$$

where V_i^f is the fault voltage of the ith measurement, stored in advance as in the dc dictionary approach, corresponding to the fth fault case and the derviatives are evaluated at the parameters of the fth fault case $\boldsymbol{\phi}^f$. Similarly to (2.25) the conditional probability of obtaining measurements $\mathbf{V}^m$ when f is the fault case is given by

$$\text{Prob}\,(\mathbf{V}^m | \, f) = \frac{\exp\{-\frac{1}{2}(\mathbf{V}^m - \mathbf{V}^f)^T (\boldsymbol{\Lambda}^f_{mm})^{-1} (\mathbf{V}^m - \mathbf{V}^f)\}}{(2\pi)^{1/2} |\boldsymbol{\Lambda}^f_{mm}|^{1/2}}, \tag{2.34}$$

where the elements of the matrix $\boldsymbol{\Lambda}_{mm}{}^f$ are as given by (2.26) except that the partial derivatives are computed at $\boldsymbol{\phi} = \boldsymbol{\phi}^f$, the assumed values of the network elements for the fth fault case.

The probability of classifying the fault to be the fth fault case given the measurements $\mathbf{V}^m$ is denoted by Prob (f $|\mathbf{V}^m$) and is expressed using Bayes' relation as

$$\text{Prob}\,(f | \, \mathbf{V}^m) = \frac{\text{Prob}\,(\mathbf{V}^m | \, f)\,\text{Prob}\,(f)}{\text{Prob}\,(\mathbf{V}^m)}, \tag{2.35}$$

where Prob(f) is the prior probability that the CUT corresponds to the fth fault case. Prob($\mathbf{V}^m$) is the overall probability of measuring $\mathbf{V}^m$ and is given by

$$\text{Prob}\,(\mathbf{V}^m) = \sum_{f \in F} \text{Prob}(\mathbf{V}^m | \, f)\,\text{Prob}\,(f). \tag{2.36}$$

The isolation criterion is to pick the fault case that results in the highest value of (2.35). Using (2.34) this can be expressed as: Choose $f \in F$ that minimizes

$$(\mathbf{V}^m - \mathbf{V}^f)^T (\Lambda^f_{mm})^{-1} (\mathbf{V}^m - \mathbf{V}^f) + \log_e [|\Lambda^f_{mm}| / (\text{Prob}(f))^2] \ . \tag{2.37}$$

Under the assumption that all faults are of equal probability (2.37) reduces to

$$(\mathbf{V}^m - \mathbf{V}^f)^T (\Lambda^f_{mm})^{-1} (\mathbf{V}^m - \mathbf{V}^f) + \log_e |\Lambda^f_{mm}| \ . \tag{2.38}$$

Suppose further that the variance-covariance matrix $\Lambda_{mm}{}^f$ is independent of the fault type. In this case we drop the superscript f and (2.36) is given by

$$(\mathbf{V}^m - \mathbf{V}^f)^T \Lambda^{-1}_{mm} (\mathbf{V}^m - \mathbf{V}^f) \ . \tag{2.39}$$

(2.39) could be also used if Λ_{mm} is the pooled covariance matrix [55], i.e., the matrix obtained by taking the average of the different $\Lambda_{mm}{}^f$, $f = 1, 2, \ldots, n_f$. Expression (2.39) should be compared with the well known nearest-neighbour rule criterion for fault isolation which is widely used [53], [87], [168] - [170]. The nearest-neighbour rule is given by minimizing over all f the value of

$$(\mathbf{V}^m - \mathbf{V}^f)^T (\mathbf{V}^m - \mathbf{V}^f) \ , \tag{2.40}$$

which is the Euclidean distance between the measured and stored quantities. It is to be noted that (2.39) could be reduced to (2.40) under the assumption that the variances of the measurement errors $\xi_i{}^2$ of (2.26) greatly outweigh all the other terms involving the variances of the network parameter deviations $\varepsilon_k{}^2$ of (2.26). As such Λ_{mm} could be considered as a diagonal matrix. If all $\xi_i{}^2$ are equal, the criterion cited in (2.40) could be used instead of (2.39). The immediate advantage of using (2.40) is its simplicity. Nevertheless, the criterion of (2.37) is more general as well as being closer to the practical situation. Implementation of the criterion (2.37) implies:

1) Utilizing reliability data in assessing the likelihood of every fault case.

2) Employing information on circuit parameter tolerances.

3) Errors and inaccuracies in measurement devices are taken into consideration.

For the video amplifier circuit of Fig. 3, three faults were actually induced on a breadboard [53] and the resultant nodal voltages at the five test points were measured. Table

2.9 summarizes the results for the application of the nearest-neighbor rule for the three induced faults. For the induced faults 4 and 14 (see Table 2.1) the minimum distance occured correctly at faults 4 and 14, respectively. For the induced fault 10, the minimum distance resulted in a tie between faults 10 and 12. These faults could not be uniquely identified and, therefore, have to be replaced together [53].

For the passive network of Fig. 4, a comparison between the criterion of (2.39) and the criterion of (2.40) is provided in Fig. 11 for the 14 fault cases. This comparison must, however, be interpreted with care, owing to the use of different measurement conditions. Curve a is obtained [55] using the pooled covariance matrix criterion for seven diagnostic measurements, with tolerances on the nonfaulty elements assumed to be $\pm$ 5%. Curve b is obtained using the nearest-neighbour rule for only five diagnostic measurements, with tolerances on the nonfaulty elements assumed to be $\pm$ 3% [170].

2.3.2 *Fuzzy Concept Criterion* [62]

In actual practice, it has been noticed by Bedrosian et al.[11]-[13], [62] that imprecision and indeterminancy of a faulty circuit often outweigh the statistical randomness and are difficult to overcome. As such, they considered faulty circuits as fuzzy systems.

For an ordinary set the element is either "included in" or "not included in" the set. For a fuzzy set every element has a degree of belonging to the set, grade of membership, P, and the grade takes values on the interval [0,1].

Similarly to the probability measure a fuzzy measure P is defined on the Borel field B of subsets of the real line Ω which has the following properties:

$$P(\varnothing) = 0 \ (\varnothing \text{ is the empty subset}), \tag{2.41a}$$

$$P(\Omega) = 1, \tag{2.41b}$$

if $\alpha,\beta \in B$ with $\alpha \subset \beta$, then

$$P(\alpha) \leq P(\beta), \tag{2.41c}$$

if $\{\alpha_j | 1 \leq j < \infty\}$ is a monotone sequence, then

$$\underset{j\to\infty}{\text{Limit}}\,[P(a_j)] = P\,[\underset{j\to\infty}{\text{Limit}}\,(a_j)] \tag{2.41d}$$

A fuzzy expected value FEV of χ over a set A, with respect to measure P is defined as

$$FEV(\chi) \triangleq \sup_{x\in A} \{\min[\chi(x), P(E_x)]\}\ , \tag{2.42a}$$

where

$$E_x = \{V|V \geq x\} \subset A, \tag{2.42b}$$

$$\chi\colon \Omega \to [0, 1] \tag{2.42c}$$

and

$$P\colon \{V|V \geq x\} \to [0, 1]\,. \tag{2.42d}$$

The fuzzy entropy FET of χ over a set A with respect to measure P is defined as

$$FET(\chi) \triangleq -FEV(\chi)\log_2 FEV(\chi) \tag{2.43}$$

and the fuzzy entropy of χ, given x, over a set A with respect to measure P is given by

$$FET(\chi|x) = -\lambda\,\chi(x)\log_2\chi(x) - (1-\lambda)\,P(E_x)\log_2 P(E_x)\ , \tag{2.44a}$$

where

$$\lambda \triangleq \frac{FEV(\chi) - P(E_x)}{\chi(x) - P(E_x)}\ . \tag{2.44b}$$

The fuzzy mutual information defined by $[FET(\chi) - FET(\chi|x)]$ is a positive number and is used as a criterion for fault isolation.

The implementation of this approach to dc network testing will proceed as follows.

Step 1 — Calculate the network fault membership function due to the fth fault component for the ith measurement.

Comment — The membership function $\overline{P}_{if}(V_i)$, $f = 1, 2, \ldots, n_f$ varies between 0 and 1 and is usually constructed depending on the designer's experience, network simulation and reliability data.

Step 2 — Calculate the fuzzy measure $P(E_{x_{if}})$

$$P(E_{x_{if}}) = \frac{\int_{x}^{V_i^u} \overline{P}_{if}(V_i)\, dV_i}{\int_{V_i^\ell}^{V_i^u} \overline{P}_{if}(V_i)\, dV_i} , \tag{2.45}$$

where V_i^u and V_i^ℓ are the upper and lower limits of the response V_i.

Step 3 Using (2.42a) compute FEV (F_{if}) as

$$FEV(F_{if}) = \sup_{x \in A} \{\min[\overline{P}_{if}(x),\ P(E_{x_{if}})]\} , \tag{2.46}$$

where A is the set of all possible values of the ith measurement V_i.

Step 4 Compute using measurements V_i^m, $i = 1, 2, \ldots, n_m$ the fuzzy mutual information

$$d_{if} \triangleq FET(F_{if}) - FET(F_{if}|V_i^m) , \ i \in I_M, f \in F . \tag{2.47}$$

Step 5 Find f corresponding to the minimum value of

$$\sum_{i \in I_M} d_{if} . \tag{2.48}$$

Learning could be incorporated in the diagnostic scheme to improve the diagnostic performance. After gathering some correctly decided data the fuzzy measure $P(E_{x_{if}})$ is updated as

$$P(E_{x_{if}}) = \frac{\int_{x}^{V_i^u} \overline{P}_{if}(V_i)\, dV_i + \int_{x}^{V_i^u} c\, u(V_i - V_i^*)\, dV_i}{\int_{V_i^\ell}^{V_i^u} \overline{P}_{if}(V_i)\, dV_i + c} , \tag{2.49}$$

where $u(V_i)$ is a unit impulse function, V_i^* denotes a correct observation and c is an enhancement constant lying between 0 and 1.

Fuzzy distance has also been proposed [62] instead of the fuzzy entropy (2.47) to isolate faults. Other fuzzy measures [12] have been proposed. The problems with the approach is its difficulty and subjectivity, and it has not found any enthusiastic attention from other researchers.

2.3.3 *Voting Technique* [141], [143]

The voting technique is based upon comparing the stored quantized dictionary entries with the corresponding quantized values of the measured quantities. Then votes are cast for and against the likelihood of a certain fault f. Recalling (2.5), d_{if} constitutes the stored dictionary quantities $\{1, 0, -1\}$. The measured values of real gain and phase quantities H_i^m are quantized such that

$$\overline{H}_i^m = \begin{cases} 1 & \text{for} \quad H_i^0 - H_i^m > \psi_i \,, \\ 0 & \text{for} \quad |H_i^0 - H_i^m| \le \psi_i \,, \\ -1 & \text{for} \quad H_i^0 - H_i^m < -\psi_i \,. \end{cases} \tag{2.50}$$

Let

$$d_f \triangleq \sum_{i \in I_M} d_{if} \overline{H}_i^m \,, \tag{2.51a}$$

which is a measure of the correlation between the stored and measured values. Let

$$d_{\bar{f}} \triangleq \sum_{i \in I_M} |d_{if}| \, (1 - |\overline{H}_i^m|) \,, \tag{2.51b}$$

which accounts for the case when $\overline{H}_i^m$ is zero but d_{if} is not. Then

$$d_f^* = \begin{cases} (\operatorname{sign} d_f)\,[|d_f| - d_{\bar{f}}] \,, & \text{for } |d_f| > d_{\bar{f}} \,, \end{cases} \tag{2.51c}$$

$$\begin{cases} 0 \,, & \text{otherwise} \,, \end{cases} \tag{2.51d}$$

could represent the probability of obtaining measurements H_i^m for the fth fault case.

If Prob(f) is the prior relative probability of each fault occuring, then the posterior relative probability of the fault f is given by

$$\text{Prob}(f) \triangleq \begin{cases} \dfrac{\text{Prob}\,(f)\, d_f^*}{\sum_{f \in F} \text{Prob}(f)\, d_f^*} \,, & \text{(2.52a)} \\ 0 \,, \quad \text{if} \sum_{f \in F} \text{Prob}(f)\, d_f^* = 0 \,. & \text{(2.52b)} \end{cases}$$

The faults are ranked according to the relative probability of each fault. It has been shown that (2.52) is valuable in identifying an ambiguity group that contains the fault [143], namely, to consider a group of elements having the highest values of d_f^* as the elements of an ambiguity set that contains the faulty element.

2.3.4 *Matching Techniques*

These techniques are quite simple. If the fault dictionary is represented by a set of loci as in [81] and [131], the output responses are located on the graphs and the closest responses to the loci of certain fault cases are identified usually by the naked eye. For other techniques [135], [144] that utilize a code for every fault case, the measured responses are coded in a similar way and template matching is conducted to identify the fault that produces the same code as that of the measured response.

2.4 *Efficient Methods of Fault Simulation*

It is conceivable that excessive computer time may be required to develop a fault dictionary for large networks. Efficient algorithms have been proposed for the simulation of multiple faults in linear and nonlinear networks [33], [69], [151]. Furthermore, computationally efficient approximations to the fault bands, namely, band faults, were developed by Pawha and Rohrer [100].

2.4.1 *Application of Householder's Formula* [151]

Temes [151] has proposed the use of Householder's formula for fault simulation. This technique is primarily applicable to fault simulation in linear networks. Let the node admittance equations of the nominal circuit be

$$\mathbf{Y}_n \mathbf{V}^n = \mathbf{I}^n, \tag{2.53}$$

where $\mathbf{Y}_n$ is the nodal admittance matrix, $\mathbf{V}^n$ is the node voltage vector and $\mathbf{I}^n$ is the current source vector (forcing function).

For the faulty circuit, with its current sources unchanged, the nodal equations are given by

$$(\mathbf{Y}_n + \Delta\mathbf{Y}^n)(\mathbf{V}^n + \Delta\mathbf{V}^n) = \mathbf{I}^n. \tag{2.54}$$

Consequently, the change in nodal voltages is given by

$$\Delta\mathbf{V}^n = [(\mathbf{Y}_n + \Delta\mathbf{Y}_n)^{-1} - \mathbf{Y}_n{}^{-1}]\,\mathbf{I}^n. \tag{2.55}$$

For a single fault, let Δy_f be the change in the admittance value of the faulty element. In general, this element could be modeled by a voltage controlled current source connected between nodes ℓ_1 and ℓ_2 and controlled by the difference between the voltages of nodes k_1 and k_2. If the element is passive, then $\ell_1 = k_1$ and $\ell_2 = k_2$. The change in the admittance matrix $\Delta \mathbf{Y}_n$ could be represented by

$$\Delta \mathbf{Y}_n = \mathbf{a}_f \Delta y_f \bar{\mathbf{a}}_f^T \tag{2.56}$$

where the entries of the vectors $\mathbf{a}_f$ and $\mathbf{a}_f$ are zeros except for entries

$$a_{\ell_1} = \bar{a}_{k_1} = 1\,, \tag{2.57a}$$

$$a_{\ell_2} = \bar{a}_{k_2} = -1 \tag{2.57b}$$

and we assumed neither ℓ_1, ℓ_2, k_1 nor k_2 is a ground reference node.

Utilizing Householder's formula (2.55) can be written as

$$\Delta \mathbf{V}^n = -\frac{\Delta y_f \mathbf{Y}_n^{-1} \mathbf{a}_f \bar{\mathbf{a}}_f^T}{1 + \Delta y_f \bar{\mathbf{a}}_f^T \mathbf{Y}_n^{-1} \mathbf{a}_f} \mathbf{V}^n\,. \tag{2.58}$$

Since the LU factors of $\mathbf{Y}_n$ are already known from a nominal analysis, $\mathbf{Y}_n^{-1}\,\mathbf{a}_f$ is easily computed in terms of them using forward and backward substitution (FBS) operations. Since the FBS requires the maximum number of multiplications, the effort in computing (2.58) is approximately the cost of FBS compared with the full solution of the system of equations (2.54).

Considering n_f faulty elements simultaneously changed, a generalization of (2.56) is given by

$$\Delta \mathbf{Y}_n = \mathbf{A}_f \Delta \mathbf{Y}_f \bar{\mathbf{A}}_f^T \tag{2.59a}$$

where

$$\mathbf{A}_f = [\mathbf{a}_1\ \mathbf{a}_2 \ldots \mathbf{a}_{n_f}]\,, \tag{2.59b}$$

$$\bar{\mathbf{A}}_f = [\bar{\mathbf{a}}_1\ \bar{\mathbf{a}}_2 \ldots \bar{\mathbf{a}}_{n_f}]\,, \tag{2.59c}$$

and

$$\Delta \mathbf{Y}_f = \mathrm{diag}\{\Delta y_{i_1}, \Delta y_{i_2}, \ldots, \Delta y_{i_{n_f}}\}\,. \tag{2.59d}$$

For multiple fault case (2.55) is given by

$$\Delta \mathbf{V}^n = -\mathbf{Y}_n^{-1}\,\mathbf{A}_f [\Delta \mathbf{Y}_f^{-1} + \bar{\mathbf{A}}_f^T \mathbf{Y}_n^{-1}\,\mathbf{A}_f]^{-1}\,\bar{\mathbf{A}}_f^T\,\mathbf{V}^n. \tag{2.60}$$

In this case the computational effort will be mainly due to the evaluation of the inverse of the matrix

$$[\Delta \mathbf{Y}_f^{-1} + \bar{\mathbf{A}}_f^T \mathbf{Y}_n^{-1} \mathbf{A}_f], \tag{2.61}$$

which is proportional to $n_f^3/3$ compared to the inversion of the matrix $(\mathbf{Y}_n + \Delta \mathbf{Y}_n)$, which is proportional to $n_t^3/3$, where n_t is the total number of the network nodes excluding the reference node.

2.4.2 *Application of Complementary Pivot Theory* [69]

Lin [69] applied the complementary pivot theory to nonlinear network dc fault simulation. The procedure consists of representing nonlinearities by piecewise-linear characteristics, representing faults by switch conditions, using multiport theory to formulate the fault equations and finally using the complementary pivot algorithm to solve the equations. This technique has the advantage of a faster dc analysis and establishing a data base so that the fault dictionary can be easily expanded without resorting to an analog circuit simulator.

A fixed change in any parameter can be modeled, as shown in Fig. 12, by a switch. The nonlinear resistive network under consideration is modeled with linear resistors, controlled sources, dc independent sources and ideal diodes. Let n_d be the number of diodes, n_m the number of measurement nodes and n_s the number of switches modeling faults. There are 2^{n_s} combinations of switch conditions, only n_f of them corresponding to the assumed fault cases (single or multiple faults).

We extract $(n_d + n_m + n_s)$ elements corresponding to diodes, switches and measurements to form the $(n_d + n_m + n_s)$-port network shown in Fig. 13. For a certain fault f some of the switches are open with their corresponding currents $\mathbf{I}^{so}$ equal to $\mathbf{0}$ and the rest are closed with their corresponding voltages $\mathbf{V}^{ss}$ equal to $\mathbf{0}$.

The hybrid equation for the multiport under fault f is given by [69]

$$\begin{bmatrix} H_{s1} & 0 & 0 & H_{s2} & H_{s3} & H_{s4} \\ H_{m1} & 1 & 0 & H_{m2} & H_{m3} & H_{m4} \\ H_{d1} & 0 & 1 & H_{d2} & H_{d3} & H_{d4} \end{bmatrix} \begin{bmatrix} \mathbf{O} \\ \mathbf{V}^m \\ \mathbf{I}^d \\ \overline{\mathbf{O}} \\ \mathbf{I}^m \\ \mathbf{V}^d \end{bmatrix} = \begin{bmatrix} \mathbf{J}^s \\ \mathbf{J}^m \\ \mathbf{J}^d \end{bmatrix} , \qquad (2.62a)$$

where

$$\mathbf{O} \triangleq \begin{bmatrix} \mathbf{V}^{so} \\ \mathbf{I}^{ss} \end{bmatrix} , \quad \overline{\mathbf{O}} \triangleq \begin{bmatrix} \mathbf{I}^{so} \\ \mathbf{V}^{ss} \end{bmatrix} . \qquad (2.62b)$$

$\mathbf{J}^s$, $\mathbf{J}^m$ and $\mathbf{J}^d$ are due to the dc independent sources inside the multiport. Since $\overline{\mathbf{O}}$ and $\mathbf{I}^m$ are zero (2.62a) can be written as

$$\begin{bmatrix} H_{s1} & 0 & 0 & H_{s4} \\ H_{m1} & 1 & 0 & H_{m4} \\ H_{d1} & 0 & 1 & H_{d4} \end{bmatrix} \begin{bmatrix} \mathbf{O} \\ \mathbf{V}^m \\ \mathbf{I}^d \\ \mathbf{V}^d \end{bmatrix} = \begin{bmatrix} \mathbf{J}^s \\ \mathbf{J}^m \\ \mathbf{J}^d \end{bmatrix} . \qquad (2.63)$$

Eliminating $\mathbf{O}$ we get

$$\mathbf{V}^m = [H_{m1} H_{s1}^{-1} H_{s4} - H_{m4}] \mathbf{V}^d + [\mathbf{J}^m - H_{m1} H_{s1}^{-1} \mathbf{J}^s] \qquad (2.64a)$$

and

$$\mathbf{I}^d = [H_{d1} H_{s1}^{-1} H_{s4} - H_{d4}] \mathbf{V}^d + [\mathbf{J}^d - H_{d1} H_{s1}^{-1} \mathbf{J}^s] . \qquad (2.64b)$$

Equation (2.64b) together with the ideal diode constraints

$$V_i^d \geq 0, I_i^d \geq 0, \; V_i^d I_i^d = 0, i = 1, 2, ..., n_d , \qquad (2.64c)$$

form a complementary problem which may be solved by the complementary pivot algorithm [69]. In implementation H_{s1}^{-1} is not found explicitly. Row echelon reduction is employed to get (2.64) from (2.63). A very comprehensive list of hard failures may be considered initially to set up the data base given by the left-hand-side matrix of (2.62a). It is to be noted that for a different fault condition the only operation needed to construct the multiport equations

involves interchanging matrix columns. No new information needs to be extracted from the network. This is because, for another fault, the status of some switches will change, namely, some open switches will be closed and some closed switches will be open. Consequently, some of the variables corresponding to $\mathbf{O}$ and $\overline{\mathbf{O}}$ will interchange, as well as their corresponding columns.

When the faults are arranged such that two successive faults differ by just one switch condition, then the solution of the second fault condition can be obtained much faster using the first fault condition and the total time spent in analysis will be considerably less than that required by the use of a circuit simulator like SYSCAP or SPICE2.

2.4.3 *Approximating Fault Bands* [100]

As we mentioned earlier in Section 2.2.1, fault bands are usually needed for constructing the different ambiguity groups. Since full worst-case analysis is usually very expensive, an approximation to the fault bands has been suggested by Pahwa and Rohrer for linear circuits [100]. The band fault for a measurement $i \in I_M$ is obtained as follows.

Step 1 Compute the worst-case tolerance band that occurs with no faults. This tolerance band has two extremes: worst-case low and worst-case high. The worst case responses are assumed to occur when all components are at their extremal tolerance boundaries in such a direction as to reinforce the deviation of the nominal response.

Step 2 For every fault condition find the shift of these worst-case responses (low and high). The fault band is the interval between the shifted worst-case high and the shifted worst-case low under the fault.

This should be compared with the effort needed to find the exact fault band, which is obtained by first computing the shift in the nominal response caused by the fault and then computing the worst-case tolerance band that occurs around the fault response.

Utilizing Householder's formula and assuming only single faults, the construction of band faults for n_f fault cases needs only 2 n_f FBS. For fault bands we need 3 n_f FBS + 2 n_f LUF (LU factorization). Since LUF is the most time consuming, it is clear how efficient the band fault approach is for large networks.

In the examples considered in [100], there were very few situations for which fault bands and band faults did not coincide closely.

2.4.4 *CUT Modeling* [103]

Simulation models for diagnostic test generation must accurately represent the performance of the circuit under test for all fault conditions. A good simulation model for fault diagnosis testing should satisfy the following attributes due to Plice [103].

1) Realistic fault simulation. The simulation model must accurately simulate the behaviour of the CUT for any of the specified faults.

2) Programmable. The simulation model must be easily programmed and the user should be able to specify the faults in terms of component or node names found in the as-built manufacturing documentation.

3) Modular. The simulation model of the CUT must be a composite of separately identifiable modules.

4) Two level. Each simulation module must have a high level version with low details (input–output model) and a low level version with extensive details which may be used interchangeably with no significant impact on the signal propagated through it.

5) Created from as-built documentation. The simulation model modules must be created from source data found in the as-built manufacturing documentation.

Furthermore, the fault model must be designed so that when the fault conditions are implemented, the basic topology of the original circuit is not violated. This means that shorts must be approximated by a nonzero resistor, since a zero-ohm resistor would imply that two

nodes are replaced by a single node [58]. If such a condition were allowed to occur, a singular matrix would be formed causing the solution procedure to fail.

A transistor fault model was developed [140], [165], [166] for implementation with any computer-aided-design program. In Fig. 14 the modified transistor model is shown with the different fault conditions achieved by changing the values of the added resistors.

It is also important in the practical application of all fault location techniques to model the ATE/CUT interactions. Avoiding this modeling would affect substantially the effectiveness of the isolation technique [44].

III. PARAMETER IDENTIFICATION TECHNIQUES

The parameter identification approach for fault location utilizes the measurements to identify all the parameters of the network. The faulty elements are consequently identified by determining which circuit element values fall within or outside the design tolerance margins.

The circuit under test is assumed to be of known topology. In general, a subset of the network nodes are accessible nodes (test nodes), where voltages and/or currents can be applied and/or measured, and the rest of the nodes are designated as internal nodes (inaccessible nodes), at which neither voltages nor currents can be applied or measured. The nominal element values are usually assumed known.

A network is said to be element-value-solvable [10], [14]-[16], if and only if the value of each of its elements is uniquely determinable from the network's behaviour as seen from its external or accessible terminals.

The parameter identification techniques are classified according to whether the diagnosis equations are linear or nonlinear. Nonlinear diagnosis equations usually provide a locally unique solution, whereas linear diagnosis equations normally yield a global unique solution.

3.1 *Nonlinear Techniques for Element-Value Determination*

Nonlinear diagnosis equations usually result for linear and nonlinear circuits when not all the nodes of the circuit under test are accessible. We consider dc testing and dynamic testing of nonlinear networks. The theory introduced for nonlinear network testing is applied to multifrequency linear network testing. We also consider necessary and sufficient conditions for resistive network testing.

3.1.1 *DC Testing of Nonlinear Networks*

Most of the material presented in this Section is based on the excellent work by Visvanathan and Sangiovanni-Vincentelli [172]. The nonlinear resistive circuit under test is assumed to have the input-output model

$$\mathbf{V}^m = \mathbf{h}(\mathbf{I}^m, \boldsymbol{\phi}), \tag{3.1}$$

where, without loss of generality, we assume that the outputs are the nodal voltages $\mathbf{V}^m$ and the inputs are the nodal currents $\mathbf{I}^m$. Note that the input-output function relation (3.1) for nonlinear circuits depends on the inputs and the parameters $\boldsymbol{\phi}$ of the circuit. In linear networks the input-output behaviour is usually expressed in terms of functions that are essentially independent of the circuit input.

As a consequence of the nonlinear description of the circuit the element-value-solvability definition is relaxed.

Definition 3.1 [172]: Two network parameters $\boldsymbol{\phi}^1$ and $\boldsymbol{\phi}^2 \in \mathbb{R}^{n\phi}$ are said to be observationally equivalent if and only if

$$\mathbf{h}(\mathbf{I}^m, \boldsymbol{\phi}^1) = \mathbf{h}(\mathbf{I}^m, \boldsymbol{\phi}^2) \;\forall\; \mathbf{I}^m \in \mathbb{R}^{nm}. \tag{3.2}$$

Definition 3.1 characterizes the uniqueness of the solution, namely, if for $\forall\, \boldsymbol{\phi} \in \mathbb{R}^{n\phi}$, $\boldsymbol{\phi} \neq \boldsymbol{\phi}^*$, $\exists\, \mathbf{I}^m$ such that

$$\mathbf{h}(\mathbf{I}^m, \boldsymbol{\phi}^*) \neq \mathbf{h}(\mathbf{I}^m, \boldsymbol{\phi}), \tag{3.3}$$

the solution of (3.1) will be unique at $\boldsymbol{\phi}^*$.

Definition 3.2 [172]: A parameter $\boldsymbol{\phi}^* \neq \mathbb{R}^{n\phi}$ is said to be locally diagnosable if there exists an open neighborhood of $\boldsymbol{\phi}^*$ containing no other $\boldsymbol{\phi}$ which is observationally equivalent to it. We say that the local diagnosability property holds at a point $\boldsymbol{\phi}^* \in \mathbb{R}^{n\phi}$ if $\boldsymbol{\phi}^*$ is locally diagnosable.

If the local diagnosability property is a generic property, i.e., a property that holds for almost all parameter points $\boldsymbol{\phi}$ in $\mathbb{R}^{n\phi}$, the circuit under test is said to be locally diagnosable.

Thus, the condition of the circuit to be locally diagnosable replaces the more stringent condition that the circuit be element-value-solvable. Since the network is nonlinear, any

change of the input $\mathbf{I}^m$ will produce a new set of outputs $\mathbf{V}^m$ that are, in general, independent of the outputs observed before the change. To characterize the local diagnosability of the circuit, a test matrix that is dependent only on the network parameters $\boldsymbol{\phi}$ is introduced. Let $w(\mathbf{I}^m)$ be a continuous scalar weighting function with respect to $\mathbf{I}^m$ such that $w(\mathbf{I}^m) > 0$ for all $\mathbf{I}^m \in \mathbb{R}^{n_m}$. Then the test matrix is given by

$$\mathbf{R}(\boldsymbol{\phi}) \triangleq \int_{-\infty}^{\infty}\int_{-\infty}^{\infty}\cdots\int_{-\infty}^{\infty} w(\mathbf{I}^m)[\nabla_{\phi}\,\mathbf{h}^T(\mathbf{I}^m, \boldsymbol{\phi})][\nabla_{\phi}\,\mathbf{h}^T(\mathbf{I}^m, \boldsymbol{\phi})]^T \, d\,I_1^m \, d\,I_2^m \cdots d\,I_{n_m}^m , \tag{3.4}$$

where ∇_{ϕ} indicates the gradients of the functions $\mathbf{h}$ w.r.t. the parameters $\boldsymbol{\phi}$. Note that $\mathbf{R}(\boldsymbol{\phi})$ is a symmetric positive semidefinite matrix. The elements of the matrix $\mathbf{R}(\boldsymbol{\phi})$ are continuous functions of $\boldsymbol{\phi}$. A parameter $\boldsymbol{\phi}^*$ is said to be a regular point [122] of $\mathbf{R}(\boldsymbol{\phi})$ if there exists an open neighborhood of $\boldsymbol{\phi}^*$ in which $\mathbf{R}(\boldsymbol{\phi})$ has a constant rank. The rank of $\mathbf{R}(\boldsymbol{\phi})$ plays a very important role in characterizing the local diagnosability property.

Theorem 3.1 [172]: Let $w(\cdot)$ be any weighting function such that the matrix $\mathbf{R}(\boldsymbol{\phi})$ exists $\forall\, \boldsymbol{\phi} \in \mathbb{R}^{n_\Phi}$, and let $\boldsymbol{\phi}^*$ be a regular point of $\mathbf{R}(\boldsymbol{\phi})$. The parameter point $\boldsymbol{\phi}^*$ is locally diagnosable if and only if $\mathbf{R}(\boldsymbol{\phi}^*)$ is positive definite.

If the rank of $\mathbf{R}(\boldsymbol{\phi}^*)$ is equal to ρ, then the measure of solvability of the parameter point $\boldsymbol{\phi}^*$ is defined as

$$\mu(\boldsymbol{\phi}^*) \triangleq n_{\phi} - \rho. \tag{3.5}$$

When $\rho < n_{\phi}$ there is an $(n_{\phi} - \rho)$-dimensional manifold of observationally equivalent points that contains $\boldsymbol{\phi}^*$. If $\mu(\boldsymbol{\phi}^*) = 0$, $\boldsymbol{\phi}^*$ is a locally unique solvable point. If the local diagnosability property for a parameter point is a generic property, the circuit under test will be locally diagnosable.

Theorem 3.2 [172]: Suppose that

$$\rho^* \triangleq \max_{\boldsymbol{\phi} \in \mathbb{R}^{n_\Phi}} \operatorname{rank} \mathbf{R}(\boldsymbol{\phi}) \tag{3.6}$$

is the generic rank of $\mathbf{R}(\boldsymbol{\phi})$. Then

1) almost all $\boldsymbol{\phi} \in \mathbb{R}^{n_\Phi}$ are regular points of $\mathbf{R}(\boldsymbol{\phi})$,

2) the circuit is locally diagnosable if and only if $\rho^* = n_\phi$.

When $\mathbf{h}(\mathbf{I}^m, \boldsymbol{\phi})$ is analytic in $\boldsymbol{\phi}$, then ρ^* as defined in (3.6) is the generic rank of $\mathbf{R}(\boldsymbol{\phi})$ and $\mu(\boldsymbol{\phi}^*)$ of (3.5) has a generic value μ^* which is the measure of testability of the circuit. This measure is determined by the circuit structure and the location of the inputs and outputs of the circuit. It does not depend on the choice of the test signals, the test algorithm or the parameter values. Therefore, it can be used as a design aid to check the testability of a circuit, to choose test nodes and to design testable circuits.

From the definition in (3.4), it is clear that the evaluation of $\mathbf{R}(\boldsymbol{\phi})$ is expensive since it involves an infinite multidimensional integral. Under the condition that $\mathbf{h}(\mathbf{I}^m, \boldsymbol{\phi})$ is analytic in $\mathbf{I}^m$ and $\boldsymbol{\phi}$, it is almost sufficient to check the rank of

$$\sum_{i=1}^{n_\phi} [\nabla_\phi \mathbf{h}^T(\mathbf{I}_i^m, \boldsymbol{\phi}^*)][\nabla_\phi \mathbf{h}^T(\mathbf{I}_i^m, \boldsymbol{\phi}^*)]^T \tag{3.7}$$

for any randomly chosen inputs $\mathbf{I}_i^m$, $i = 1, 2, ..., n_\phi$, and randomly chosen $\boldsymbol{\phi}^*$. If the rank of (3.7) equals n_ϕ, then the circuit is locally diagnosable and any n_ϕ randomly chosen inputs can be used to solve uniquely (locally) for the element values of the circuit. The solution is carried out by solving the equations

$$\mathbf{h}(\mathbf{I}_i^m, \boldsymbol{\phi}) - \mathbf{V}_i^m = \mathbf{0}, \; i = 1, 2, ..., n_\phi \tag{3.8}$$

for the parameters $\boldsymbol{\phi}$, using a stabilized Newton algorithm [26], [92]. Usually, the number of inputs is chosen to be greater than n_ϕ to avoid numerical difficulties. A sub-optimal algorithm proposed in [171] selects sequentially the test node among a possible set of nodes that increases as much as possible the rank of the matrix $\mathbf{R}$. The algorithm stops when rank $[\mathbf{R}(\boldsymbol{\phi})] = n_\phi$. Due to the nonlinearity of the network the number of outputs chosen is smaller than the number of network parameters n_ϕ.

Consider the diode circuit in Fig. 15 [172]. The input-output characteristic is given by

$$I^m = G\, V^m + I_s\,(e^{aV^m} - 1),$$

where I_s is the diode saturation current, α is the diode constant and G is the conductance of the linear resistor. Note that the relation is analytical with respect to V^m and $\boldsymbol{\phi} = [G\ I_s\ \alpha]^T$. We apply (3.7) to check the testability of the network. Let $V_1^m = -1$, $V_2^m = 1$, $V_3^m = 2$ and $\boldsymbol{\phi}^* = [1\ 1\ 1]^T$. Accordingly, we have

$$\sum_{j=1}^{3} \begin{bmatrix} \frac{\partial I_j^m}{\partial G} \\ \frac{\partial I_j^m}{\partial I_s} \\ \frac{\partial I_j^m}{\partial \alpha} \end{bmatrix} \begin{bmatrix} \frac{\partial I_j^m}{\partial G} & \frac{\partial I_j^m}{\partial I_s} & \frac{\partial I_j^m}{\partial \alpha} \end{bmatrix} =$$

$$\sum_{j=1}^{3} \begin{bmatrix} V_j^m \\ \left(e^{\alpha V_j^m} - 1\right) \\ I_s V_j^m e^{\alpha V_j^m} \end{bmatrix} \begin{bmatrix} V_j^m & \left(e^{\alpha V_j^m} - 1\right) & I_s V_j^m e^{\alpha V_j^m} \end{bmatrix}$$

$$= \begin{bmatrix} -1 & 1 & 2 \\ -0.632 & 1.718 & 6.389 \\ -0.367 & 2.718 & 14.778 \end{bmatrix} \begin{bmatrix} -1 & -0.632 & -0.367 \\ 1 & 1.718 & 2.718 \\ 2 & 6.389 & 14.778 \end{bmatrix}$$

$$= \begin{bmatrix} 6 & 15.128 & 32.641 \\ 15.128 & 42.936 & 99.318 \\ 32.641 & 99.318 & 225.9106 \end{bmatrix},$$

which is nonsingular. Hence, the circuit of Fig. 15 is locally diagnosable.

The problem of choosing appropriate dc biases such that the faults will not be blocked and do appear at the terminal test points is of particular importance. Conditions that depend on the network element types and connections have been given in [40].

3.1.2 *Time Domain Testing of Nonlinear Networks*

A similar theory for the diagnosability of nonlinear dynamical circuits has been developed by Saeks et al. [122]. The inputs and outputs are functions of time and could be considered as elements of an infinite dimensional Hilbert space. $\mathbf{v}^m(t)$ and $\mathbf{i}^m(t)$ are assumed to be piecewise continuous functions of time on the interval [0, T]. Let U be the space of $\mathbb{R}^{n_m}$-valued piecewise continuous functions of time on the interval [0, T]. Then, similarly to (3.4), the test matrix is defined as

$$\mathbf{R}(\boldsymbol{\phi}) \triangleq \int_U \int_0^T w(\mathbf{i}^m(t))[\nabla_{\boldsymbol{\phi}} \mathbf{h}^T(\mathbf{i}^m(t), \boldsymbol{\phi})]\,[\nabla_{\boldsymbol{\phi}} \mathbf{h}^T(\mathbf{i}^m(t), \boldsymbol{\phi})]^T\,dt\,d\mathbf{i}^m(t)\,. \tag{3.9}$$

The nonsingularity of $\mathbf{R}(\boldsymbol{\phi}^*)$ implies that $\boldsymbol{\phi}^*$ is a locally diagnosable point and if the rank of $\mathbf{R}(\boldsymbol{\phi}^*)$ is a generic property, then the local diagnosability of $\boldsymbol{\phi}^*$ implies that the circuit is locally diagnosable. Instead of performing the integral over the whole space U we usually check the diagnosability of $\boldsymbol{\phi}^*$ by computing (3.9) for a finite number of inputs $\mathbf{i}_j^m$, $j = 1, 2, \ldots, \ell \in U$.

$$\sum_{j=1}^{\ell} \int_0^T [\nabla_{\boldsymbol{\phi}} \mathbf{h}^T(\mathbf{i}_j^m(t), \boldsymbol{\phi}^*)]\,[\nabla_{\boldsymbol{\phi}} \mathbf{h}^T(\mathbf{i}_j^m(t), \boldsymbol{\phi}^*)]^T\,dt\,. \tag{3.10}$$

Consider the simple illustrative example of Fig. 16 [122]. Note that the circuit contains both linear and nonlinear resistors and inductors. The various branch relations are given by

$$i^d(t) = I_s\left(e^{\alpha v^d(t)} - 1\right),$$

$$i^G(t) = G\,v^G(t),$$

$$i^\Gamma(t) = \Gamma \int_0^t v^\Gamma(t')\,dt',$$

$$i^\Upsilon(t) = \gamma\left(\int_0^t v^\Upsilon(t')\,dt'\right)^2,$$

where the initial condition states are fixed at zero and the input-output relation is given by

$$i^m(t) = I_s\left(e^{\alpha v^m(t)} - 1\right) + G\, v^m(t) + \Gamma\int_0^t v^m(t')\,dt' + \gamma\left(\int_0^t v^m(t')\,dt'\right)^2 .$$

For $v^m(t) = t\ \forall\, t \in [0, 1]$ and the parameters $\boldsymbol{\phi}^* = [I_s\ \alpha\ G\ \Gamma\ \gamma]^T = [1\ 1\ 1\ 1\ 1]^T$ we find

$$\left[\nabla_{\phi} i^m(t)\right]^T = \left[\frac{\partial i^m(t)}{\partial I_s}\ \frac{\partial i^m(t)}{\partial \alpha}\ \frac{\partial i^m(t)}{\partial G}\ \frac{\partial i^m(t)}{\partial \Gamma}\ \frac{\partial i^m(t)}{\partial \gamma}\right],$$

$$= \left[e^{\alpha v^m(t)} - 1 \quad I_s v^m(t) e^{\alpha v^m(t)} \quad v^m(t) \quad \int_0^t v^m(t')\,dt' \quad \left(\int_0^t v^m(t')\,dt'\right)^2\right],$$

$$= \left[e^t - 1 \quad t\,e^t \quad t \quad t^2/2 \quad t^4/4\right] .$$

Therefore (3.10) becomes

$$\int_0^1 \begin{bmatrix} (e^t-1)^2 & t\,e^t(e^t-1) & t(e^t-1) & t^2(e^t-1)/2 & t^4(e^t-1)/4 \\ t\,e^t(e^t-1) & t^2 e^{2t} & t^2 e^t & t^3 e^t/2 & t^5 e^t/4 \\ t(e^t-1) & t^2 e^t & t^2 & t^3/2 & t^5/4 \\ t^2(e^t-1)/2 & t^3 e^t/2 & t^3/2 & t^4/4 & t^6/8 \\ t^4(e^t-1)/4 & t^5 e^t/4 & t^5/4 & t^6/8 & t^8/16 \end{bmatrix} dt ,$$

$$= \begin{bmatrix} 0.75786 & 1.09726 & 0.5 & 0.19247 & 0.0655 \\ 1.09726 & 1.59726 & 0.7182 & 0.28172 & 0.0998 \\ 0.5 & 0.7182 & 0.3333 & 0.125 & 0.04167 \\ 0.19247 & 0.28172 & 0.125 & 0.05 & 0.01786 \\ 0.0655 & 0.0998 & 0.04167 & 0.01786 & 0.00694 \end{bmatrix} .$$

Note that the above matrix is nonsingular. Hence $\boldsymbol{\phi}^*$ is locally diagnosable. Further since the input-output relation is analytic with respect to $\boldsymbol{\phi}$, the circuit is locally diagnosable.

In the case of circuits of any reasonable size, the explicit relation (3.1) between the inputs and outputs is difficult to obtain and usually the circuit is defined in terms of a set of sparse tableau equations [37], [173] as

$$\mathbf{h}(\mathbf{x}(t),\ \mathbf{i}^b(t),\ \mathbf{v}^b(t),\ \boldsymbol{\phi}) = \mathbf{0} , \tag{3.11a}$$

$$\mathbf{i}^m(t) = \mathbf{A}_1\ \mathbf{i}^b(t) , \tag{3.11b}$$

$$\dot{\mathbf{x}}(t) = \mathbf{A}_2 \begin{bmatrix} \mathbf{i}^b(t) \\ \mathbf{v}^b(t) \end{bmatrix}, \tag{3.11c}$$

$$\mathbf{v}^m(t) = \mathbf{A}_3\, \mathbf{v}^b(t), \tag{3.11d}$$

where $\mathbf{x}(t)$ is the vector of state variables, $\mathbf{v}^b(t)$, $\mathbf{i}^b(t)$ are the voltages and currents of the circuit branches and $\mathbf{A}_i$, i = 1, 2, 3 are appropriate transformation matrices.

The evaluation of the derivatives needed for (3.9) and (3.10) is usually not a computationally easy task. The proposal of discretizing equations (3.11) [122] has been carried out in [173]. Using a numerical backward differentiation formula, as is done in a circuit simulator, $\dot{\mathbf{x}}(t)$ at instant t_j is given by

$$\dot{\mathbf{x}}(t_j) = \frac{1}{\tau_j} \sum_{i=0}^{k} \mathbf{B}_{ij}\, \mathbf{x}(t_{j-i}), \tag{3.12a}$$

where

$$\tau_j = t_j - t_{j-1} \tag{3.12b}$$

and $\mathbf{B}_{ij}$ is formed from the coefficients of the numerical differentiation formula. Consequently, (3.11) is discretized as follows.

$$\mathbf{h}(\mathbf{x}(t_j), \mathbf{i}^b(t_j), \mathbf{v}^b(t_j), \boldsymbol{\phi}) = \mathbf{0}, \tag{3.13a}$$

$$\mathbf{i}^m(t_j) = \mathbf{A}_1\, \mathbf{i}^b(t_j), \tag{3.13b}$$

$$\frac{1}{\tau_j} \sum_{i=0}^{k} \mathbf{B}_{ij}\, \mathbf{x}(t_{j-i}) = \mathbf{A}_2 \begin{bmatrix} \mathbf{i}^b(t_j) \\ \mathbf{v}^b(t_j) \end{bmatrix}, \tag{3.13c}$$

$$\mathbf{v}^m(t_j) = \mathbf{A}_3\, \mathbf{v}^b(t_j). \tag{3.13d}$$

$\mathbf{v}^m(t_j)$ is assumed to be an analytic function in $\boldsymbol{\phi}$ and $\mathbf{i}^m(t_i)$, i = 1, 2, ..., j for all j = 1, 2, ... Moreover, it is assumed that the circuit has a unique dc bias point and for a given sequence of inputs $\mathbf{i}^m(t_i)$, i = 1, 2, ... j, it has unique solutions $\mathbf{x}(t_j)$, $\mathbf{i}^b(t_j)$, $\mathbf{v}^b(t_j)$ and $\mathbf{v}^m(t_j)$.

Definition 3.3 [173]: The discretized circuit (3.13) is said to be locally diagnosable in K steps if there exists a sequence of inputs $\mathbf{i}^m(t_i)$, i = 1, 2, ..., K such that for almost all $\boldsymbol{\phi}^* \in \mathbb{R}^{n_\Phi}$ there exists an open neighborhood of $\boldsymbol{\phi}^*$ containing no other $\boldsymbol{\phi}$ which is observationally equivalent to it, i.e., $\mathbf{v}^m(t_i, \boldsymbol{\phi}) \neq \mathbf{v}^m(t_i, \boldsymbol{\phi}^*)$ for some $i \in \{1, 2, ..., K\}$.

The test matrix corresponding to the above definition is defined as

$$\mathbf{R}^K(\boldsymbol{\phi}, \{\mathbf{i}^m(t_K)\}) \triangleq \sum_{i=1}^{K} [\nabla_{\phi} \mathbf{v}^m{}^T(t_i)][\nabla_{\phi} \mathbf{v}^m{}^T(t_i)]^T , \tag{3.14}$$

where $\{\mathbf{i}^m(t_K)\}$ refers to the sequence of inputs $\mathbf{i}^m(t_1)$, $\mathbf{i}^m(t_2)$, ..., $\mathbf{i}^m(t_K)$ and $\mathbf{v}^m(t_i)$ is evaluated for this sequence of inputs.

The discretized system is said to be locally diagnosable in K steps if and only if the generic rank of $\mathbf{R}^K(\boldsymbol{\phi}, \{\mathbf{i}^m(t_K)\})$ is n_{ϕ}.

From the examples given in [122], it has been shown that, unlike the nonlinear dc testing case, a nonlinear dynamical circuit can be tested with fewer test input signals than the number of parameters and with fewer outputs [173]. The inverter circuit of Fig. 17a was considered in [173] for both dc testing and time-domain testing, with the nonlinear transistor model of Fig. 17b. Parameters β_F, β_R, $r_{bb'}$, $r_{cc'}$ and $r_{ee'}$ are assumed to be fault free.

For dc-testing they have considered the four resistors R_1 through R_4, I_{sd} and the I_s associated with each transistor as the possibly faulty parameter. Therefore, there are a total of nine parameters. Note that for dc testing the capacitors are open circuits. The results given in Table 3.1 are obtained when V_{cc} was kept fixed at five volts, while various dc values between zero and five volts were used for V_{in}.

The results of time-domain testing are summarized in Table 3.2. V_{cc} was kept constant at five volts, while the input signal varied between zero and five volts with 100 picoseconds rise time, 400 picoseconds pulsewidth and 100 picoseconds fall time. Measurements were made at 100 time points, i.e., K = 100. In addition to the parameters considered for dc testing, the two capacitors C_{be} and C_{bc} are considered for each transistor. Therefore, there are a total of seventeen parameters. Although the number of unknown parameters is greater than for the dc case, fewer test points are required for the local diagnosability of the circuit, i.e., when $\mu^* = 0$.

3.1.3 *Multifrequency Testing of Linear Networks*

The theory for the diagnosability of nonlinear networks emerged from a similar theory for multifrequency testing of linear dynamic circuits [133], [134]. Both have the following features.

1) The parameter values are only locally uniquely determined.

2) The number of test nodes is much less than the number of parameters.

3) The computation of element values is expensive and involves solving a set of nonlinear equations.

Two questions, which follow, are fundamental to multifrequency testing [42], [133], [134].

1) What test frequencies should be employed to optimize the solvability of the diagnosis equations?

2) How solvable are the equations given an optimal choice of test frequencies?

These two questions are answered by developing the fault diagnosis equations under multifrequency testing and defining a measure of solvability for these equations.

The approaches outlined in [30], [110] and [134] have utilized the component-connection model (CCM) for deriving the diagnosis equations. In particular, Sen and Saeks [134] have utilized the CCM in deriving the transfer function matrix observable from the accessible nodes of the network. On the other hand, Rapisarda and DeCarlo [110] have utilized the CCM in developing a tableau system of equations and have avoided the computation of the composite system transfer function matrix. From the computational point of view the approach followed by Rapisarda et al. could be superior since the resulting diagnosis equations have a regular structure with fixed polynomial order, often quadratic.

The theoretical results are basically independent of the use of the CCM [108] representation of the network. Therefore, we give these results using the nodal approach. The voltages and currents are represented by their phasors.

Let n_t be the total number of circuit nodes excluding the reference node, n_m be the number of accessible nodes and n_b be the number of circuit branches. The element characteristics are given by

$$\mathbf{Y}_b \mathbf{V}^b = \mathbf{I}^b , \tag{3.15}$$

where, without loss of generality, we assume that

$$\mathbf{Y}_b = \text{diag}\,\{y_1(s, \boldsymbol{\Phi}_1),\ y_2(s, \boldsymbol{\Phi}_2),\ \ldots,\ y_{n_b}(s, \boldsymbol{\Phi}_{n_b})\}, \tag{3.16}$$

where $\boldsymbol{\Phi}_i$ indicates that the branch admittance could be a function in more than one parameter, i.e., $n_\Phi \geq n_b$. s is the complex frequency and

$$\mathbf{V}^b = [V_1^b\ V_2^b \ldots V_{n_b}^b]^T,\ \mathbf{I}^b = [I_1^b\ I_2^b \ldots I_{n_b}^b]^T \tag{3.17}$$

are the voltages and currents of the n_b branches, respectively.

Let $\mathbf{Q}$ be the incidence matrix of the circuit. Then the nodal equations are given by

$$\mathbf{Q}\,\mathbf{Y}_b\,\mathbf{Q}^T\mathbf{V}^n = \mathbf{Y}_n\,\mathbf{V}^n = \mathbf{I}^n , \tag{3.18}$$

where $\mathbf{Y}_n$ is the nodal admittance matrix, $\mathbf{V}^n$ is the vector of nodal voltages and $\mathbf{I}^n$ is the vector representing the nodal current sources of the network.

Let the first n_m nodes correspond to the accessible nodes. We partition the incidence matrix as

$$\mathbf{Q} = \begin{bmatrix} \mathbf{Q}_m \\ \mathbf{Q}_{n-m} \end{bmatrix} , \tag{3.19}$$

where $\mathbf{Q}_m$ is the incidence matrix of accessible nodes and $\mathbf{Q}_{n-m}$ is the incidence matrix of inaccessible nodes. Accordingly, the nodal equations are partitioned as [59]

$$\begin{bmatrix} \mathbf{Q}_m\,\mathbf{Y}_b\,\mathbf{Q}_m^T & \mathbf{Q}_m\,\mathbf{Y}_b\,\mathbf{Q}_{n-m}^T \\ \mathbf{Q}_{n-m}\,\mathbf{Y}_b\,\mathbf{Q}_m^T & \mathbf{Q}_{n-m}\,\mathbf{Y}_b\,\mathbf{Q}_{n-m}^T \end{bmatrix} \begin{bmatrix} \mathbf{V}^m \\ \mathbf{V}^{n-m} \end{bmatrix} = \begin{bmatrix} \mathbf{I}^m \\ \mathbf{I}^{n-m} \end{bmatrix} , \tag{3.20}$$

where the vectors $\mathbf{V}^n$ and $\mathbf{I}^n$ are partitioned to correspond to accessible and inaccessible nodes. Eliminating $\mathbf{V}^{n-m}$, namely, the voltages of the inaccessible nodes, and assuming $\mathbf{I}^{n-m} = \mathbf{0}$, a reduced system of equations which corresponds to the input-output equations is

$$\mathbf{I}^m = \mathbf{Q}_m\,\mathbf{Y}_b[1_{n_b} - \mathbf{Q}_{n-m}^T(\mathbf{Q}_{n-m}\,\mathbf{Y}_b\,\mathbf{Q}_{n-m}^T)^{-1}\mathbf{Q}_{n-m}\,\mathbf{Y}_b]\mathbf{Q}_m^T\,\mathbf{V}^m , \tag{3.21}$$

where 1_{n_b} is a unity matrix of order n_b. We let

$$\mathbf{Y}(s, \boldsymbol{\phi}) = \mathbf{Q}_m \mathbf{Y}_b [1_{n_b} - \mathbf{Q}_{n-m}{}^T (\mathbf{Q}_{n-m} \mathbf{Y}_b \mathbf{Q}_{n-m}{}^T)^{-1} \mathbf{Q}_{n-m} \mathbf{Y}_b] \mathbf{Q}_m{}^T \tag{3.22}$$

be the transfer function matrix of the network, which could be constructed by direct voltage measurements at the accessible nodes using different independent input excitations $\mathbf{I}_i^m$, $i = 1, 2, ..., n_m$. Moreover, being rational, it is completely determined by its value at a finite number of frequencies. $\mathbf{Y}(s, \boldsymbol{\phi})$ is, in general, a matrix. We transform it to a column vector to simplify the required mathematical manipulations. So, we assume that vec $(\mathbf{Y}(s, \boldsymbol{\phi}))$ transforms $\mathbf{Y}(s, \boldsymbol{\phi})$ to a column vector. For n_ω different frequencies the diagnosis equations take the form of the column vector

$$\mathbf{H}(\boldsymbol{\phi}) = \begin{bmatrix} \text{vec}\,(\mathbf{Y}(s_1, \boldsymbol{\phi})) \\ \text{vec}\,(\mathbf{Y}(s_2, \boldsymbol{\phi})) \\ \vdots \\ \text{vec}\,(\mathbf{Y}(s_{n_\omega}, \boldsymbol{\phi})) \end{bmatrix} . \tag{3.23}$$

Let the test matrix be defined as

$$\mathbf{R}(\boldsymbol{\phi}) = [\nabla_\phi \mathbf{H}^T(\boldsymbol{\phi})] [\nabla_\phi \mathbf{H}^T(\boldsymbol{\phi})]^*, \tag{3.24}$$

where * indicates the conjugate transpose. Similarly to the previous results we define the measure of solvability of $\boldsymbol{\phi}^*$ as

$$\mu(\boldsymbol{\phi}^*) = n_\phi - \rho, \tag{3.25}$$

where ρ is the rank of test matrix $\mathbf{R}(\boldsymbol{\phi}^*)$. For each $y_i(s, \boldsymbol{\phi}_i)$, $i = 1, 2, ..., n_b$ being a rational function of $\boldsymbol{\phi}_i$, it can be proved that $\mu(\boldsymbol{\phi}^*)$ is almost constant, i.e., it is the generic measure of solvability for the whole network. It is clear that the construction of $\mathbf{H}(\boldsymbol{\phi})$ depends on the choice of the number of test frequencies. It has been proved in [134] that if ρ^* is the generic number of linearly independent rows of $[\nabla_\phi [\text{vec}\ \mathbf{Y}(s, \boldsymbol{\phi}^*)]^T]^T$ over the field of complex numbers, then the minimum value of μ, the measure of testability, is given by

$$\mu^* = n_\phi - \rho^* \tag{3.26}$$

and it is achieved by almost any choice of $n_\phi - \mu^*$ distinct complex frequencies.

The above result does not take numerical considerations into account and it has been noticed [134] that the solution of the diagnosis equations is quite sensitive to the choice of test frequencies. There is not yet a theory for the optimum choice of test frequencies so heuristic choices are followed similar to those used in the dictionary approach.

μ^* characterizes the degree to which the diagnosis equations can be solved given an optimum choice of test frequencies. It provides a means of choosing the accessible nodes, so that a specified minimum value of μ^* is achieved (if $\mu^* = 0$ the network is locally diagnosable in the same sense as defined before).

For the purpose of illustration we consider the simple example of Fig. 18. If V_2 is the only output, then

$$\frac{V_2}{I_{in}} = \frac{sC\,R_1\,R_2}{1 + sC\,(R_1 + R_2)}$$

and

$$\nabla_{\phi}^{T}(V_2/I_{in}) = \left[\frac{\partial(V_2/I_{in})}{\partial R_1} \quad \frac{\partial(V_2/I_{in})}{\partial R_2} \quad \frac{\partial(V_2/I_{in})}{\partial C} \right],$$

$$= \left[\frac{sC\,R_2\,(1 + sC\,R_2)}{[1 + sC\,(R_1+R_2)]^2} \quad \frac{sC\,R_1\,(1 + sC\,R_1)}{[1 + sC\,(R_1+R_2)]^2} \quad \frac{s\,R_1\,R_2}{[1 + sC\,(R_1+R_2)]^2} \right].$$

For $\boldsymbol{\phi}^* = [1\ 1\ 1]^T$, we have

$$\nabla_{\phi}^{T}(V_2/I_{in}) = \left[\frac{s(1+s)}{(1+2s)^2} \quad \frac{s(1+s)}{(1+2s)^2} \quad \frac{s}{(1+2s)^2} \right],$$

which has 2 independent columns over the field of complex numbers, as such the measure of testability $\mu^* = 1$ and the circuit is not locally diagnosable using V_2 as the only output.

If V_1 is the only measured output, then

$$\frac{V_1}{I_{in}} = \frac{R_1\,(sC\,R_2+1)}{1 + sC\,(R_1 + R_2)}$$

and

$$\nabla_{\phi}^{T}(V_1/I_{in}) = \left[\frac{(1 + sC\,R_2)^2}{[1 + sC\,(R_1+R_2)]^2} \quad \frac{(sC\,R_1)^2}{[1 + sC\,(R_1+R_2)]^2} \quad \frac{-s\,R_1^2}{[1 + sC\,(R_1+R_2)]^2} \right].$$

For $\boldsymbol{\phi}^*$ it is equal to

$$\left[\frac{(1+s)^2}{(1+2s)^2} \quad \frac{s^2}{(1+2s)^2} \quad \frac{-s}{(1+2s)^2} \right],$$

which has 3 independent columns over the field of complex numbers, therefore the measure of testability $\mu^* = 0$ and the circuit is locally diagnosable using V_1 alone.

In fact, by measuring (V_1/I_{in}) at three independent frequencies we can compute the coefficients of the transfer function, namely R_1, CR_1R_2 and $C(R_1 + R_2)$, and utilize these coefficients in computing R_1, R_2 and C using simple algebraic manipulations.

A quadratic system of equations for diagnosis could be constructed using equation (3.18) in which both $\mathbf{V}^{n-m}$ and the diagonal entries of $\mathbf{Y}_b$ are unknowns. This system of equations is quite similar to the tableau system of equations developed in [110]. We may rewrite (3.18) as

$$[\mathbf{Q}\,\mathbf{Y}_b(s, \boldsymbol{\phi})]\,[\mathbf{Q}_m{}^T\,\mathbf{V}^m(s) + \mathbf{Q}_{n-m}{}^T\,\mathbf{V}^{n-m}(s)] = \mathbf{I}^n(s), \tag{3.27}$$

where the arguments s, $\boldsymbol{\phi}$ are indicated to illustrate that for a given frequency s_i the terms in the first brackets in (3.27) are dependent on the parameters $\boldsymbol{\phi}$ only and the terms in the second brackets are functions of the unknowns $\mathbf{V}^{n-m}(s)$. Both $\mathbf{V}^m(s)$ and $\mathbf{I}^n(s)$ are assumed known. The main difference between this set of equations and equations (3.21) is that the variables $\mathbf{V}^{n-m}(s)$ are not eliminated. Therefore, for every new frequency a set of new variables, $\mathbf{V}^{n-m}(s)$, are added to the unknown variables. For n_ω frequencies the diagnosis equations are given by

$$\mathbf{H}(\bar{\boldsymbol{\phi}}) = \begin{bmatrix} \mathbf{H}_{\phi 1}(\boldsymbol{\phi})\,\mathbf{H}_{v1}(\mathbf{V}_1^{n-m}) - \mathbf{I}^n(s_1) \\ \mathbf{H}_{\phi 2}(\boldsymbol{\phi})\,\mathbf{H}_{v2}(\mathbf{V}_2^{n-m}) - \mathbf{I}^n(s_2) \\ \vdots \\ \mathbf{H}_{\phi n_\omega}(\boldsymbol{\phi})\,\mathbf{H}_{vn_\omega}(\mathbf{V}_{n_\omega}^{n-m}) - \mathbf{I}^n(s_{n_\omega}) \end{bmatrix} = \mathbf{0}\,, \tag{3.28}$$

where

$$\mathbf{I}^n(s_i) = \begin{bmatrix} \mathbf{I}^m(s_i) \\ \mathbf{0} \end{bmatrix}, \tag{3.29}$$

$$\mathbf{H}_{\phi i}(\boldsymbol{\phi}) = [\mathbf{Q}\,\mathbf{Y}_b(s_i, \boldsymbol{\phi})]\,, \tag{3.30}$$

$$\mathbf{H}_{vi}(\mathbf{V}_i^{n-m}) = [\mathbf{Q}_m{}^T\,\mathbf{V}^m(s_i) + \mathbf{Q}_{n-m}{}^T\,\mathbf{V}^{n-m}(s_i)], \tag{3.31}$$

$$\mathbf{V}_i^{n-m} \triangleq \mathbf{V}^{n-m}(s_i) \tag{3.32}$$

and

$$\overline{\boldsymbol{\Phi}} \triangleq \begin{bmatrix} \boldsymbol{\Phi} \\ \mathbf{V}_1^{n-m} \\ \cdot \\ \cdot \\ \cdot \\ \mathbf{V}_{n_\omega}^{n-m} \end{bmatrix} . \tag{3.33}$$

Theorem 3.3 [110]: Let $\overline{\boldsymbol{\Phi}}^*$ be a solution to (3.28). The circuit is diagnosable for the parameter vector $\boldsymbol{\phi}^*$ if there are sufficient test frequencies s_i and corresponding inputs $\mathbf{I}^n(s_i)$, $i = 1, 2, \ldots, n_\omega$, with n_ω finite, such that the matrix $[\nabla_{\overline{\Phi}}\,\mathbf{H}^T(\overline{\boldsymbol{\Phi}}^*)]^T$ is of full column rank.

Due to the structure of the diagnosis equations it can be shown that if the gradient matrix $[\nabla_{\overline{\Phi}}\,\mathbf{H}^T(\overline{\boldsymbol{\Phi}})]^T$ has full column rank for certain $\overline{\boldsymbol{\Phi}}^*$, then it has full column rank for almost all $\overline{\boldsymbol{\Phi}}$. Therefore the circuit is diagnosable for almost all $\boldsymbol{\phi} \in \mathbb{R}^{n_\Phi}$.

Using the diagnosis equations we can place some bounds on the number of test frequencies n_ω (nothing is mentioned about their optimal choice). The number of complex unknowns of the vector $\mathbf{V}_i^{n-m}$ equals $(n_t - n_m)$. The number of complex equations in (3.28) for n_ω frequencies is equal to $n_\omega n_t$. Therefore, the following bound should be observed such that the number of real equations is greater than or equal to the number of unknowns.

$$2\,n_\omega n_t \geq 2\,n_\omega\,(n_t - n_m) + n_\phi, \tag{3.34a}$$

which implies the bound

$$n_\omega \geq \frac{n_\phi}{2n_m} . \tag{3.34b}$$

On the other hand if Theorem 3.3 is satisfied it can be proved that $n_\omega \leq n_\phi$ [110].

3.1.4 *Element-Value-Solvability of Linear Resistive Networks*

Navid and Willson [91], [92] have given necessary and sufficient conditions for the element-value-solvability of a linear resistive network. Their technique is also applicable to nonlinear resistive networks that can be effectively modeled by their small signal linear resistive model.

The admittance transfer function matrix of (3.22) provides the possible observable information (note that it is no longer a function of frequency). For a reciprocal resistive network the maximum number of independent entries of (3.22) is equal to

$$1/2\, n_m (n_m + 1)\,. \tag{3.35}$$

Therefore, the maximum number of resistors n_ϕ in the network should be less than or equal to $1/2\, n_m(n_m + 1)$. This is a necessary condition for the solvability of the network. The transfer admittance between any accessible nodes $i, j \in M$, where M is the set of accessible nodes, is given by the negative of the entry y_{ij} of the matrix (3.22). The transfer admittance between any accessible node i and the ground node 0 is given by the sum of the entries of the ith row or column of the matrix (3.22), namely,

$$y_{io} = \sum_{j=1}^{n_m} y_{ij},\ i \in M\,. \tag{3.36}$$

The set of network branches consists of the subset of $n_{\phi 1}$ <u>free branches</u> $I_{\phi 1}$, which includes those branches not incident with internal nodes and the subset of $n_{\phi 2}$ <u>fundamental branches</u> $I_{\phi 2}$, defined to be those which have at least one terminal connected to an internal node and $n_\phi = n_{\phi 1} + n_{\phi 2} = n_b$. The subgraph obtained by deleting the free branches from the network graph is called the <u>fundamental subgraph</u>. The solvability of the network depends upon the solvability of the fundamental subgraph, in particular, if the admittances of the fundamental branches are known then the admittances of the free branches can be directly obtained.

Recalling (3.22), the transfer admittance between any two accessible nodes is the sum of two terms. The first term corresponds to the admittance of the free branch which is

connected directly between the accessible nodes. The second term arises from the elimination of the internal nodes and is a function of the admittances of the fundamental branches only. Moreover, the transfer admittance of a linear network, as has been indicated earlier, is a bilinear function of each branch admittance. Therefore, the transfer admittance between any two accessible nodes has the form [51]

$$y_i + \frac{\sum_j g_j}{\Delta}, \tag{3.37}$$

where y_i, $i \in I_{\phi 1}$ is the admittance of the free branch which directly connects the two accessible nodes. Δ is the determinant of the matrix $\mathbf{Q}_{n-m}\ \mathbf{Y}_b\ \mathbf{Q}_{n-m}^T$. Each term of Δ consists of a different product of $(n_t - n_m)$ fundamental branches. In the numerator every g_j term is the product of $(n_t - n_m + 1)$ fundamental branches, i.e.,

$$g_j = y_{j_1} y_{j_2} \cdots y_{j_{n_t - n_m + 1}}, \quad j_i \in I_{\phi 2}. \tag{3.38}$$

In general, no two terms of the numerator are alike, moreover, there is no identical numerator term between various transfer admittances. If the values of the fundamental branches are known it is readily clear from (3.37) that the admittances of free branches, y_i, can be directly obtained. Therefore, we consider only the transfer admittances between nodes that are not connected with any free branch, i.e., have only the second term in (3.37). It is possible to eliminate the denominator Δ by the following transformation [51]

$$y_j' = y_j/(\Delta^{1/(n_t - n_m + 1)}), \quad j \in I_{\phi 2}. \tag{3.39}$$

In this case the resulting equations are multilinear in y'_j and they have the form

$$\sum_j g_j', \tag{3.40a}$$

where

$$g_j' = y_{j_1}' y_{j_2}' \cdots y_{j_{n_t - n_m + 1}}'. \tag{3.40b}$$

The transfer admittances are linearly related to the variables g'_j, which can be represented as

$$\mathbf{H}(\phi) = \mathbf{A}\,\mathbf{g}', \tag{3.41}$$

where $\mathbf{g}'$ is a k′-vector of the k′ different g'_j terms, $\mathbf{H}(\boldsymbol{\phi})$ is a n'_m-vector of transfer admittances that does not depend on the admittances of free branches and $\mathbf{A}$ is a n'_m x k′ matrix consisting of zeros and ones with exactly one nonzero element in each column. Let

$$\begin{bmatrix} g''_1 \\ g''_2 \\ \cdot \\ \cdot \\ \cdot \\ g''_{k'} \end{bmatrix} \triangleq \begin{bmatrix} \log_e g'_1 \\ \log_e g'_2 \\ \cdot \\ \cdot \\ \cdot \\ \log_e g'_{k'} \end{bmatrix} , \tag{3.42a}$$

or, more compactly,

$$\mathbf{g}'' = \log_e \mathbf{g}' , \tag{3.42b}$$

where $\log_e$ is the natural logarithm function. Using (3.40b) we have

$$\mathbf{g}'' = \mathbf{B}\,\mathbf{y}'' , \tag{3.43a}$$

where

$$\mathbf{y}'' = \log_e \mathbf{y}' \tag{3.43b}$$

and $\mathbf{B}$ is a k′ x $n_{\phi 2}$ matrix consisting of zeros and ones, with exactly $(n_t - n_m + 1)$ nonzero elements in each row. Using (3.42), we can find $\mathbf{g}'$ in terms of $\mathbf{g}''$ as

$$\begin{bmatrix} g'_1 \\ g'_2 \\ \cdot \\ \cdot \\ \cdot \\ g'_{k'} \end{bmatrix} \triangleq \begin{bmatrix} \exp(g''_1) \\ \exp(g''_2) \\ \cdot \\ \cdot \\ \cdot \\ \exp(g''_{k'}) \end{bmatrix} , \tag{3.44a}$$

or, more compactly,

$$\mathbf{g}' = \exp(\mathbf{g}'') , \tag{3.44b}$$

where exp is the exponential function. Using (3.43) and (3.44) we may write (3.41) as

$$\mathbf{H} = \mathbf{A} \exp[\mathbf{B} \log_e \mathbf{y}'] \tag{3.45}$$

and the gradients with respect to $\mathbf{y}'$ are given by

$$[\nabla_{y'} \mathbf{H}^T]^T = \mathbf{A}\,\mathbf{D}\,\mathbf{B}\,\mathbf{D}_{y'} , \tag{3.46a}$$

where

$$\mathbf{D} \triangleq \text{diag}\{g'_1, g'_2, \ldots, g'_{k'}\}\,, \tag{3.46b}$$

and

$$\mathbf{D}_{y'} \triangleq \text{diag}\{1/y'_{j_1}, 1/y'_{j_2}, \ldots, 1/y'_{j_{n_{\phi 2}}}\}\,. \tag{3.46c}$$

Theorem 3.4 [92]: The values of the unknowns y'_j, $j \in I_{\phi 2}$, which satisfy the system of nonlinear equations (3.45) are unique if and only if the matrix $\mathbf{A\,D\,B}$ has rank $n_{\phi 2}$ for every diagonal matrix $\mathbf{D} > \mathbf{0}$, i.e., all diagonal elements are positive.

The system of equations (3.45) is usually solved using a modified Newton's method [92]. After finding $y'_j, j \in I_{\phi 2}$ all y_j could be found using the inverse relation

$$y_j = y'_j\,\Delta'\,, \tag{3.47a}$$

where

$$\Delta' = \Delta^{1/(n_t - n_m + 1)} \tag{3.47b}$$

is the determinant obtained by substituting the values y'_j, $j \in I_{\phi 2}$, instead of the original values y_j.

For the linear resistive network of Fig. 19, nodes 5 and 6 are the only inaccessible nodes. The measurable transfer admittances are given by the following relations [92].

$$y_{12} = \frac{G_1 G_2 G_3}{\Delta}\,,\; y_{13} = \frac{G_1 G_4 (G_2 + G_3 + G_5)}{\Delta}\,,\; y_{14} = \frac{G_1 G_2 G_5}{\Delta}\,,$$

$$y_{23} = \frac{G_2 G_3 G_4}{\Delta}\,,\; y_{24} = \frac{G_3 G_5 (G_1 + G_2 + G_4)}{\Delta} \text{ and } y_{34} = G_6 + \frac{G_2 G_4 G_5}{\Delta}\,,$$

where $\Delta = (G_1 + G_4)(G_2 + G_3 + G_5) + G_2(G_3 + G_5)$. From y_{34} it is clear that G_6 could be directly found if the G_1 to G_5 elements, that constitute the fundamental branches, are first identified. Therefore, we consider only y_{12}, y_{13}, y_{14}, y_{23} and y_{24}. Utilizing (3.39) we get $y_{12} = G'_1 G'_2 G'_3$, $y_{13} = G'_1 G'_4 (G'_2 + G'_3 + G'_5)$, $y_{14} = G'_1 G'_2 G'_5$, $y_{23} = G'_2 G'_3 G'_4$ and $y_{24} = G'_3 G'_5 (G'_1 + G'_2 + G'_4)$. Consequently,

$$\mathbf{g}' = [G'_1 G'_2 G'_3 \quad G'_1 G'_4 G'_2 \quad G'_1 G'_2 G'_5 \quad G'_2 G'_3 G'_4$$

$$G'_3 G'_5 G'_1 \quad G'_1 G'_4 G'_3 \quad G'_1 G'_4 G'_5 \quad G'_3 G'_5 G'_2 \quad G'_3 G'_5 G'_4]^T$$

Accordingly, we may write the matrix **A** of (3.41) as

$$\mathbf{A} = \begin{array}{c} \\ y_{12} \\ y_{13} \\ y_{14} \\ y_{23} \\ y_{24} \end{array} \begin{array}{c} \begin{array}{ccccccccc} g'_1 & g'_2 & g'_3 & g'_4 & g'_5 & g'_6 & g'_7 & g'_8 & g'_9 \end{array} \\ \begin{bmatrix} 1 & 0 & 0 & 0 & 0 & 0 & 0 & 0 & 0 \\ 0 & 1 & 0 & 0 & 0 & 1 & 1 & 0 & 0 \\ 0 & 0 & 1 & 0 & 0 & 0 & 0 & 0 & 0 \\ 0 & 0 & 0 & 1 & 0 & 0 & 0 & 0 & 0 \\ 0 & 0 & 0 & 0 & 1 & 0 & 0 & 1 & 1 \end{bmatrix} \end{array}$$

and the matrix **B** of (3.43a) as

$$\mathbf{B} = \begin{array}{c} \\ g''_1 \\ g''_2 \\ g''_3 \\ g''_4 \\ g''_5 \\ g''_6 \\ g''_7 \\ g''_8 \\ g''_9 \end{array} \begin{array}{c} \begin{array}{ccccc} G''_1 & G''_2 & G''_3 & G''_4 & G''_5 \end{array} \\ \begin{bmatrix} 1 & 1 & 1 & 0 & 0 \\ 1 & 1 & 0 & 1 & 0 \\ 1 & 1 & 0 & 0 & 1 \\ 0 & 1 & 1 & 1 & 0 \\ 1 & 0 & 1 & 0 & 1 \\ 1 & 0 & 1 & 1 & 0 \\ 1 & 0 & 0 & 1 & 1 \\ 0 & 1 & 1 & 0 & 1 \\ 0 & 0 & 1 & 1 & 1 \end{bmatrix} \end{array}$$

and it can be shown that rank (**A D B**) = 5 for all diagonal matrices **D** > **0**. Therefore, by Theorem 3.4 the network is element-value-solvable. (Note that if rank **A D B** ≠ 0 for specific **D** > **0** it is almost ≠ 0 for all possible **D** > **0**).

3.2 *Linear Techniques for Element-Value Determination*

We refer to those techniques that involve only the solution of linear systems of equations as the linear techniques for element-value determination.

3.2.1 *Generalized Star-Delta Transformation Technique* [97]

Without loss of generality, we assume that there is only one inaccessible node in the network. Consequently, the transfer admittance $H_j(\phi)$ between any two accessible nodes that are not connected by a free branch has the form

$$H_j(\phi) = \frac{y_{j_1} y_{j_2}}{\Delta} \quad , \quad j_i \in I_{\phi 2} \ , \ j \in I'_m \ , \tag{3.48a}$$

where

$$I'_m = \{1, 2, ..., n'_m\}. \tag{3.48b}$$

Utilizing the transformation of (3.39) and taking the logarithm of (3.48a) we get

$$\log_e H_j(\phi) = \log_e y'_{j_1} + \log_e y'_{j_2} \ , \qquad j_i \in I_{\phi 2} \ , \ j \in I'_m \ , \tag{3.49}$$

which, in matrix form, is given by

$$\log_e \mathbf{H}(\phi) = \mathbf{B} \log_e \mathbf{y}', \tag{3.50}$$

where $\mathbf{B}$ is a $n'_m \times n_{\phi 2}$ matrix consisting of zeros and ones, with exactly two nonzero elements in each row. If there exists a $n_{\phi 2} \times n_{\phi 2}$ nonsingular submatrix of $\mathbf{B}$ the system of equations in (3.50) is solvable and the elements $\mathbf{y}'$ could be obtained. This condition is easily checked by constructing an auxillary graph G.

G contains $n_{\phi 2}$ vertices, each of which corresponds to an element $y'_{j_i}, j_i \in I_{\phi 2}$. Edges in G correspond to equations (3.50). For example, from (3.49), G contains an edge that connects vertices y'_{j_1} and y'_{j_2}. A particular subgraph of G that contains all the vertices of G such that each of the connected components of the subgraph contains exactly one cycle with an odd number of edges (greater than or equal to three) is called a dendroid [136].

Theorem 3.5 [97]: If G contains a dendroid then equations (3.50) are uniquely solvable for the variables $\log_e \mathbf{y}'$.

Due to the logarithmic transformation the elements y'_j can not be uniquely obtained unless more information about the element types, namely, the sign of the real and imaginary parts are known [138]-[139] or in Theorem 3.5, we restrict the dendroid to be connected and to contain exactly one cycle. Obviously, for resistive circuits, where all element-values are real

and positive, we can also obtain unique element solvability from a set of equations corresponding to a disconnected dendroid.

The elimination of an internal node could be viewed as a generalized star-delta transformation [8], [9], [174]. The inverse transformation corresponds to the restoration of the node and all elements incident with the node [35]. The foregoing theorem and the subsequent discussion provides the conditions for such a transformation.

In the general case we will have a number of internal nodes. It is then required to find the element values of the network from measurements at the accessible nodes only. We may assume that the inaccessible nodes in a network are eliminated one by one, in a certain order, and a sequence of networks $N_0, N_1, \ldots, N_{n_t - n_m}$ are obtained, where N_0 is the original network and $N_{n_t - n_m}$ is the final network, which contains accessible nodes only, and whose parameter values can be determined from measurements.

Theorem 3.6 [97]: N_0 can be revived from $N_{n_t - n_m}$ if, for a sequence of all the inaccessible nodes of N_0, N_{k-1} can be revived uniquely from N_k for all $k = 1, 2, \ldots, n_t - n_m$.

The revival of inaccessible nodes is done one by one and the condition for the inverse transformation (Theorem 3.5) is applied to determine, if possible, the element values of $N_{n_t - n_m - 1}$ from $N_{n_t - n_m}$, those of $N_{n_t - n_m - 2}$ from $N_{n_t - n_m - 1}$ and so on until those in N_0 are calculated.

The possibility of reviving N_0 uniquely from $N_{n_t - n_m}$ depends on the order of eliminating the internal nodes. At present, there has not been any suggestions for determining the best order with which all elements can be calculated.

Theorem 3.6 provides a sufficient condition for determining all the element values of a network using only linear equations, without the need of accessing all the nodes.

For the circuit of Fig. 19, after eliminating nodes 5 and 6 successively, we get the circuits N_1 and N_2 shown in Fig. 20a and Fig. 20b, respectively. The elements of the circuit N_2 are measured directly through the accessible nodes. The question is now whether we can revive N_1 from N_2, i.e., revive node 6. In N_1 node 6 is connected to 4 branches G_3, G_5,

$$G_7 = \frac{G_1 G_2}{G_1 + G_2 + G_4} \text{ and } G_8 = \frac{G_2 G_4}{G_1 + G_2 + G_4},$$

which are related to the measurements as follows.

$$y_{24} = \frac{G_3 G_5}{G_3 + G_5 + G_7 + G_8} = G_3' G_5',$$

$$y_{23} = \frac{G_3 G_8}{G_3 + G_5 + G_7 + G_8} = G_3' G_8',$$

$$y_{14} = \frac{G_5 G_7}{G_3 + G_5 + G_7 + G_8} = G_5' G_7',$$

and

$$y_{12} = \frac{G_3 G_7}{G_3 + G_5 + G_7 + G_8} = G_3' G_7'.$$

Using the logarithmic transformation, a linear system of equations results that is similar to (3.50) and is represented by the graph shown in Fig. 20c. This graph is a connected dendroid, therefore from Theorem 3.5 we can revive node 6 and get network N_1 from N_2. Similarly, to restore the original network, we revive node 5, which is connected to branches G_1, G_2 and G_4 in the original network N_0. These branches are related to the measurements as follows.

$$y_{13} - \frac{G_7 G_8}{G_3 + G_5 + G_7 + G_8} = G_9 = \frac{G_1 G_4}{G_1 + G_2 + G_4} = G_1' G_4',$$

$$G_7 = \frac{G_1 G_2}{G_1 + G_2 + G_4} = G_1' G_2',$$

and

$$G_8 = \frac{G_2 G_4}{G_1 + G_2 + G_4} = G_2' G_4'.$$

Note that G_7 and G_8 are obtained after we revived node 6. It is clear from Fig. 20d that the condition of Theorem 3.5 is satisfied, and we can revive node 5 and restore the original network. Note that the last step is equivalent exactly to the well-known delta-star transformation. Ozawa et al. [97] have given examples for active networks.

3.2.2 *Component Simulation Techniques*

If enough information is available about the network, the element values of the network could be evaluated using a linear system of equations. We consider two main cases. The first case utilizes just a single excitation and where both currents and voltages could be measured. The second case considers only voltage measurements, with all nodes of the network assumed accessible.

3.2.2.1 *Single Excitation Element-Value-Evaluation Technique* [123]

Let T be a given tree of the network under test. The branch currents and the branch voltages in T (and its cotree) are denoted by $\mathbf{V}^t(\mathbf{V}^c)$ and $\mathbf{I}^t$ $(\mathbf{I}^c)$, respectively. Accordingly, we may write KCL as

$$\mathbf{Q}\,\mathbf{I}^b = [\mathbf{1}_{n_t}\ \mathbf{Q}_c]\begin{bmatrix}\mathbf{I}^t\\ \mathbf{I}^c\end{bmatrix} = \mathbf{0} \tag{3.51}$$

and KVL as

$$[-\mathbf{Q}_c^T\ \mathbf{1}_{n_c}]\begin{bmatrix}\mathbf{V}^t\\ \mathbf{V}^c\end{bmatrix} = \mathbf{0}\ , \tag{3.52}$$

where $\mathbf{1}_{n_t}$ and $\mathbf{1}_{n_c}$ are unit matrices of appropriate order.

We assume that the measured currents and voltages are related to $\mathbf{I}^c$ and $\mathbf{V}^t$ respectively, with the following transformation.

$$\mathbf{I}^c = \mathbf{A}_1\,\mathbf{I}^m\ , \tag{3.53}$$

$$\mathbf{V}^t = \mathbf{A}_2\,\mathbf{V}^m\ . \tag{3.54}$$

We may directly express $\mathbf{I}^b$ and $\mathbf{V}^b$ in terms of $\mathbf{I}^m$ and $\mathbf{V}^m$ as follows

$$\mathbf{I}^b = \begin{bmatrix}-\mathbf{Q}_c\\ \mathbf{1}_{n_c}\end{bmatrix}\mathbf{A}_1\,\mathbf{I}^m\ , \tag{3.55}$$

$$\mathbf{V}^b = \begin{bmatrix}\mathbf{1}_{n_t}\\ \mathbf{Q}_c^T\end{bmatrix}\mathbf{A}_2\,\mathbf{V}^m\ . \tag{3.56}$$

Therefore, all branch currents and voltages are known and, consequently, all branch admittances of the network could be computed from (3.15). The problem with this approach is that we need n_b simultaneous measurements of voltages and currents. The current measurements are essential and the minimum number required by this approach is equal to the number of fundamental loops of the network, namely, $n_b - n_t$. As such, the approach is not practically attractive and other approaches that utilize nodal voltage measurements only have been developed.

For the passive resistive network of Fig. 21a, the network is excited at node 1 and the nodal voltages V_1^n, V_2^n and V_3^n are measured as well as the branch currents I_2^b and I_4^b. For $I_{in} = 1$ A we have $V_1^n = 5/8$ V, $V_2^n = 2/8$ V, $V_3^n = 1/8$ V, $I_2^b = 3/8$ A and $I_4^b = 1/8$ A. A proper tree of the network is indicated by the solid lines in Fig. 21b and the corresponding incidence matrix is given by

$$\mathbf{Q} = \begin{array}{c} \\ \text{Node 1} \\ \text{Node 2} \\ \text{Node 3} \end{array} \begin{array}{c} \begin{array}{cccccc} G_1 & G_3 & G_5 & I_{in} & G_2 & G_4 \end{array} \\ \begin{bmatrix} 1 & 0 & 0 & -1 & 1 & 0 \\ 0 & 1 & 0 & 0 & -1 & 1 \\ 0 & 0 & 1 & 0 & 0 & -1 \end{bmatrix} \end{array} = [\mathbf{1}_{n_t} \ \mathbf{Q}_c] \ .$$

Therefore, from (3.55) and (3.56) with both $\mathbf{A}_1$ and $\mathbf{A}_2$ being unit matrices of proper orders we have

$$\begin{bmatrix} I_1^b \\ I_3^b \\ I_5^b \\ I_{in}^b \\ I_2^b \\ I_4^b \end{bmatrix} = \begin{bmatrix} 1 & -1 & 0 \\ 0 & 1 & -1 \\ 0 & 0 & 1 \\ 1 & 0 & 0 \\ 0 & 1 & 0 \\ 0 & 0 & 1 \end{bmatrix} \begin{bmatrix} 1 \\ 3/8 \\ 1/8 \end{bmatrix} = \begin{bmatrix} 5/8 \\ 2/8 \\ 1/8 \\ 1 \\ 3/8 \\ 1/8 \end{bmatrix}$$

and

$$\begin{bmatrix} V_1^b \\ V_3^b \\ V_5^b \\ V_{in}^b \\ V_2^b \\ V_4^b \end{bmatrix} = \begin{bmatrix} 1 & 0 & 0 \\ 0 & 1 & 0 \\ 0 & 0 & 1 \\ -1 & 0 & 0 \\ 1 & -1 & 0 \\ 0 & 1 & -1 \end{bmatrix} \begin{bmatrix} 5/8 \\ 2/8 \\ 1/8 \end{bmatrix} = \begin{bmatrix} 5/8 \\ 2/8 \\ 1/8 \\ -5/8 \\ 3/8 \\ 1/8 \end{bmatrix} .$$

Consequently, we find that $G_1 = G_2 = G_3 = G_4 = G_5 = 1.0$ mho and all elements of the network are completely identified.

3.2.2.2 *Multiple Excitation Element-Value-Evaluation Technique*

The basic assumption behind this approach is that all network nodes are accessible [2], [18], [34], [94], [98], [99], [114], [116], [117], [118], [158], [163]. From KCL and (3.18) we may write

$$\mathbf{Q}\,\mathbf{V}_b\,\mathbf{y}^b = \mathbf{I}^n, \tag{3.57a}$$

where

$$\mathbf{V}_b = \text{diag}\,\{V_1^b, V_2^b, \ldots, V_{n_b}^b\} \tag{3.57b}$$

and

$$\mathbf{y}^b = [y_1 \;\; y_2 \cdots y_{n_b}]^T . \tag{3.57c}$$

For multiple excitations $\mathbf{I}_j^n, j = 1, 2, \ldots, k$ at the same frequency we have

$$\begin{bmatrix} \mathbf{Q}\,\mathbf{V}_{b1} \\ \mathbf{Q}\,\mathbf{V}_{b2} \\ \vdots \\ \mathbf{Q}\,\mathbf{V}_{bk} \end{bmatrix} \mathbf{y}^b = \begin{bmatrix} \mathbf{I}_1^n \\ \mathbf{I}_2^n \\ \vdots \\ \mathbf{I}_k^n \end{bmatrix} . \tag{3.58}$$

The number of equations in (3.58) is equal to $k\,n_t$. Therefore, we should have $n_b \leq k\,n_t$. This is a necessary but not sufficient condition for determining $\mathbf{y}^b$. A necessary and sufficient condition is to find n_b independent equations.

Similarly, several frequencies could be utilized to obtain the required independent equations. For passive elements the admittance y_i could be expressed as

$$y_i = (j\omega)^{\alpha_i} \phi_i , \tag{3.59}$$

where $\alpha_i = 0, +1$, or -1 depending on whether the ith branch is a resistor, capacitor or inductor, respectively, and j is the complex square root of -1. Accordingly, (3.57a) becomes

$$\mathbf{Q}\,\overline{\mathbf{V}}_b\,\boldsymbol{\phi} = \mathbf{I}^n , \tag{3.60a}$$

where

$$\overline{\mathbf{V}}_b = \text{diag}\{\overline{V}_1{}^b, \overline{V}_2{}^b, \ldots, \overline{V}_{n_b}{}^b\} \tag{3.60b}$$

and

$$\overline{V}_i{}^b = V_i{}^b (j\omega)^{\alpha_i} \tag{3.60c}$$

is referred to as the modified branch voltage. For k independent excitations at different or the same frequencies we have

$$\begin{bmatrix} \mathbf{Q}\,\overline{\mathbf{V}}_{b1} \\ \mathbf{Q}\,\overline{\mathbf{V}}_{b2} \\ \vdots \\ \mathbf{Q}\,\overline{\mathbf{V}}_{bk} \end{bmatrix} \boldsymbol{\phi} = \begin{bmatrix} \mathbf{I}_1{}^n \\ \mathbf{I}_2{}^n \\ \vdots \\ \mathbf{I}_k{}^n \end{bmatrix} . \tag{3.61}$$

For ladder networks two independent excitations were found necessary and sufficient for the identification of all ladder network branch admittances [18], [163]. We excite the ladder circuit of Fig. 21a twice, once at node 1 and once at node 3. Constructing the system of equations corresponding to (3.57), we get

$$\begin{array}{ccccc} G_1 & G_3 & G_5 & G_2 & G_4 \end{array}$$

$$\begin{bmatrix} 1 & 0 & 0 & 1 & 0 \\ 0 & 1 & 0 & -1 & 1 \\ 0 & 0 & 1 & 0 & -1 \end{bmatrix} \begin{bmatrix} 5/8 & & & & \\ & 2/8 & & \mathbf{0} & \\ & & 1/8 & & \\ & \mathbf{0} & & 3/8 & \\ & & & & 1/8 \end{bmatrix} \begin{bmatrix} G_1 \\ G_3 \\ G_5 \\ G_2 \\ G_4 \end{bmatrix} = \begin{bmatrix} 1 \\ 0 \\ 0 \end{bmatrix}$$

for the excitation at node 1 and

$$\begin{matrix} G_1 & G_3 & G_5 & G_2 & G_4 \end{matrix}$$

$$\begin{bmatrix} 1 & 0 & 0 & 1 & 0 \\ 0 & 1 & 0 & -1 & 1 \\ 0 & 0 & 1 & 0 & -1 \end{bmatrix} \begin{bmatrix} 1/8 & & & & \\ & 2/8 & & 0 & \\ & & 5/8 & & \\ & 0 & & -1/8 & \\ & & & & -3/8 \end{bmatrix} \begin{bmatrix} G_1 \\ G_3 \\ G_5 \\ G_2 \\ G_4 \end{bmatrix} = \begin{bmatrix} 0 \\ 0 \\ 1 \end{bmatrix}$$

for the excitation at node 3. Combining these two systems of equations together we get

$$\begin{bmatrix} 5/8 & 0 & 0 & 3/8 & 0 \\ 0 & 2/8 & 0 & -3/8 & 1/8 \\ 0 & 0 & 1/8 & 0 & -1/8 \\ -- & -- & -- & -- & -- \\ 1/8 & 0 & 0 & -1/8 & 0 \\ 0 & 2/8 & 0 & 1/8 & -3/8 \\ 0 & 0 & 5/8 & 0 & 3/8 \end{bmatrix} \begin{bmatrix} G_1 \\ G_3 \\ G_5 \\ G_2 \\ G_4 \end{bmatrix} = \begin{bmatrix} 1 \\ 0 \\ 0 \\ -- \\ 0 \\ 0 \\ 1 \end{bmatrix},$$

which has 5 independent equations that yield $G_1 = G_2 = G_3 = G_4 = G_5 = 1.0$.

Recalling (3.18), with n_t independent excitations we have

$$\mathbf{Y}_n \mathbf{V}_n = \mathbf{I}_n, \tag{3.62a}$$

where

$$\mathbf{V}_n = [\mathbf{V}_1^n \ \mathbf{V}_2^n \dots \mathbf{V}_{n_t}^n] \tag{3.62b}$$

and

$$\mathbf{I}_n = [\mathbf{I}_1^n \ \mathbf{I}_2^n \dots \mathbf{I}_{n_t}^n]. \tag{3.62c}$$

From (3.62a) the unknown matrix $\mathbf{Y}_n$ is given by

$$\mathbf{Y}_n = \mathbf{V}_n^{-1} \mathbf{I}_n, \tag{3.62d}$$

provided that $\mathbf{V}_n$ is nonsingular. As a consequence of equations (3.62a) and (3.62d) the following theorem gives general sufficient conditions for the identification of $\mathbf{Y}_n$ [20], [21].

Theorem 3.7: If a given linear network can be described by nodal equations and test excitations are chosen in such a way that $\mathbf{I}_n$ is a nonsingular matrix then $\mathbf{V}_n$ is also nonsingular and the solution (3.62d) exists.

One of the possible choices of independent excitations is to apply a unit current consecutively to all n_t nodes, i.e., $\mathbf{I}_n = \mathbf{1}_{n_t}$ [114]. This, however, could be redundant and, in general, the number of necessary and sufficient excitations for identifying all network elements is far less than n_t.

If the passive ladder network of Fig. 21a is excited at nodes 1, 2 and 3, successively, we get

$$\mathbf{V}_n = \begin{bmatrix} 5/8 & 1/4 & 1/8 \\ 1/4 & 1/2 & 1/4 \\ 1/8 & 1/4 & 5/8 \end{bmatrix}.$$

Therefore,

$$\mathbf{Y}_n = \mathbf{V}_n^{-1} = \begin{bmatrix} 2 & -1 & 0 \\ -1 & 3 & -1 \\ 0 & -1 & 2 \end{bmatrix}$$

and immediately we can identify $G_1 = G_2 = G_3 = G_4 = G_5 = 1.0$. Clearly, three excitations are sufficient to identify all network elements although only two of them, as we indicated before, are necessary and sufficient.

3.2.2.3 *Conditions for Sufficient Excitations* [147], [149]

The question of characterizing the minimum number of necessary and sufficient excitations for identifying network elements from node voltage measurements has been addressed utilizing topological and graph theoretical concepts [94], [98], [99], [147], [158]. The basic idea is to identify a sequence of independent cut sets CS_i, $i = 1,2,\ldots,n_t$ such that the

element values of the branches of CS_i, $i = 1, 2, \ldots, n_t$ can be determined sequentially from the node voltage measurements. Obviously, the union of these cut sets would be the total set of network branches, if all element values can be determined sequentially.

Equation (3.62a) can be written in the form [149]

$$\mathbf{V}_n^T \mathbf{Y}_n^T = \mathbf{1}_{n_t} . \tag{3.63}$$

Consider the product $\mathbf{V}_n^T$ and the jth column of $\mathbf{Y}_n^T$. We have

$$\mathbf{V}_n^T \mathbf{y}_j = \begin{bmatrix} (\mathbf{V}_1^n)^T \\ (\mathbf{V}_2^n)^T \\ . \\ . \\ . \\ (\mathbf{V}_{n_t}^n)^T \end{bmatrix} \begin{bmatrix} y_{j1} \\ y_{j2} \\ . \\ . \\ . \\ y_{jn_t} \end{bmatrix} = \mathbf{e}_j , \tag{3.64}$$

where $\mathbf{e}_j$ is a vector with elements zero except at the jth position, where it has a value of one. Some of the elements of $\mathbf{y}_j$ could be known or zeros. Let the k unknown elements of $\mathbf{y}_j$ be identified by the set of indices $I_C = \{i_1, i_2, \ldots, i_k\}$. The set of elements y_{ji}, $i \in I_C$ are called a reduced cut set. Transferring the known terms from the left-hand side to the righ-hand side of (3.64) and adjusting $\mathbf{e}_j$ appropriately we get

$$\mathbf{V}_n^T \begin{bmatrix} \mathbf{0} \\ y_{ji_1} \\ y_{ji_2} \\ . \\ . \\ . \\ y_{ji_k} \\ \mathbf{0} \end{bmatrix} = \mathbf{V}_{nC}^T \mathbf{y}_j^c = \mathbf{e}_j^c , \tag{3.65}$$

where $\mathbf{e}_j^c$ is the modified right-hand side, $\mathbf{y}_j^c$ is the reduced cut set admittance vector and $\mathbf{V}_{nC}^T$ consists of columns I_C from $\mathbf{V}_n^T$. In order to determine $\mathbf{y}_j^c$ we have to find k rows of (3.65) such that the resulting square submatrix of $\mathbf{V}_{nC}^T$ is nonsingular and the corresponding

right hand side vector is nonzero. Let I_B be the index set of these rows. Accordingly, we may write (3.65) as

$$\mathbf{V}_{BC}^{T}\ \mathbf{y}_{j}^{c} = \mathbf{e}_{jB}^{c}, \tag{3.66}$$

where $\mathbf{V}_{BC}{}^{T}$ consists of rows I_B from $\mathbf{V}_{nC}{}^{T}$ and $\mathbf{e}_{jB}{}^{c}$ consists of rows I_B from $\mathbf{e}_{j}^{c}$.

From (3.63) we have

$$\mathbf{V}_{BC}^{T} = (\mathbf{Y}_{n}^{T})_{BC}^{-1}. \tag{3.67}$$

Consequently, the matrix $\mathbf{V}_{BC}{}^{T}$ is nonsingular if and only if $(\mathbf{Y}_n{}^{T})_{BC}{}^{-1}$ is nonsingular. From matrix theory this implies that the matrix $\mathbf{Y}_{\bar{B}\bar{C}}$ obtained by deleting I_B rows and I_C columns from $\mathbf{Y}_n$ is nonsingular. It is to be noted that the I_B rows of $\mathbf{V}_n{}^{T}$ correspond to different excitations applied to the subset of nodes identified by the index set I_B.

Consider a sequence of sets I_{Cj} = j = 1, 2, ..., n_t which corresponds to a sequence of reduced cutsets of the network.

Theorem 3.8 [149]: If independent excitations which are applied at a subset of the network nodes I_A are sufficient for the identification of all elements of $\mathbf{Y}_n$ then

$$\forall\, I_{Cj}\ \exists\, I_{Bj} \subset I_A : |\mathbf{Y}_{\bar{B}j\bar{C}j}| \neq 0. \tag{3.68}$$

The excitation nodes I_A are usually called the injection nodes.

Other graph theoretical conditions for determining parameter values from node-voltage measurements are given in [98], [99] for single and multifrequency measurements. The concept of basis voltages [94] is applied and extended to find the injection nodes as well as the sequence of independent cut sets. Using Theorem 3.8 we can show that excitations at nodes 1 and 3 are sufficient for identification of all elements of the network of Fig. 21a. In this case I_A = {1, 3}. Consider the sequence I_{C1} = {1}, I_{C2} = {3} and I_{C3} = {2} and the corresponding sequence I_{B1} = {1}, I_{B2} = {3} and I_{B3} = {1} such that $I_{Bj} \subset I_A$. Since Theorem 3.8 is sufficient topologically then it is readily clear that $|\mathbf{Y}_{\bar{B}j\bar{C}j}| \neq 0$, j = 1, 2, 3 for almost all values of the network elements G_1, G_2, G_3, G_4 and G_5. It can be zero for only very few specific values of the network elements.

3.2.2.4 *Adjoint Network Approach* [163]

Trick et al. utilized Tellegen's theorem and the adjoint network concept to calculate the component value changes in a circuit from node voltage measurements. The differential form of Tellegen's theorem is given by

$$\sum_{k=1}^{n_b} \left(\hat{V}_k^b \Delta I_k^b - \hat{I}_k^b \Delta V_k^b \right) = - \sum_{j=1}^{n_m} \left(\hat{V}_j^m \Delta I_j^m - \hat{I}_j^m \Delta V_j^m \right) , \tag{3.69}$$

where $\hat{I}_k^{\,b}$, $\hat{I}_j^{\,m}$, $\hat{V}_k^{\,b}$ and $\hat{V}_j^{\,m}$ are the currents and voltages in the adjoint network, which is topologically identical to the original network. $\Delta I_k^{\,b}$ and $\Delta V_k^{\,b}$ are the changes in the n_b network branches due to the changes of the network elements from nominal. $\Delta I_j^{\,m}$ and $\Delta V_j^{\,m}$ are the changes in the n_m port currents and voltages due to the changes of network branches. For a current excited network $\Delta I_j^{\,m} = 0$. For passive networks the change in branch current $\Delta I_k^{\,b}$ is given by

$$\Delta I_k^b = \Delta y_k (V_k^b + \Delta V_k^b) + y_k \Delta V_k^b , \tag{3.70}$$

and the branch constraint for the adjoint network is given by

$$\hat{I}_k^b = y_k \hat{V}_k^b . \tag{3.71}$$

Hence, equation (3.69) becomes

$$\sum_{k=1}^{n_b} (V_k^b + \Delta V_k^b) \hat{V}_k^b \Delta y_k = \sum_{j=1}^{n_m} \Delta V_j^m \hat{I}_j^m . \tag{3.72}$$

In order to evaluate Δy_k we need a set of n_b independent equations of the type (3.72). We can get these equations by using different excitation conditions. However, the maximum number of independent sets of branch voltages at a certain frequency which we can generate in an n_m-port network is no more than n_m [115]. Consequently, the adjoint network concept is used to partition the network elements into subsets containing the smallest number of elements. It is clear from (3.72) that by forcing $\hat{V}_k^{\,b} = 0$ the corresponding change Δy_k will not appear in (3.72). An efficient way to divide the elements is to use the concept of independent cut sets.

Since all the network nodes are accessible we have $n_m = n_t$, the total number of network nodes excluding the reference node. The measurement ports are assumed to be connected between the network nodes and the ground node. As such V_j^m is the voltage of node j. We consider the situation when the cut set is formed of a set of passive elements connected to node ℓ. Let $I_{C\ell}$ be the index set of network elements connected to node ℓ and $I_{B\ell}$ be the index set of the network nodes connected to node ℓ by an element in $I_{C\ell}$.

In the adjoint network we short all nodes to ground except node ℓ, where we connect a unit current source. Then the following conditions hold:

$$\hat{V}_k^b = 0, k \notin I_{C\ell}, \tag{3.73a}$$

$$\hat{V}_{k_1}^b = \hat{V}_{k_2}^b, \forall k_1, k_2 \in I_{C\ell}, \tag{3.73b}$$

$$\hat{V}_\ell^m = \hat{V}_k^b, \forall k \in I_{C\ell}, \tag{3.73c}$$

$$\hat{V}_j^m = 0, j \neq \ell, \tag{3.73d}$$

$$\hat{I}_j^m = \hat{V}_\ell^m y_{k_j}, j \in I_{B\ell}, k_j \in I_{C\ell} \tag{3.73e}$$

$$\hat{I}_\ell^m = - \hat{V}_\ell^m \sum_k y_k, \; k \in I_{C\ell}, \tag{3.73f}$$

where y_{k_j} connects node j to note ℓ. Consequently, (3.72) becomes

$$\sum_{k \in I_{C\ell}} (V_k^b + \Delta V_k^b) \Delta y_k = - \Delta V_\ell^m \sum_{k \in I_{C\ell}} y_k + \sum_{j \in I_{B\ell}} \Delta V_j^m y_{k_j}, \tag{3.74a}$$

$$= - \sum_{k \in I_{C\ell}} \Delta V_k^b y_k. \tag{3.74b}$$

Equation (3.74) can also be derived by inspection from (3.70), applying KCL at node ℓ for the circuit under test with unknown parameters and with the known nominal values.

For a number of independent excitation conditions equal to the cardinality of $I_{C\ell}$ we can solve for the parameters Δy_k, $k \in I_{C\ell}$. The approach can be easily extended to active networks using single and multiple frequencies similarly to the approach outlined in 3.2.2.2.

For the ladder network of Fig. 21a we consider the three adjoint networks shown in Fig. 22. Utilizing the adjoint network of Fig. 22a we have $\ell = 1$ and we may write the equation corresponding to (3.74) as

$$(V_1^b + \Delta V_1^b)\,\Delta G_1 + (V_2^b + \Delta V_2^b)\,\Delta G_2 = -\,(\Delta V_1^b G_1 + \Delta V_2^b G_2)\,.$$

This equation contains two unknowns ΔG_1 and ΔG_2. Therefore, two independent excitations are required, namely, exciting nodes 1 and 3 to form two equations in two unknowns, since all branch voltages are assumed known. For the adjoint network of Fig. 22b we have $\ell = 3$ and we may write the following equation

$$-(V_4^b + \Delta V_4^b)\,\Delta G_4 + (V_5^b + \Delta V_5^b)\,\Delta G_5 = -\,(-\Delta V_4^b G_4 + \Delta V_5^b G_5)\,.$$

Again, the same two excitations are needed to solve for ΔG_4 and ΔG_5. Finally for the adjoint network of Fig. 22c we have $\ell = 2$, and we may write

$$-(V_2^b + \Delta V_2^b)\,\Delta G_2 + (V_3^b + \Delta V_3^b)\,\Delta G_3 + (V_4^b + \Delta V_4^b)\,\Delta G_4$$
$$= -\,(-\Delta V_2^b G_2 + \Delta V_3^b G_3 + \Delta V_4^b G_4)\,,$$

which has three unknowns ΔG_2, ΔG_3 and ΔG_4. But, since we have already solved for ΔG_2 and ΔG_4 only one excitation is required to get ΔG_3. Note that if we had started with node 2 we would have needed three independent excitations instead of two. This emphasizes the importance of choosing the sequence of nodes (or, more generally, the sequence of cut sets).

3.2.2.5 *Conditions for Measuring a Particular Element* [82]

Trick et al. [163] and Mayeda et al. [82] have given the conditions for measuring an element in passive networks.

Theorem 3.9 [163]: Consider an element which is connected between accessible nodes ℓ_1 and ℓ_2 in a passive network. The measurement of the admittance of this element is possible if and only if each path in the circuit from node ℓ_1 to node ℓ_2 (excluding the path through the element) contains at least one accessible node.

Based on this result some practical techniques for measuring specific circuit elements are implemented [124]. In [163] a scheme that utilizes an operational amplifier requires only one measurement. It is very easy to implement using ATE for in-circuit component measurement.

IV. FAULT VERIFICATION TECHNIQUES

Practically, the number of performed measurements n_m is less than the number of network elements n_Φ. Also, it is quite realistic to assume that the number of faulty elements n_f is very small such that the inequality $n_f < n_m < n_\Phi$ holds. A number of techniques have been proposed to address the problem of locating the faulty elements utilizing a limited number of measurements. We discuss in this section the techniques that are based upon checking the consistency of certain equations which are invariant on the changes in the faulty elements [36], [47], [60], [93], [112], [150], [155]. Unless otherwise stated, the network is assumed excited once and only voltage measurements are performed.

4.1 *Substitution Theorem Technique*

The change of value of a component with respect to nominal can be represented by either a current or a voltage source in parallel or in series, respectively, with the component [3], [148].

4.1.1 *Node-Fault Diagnosis* [57]

Without loss of generality, we assume that the changes are represented by current sources only, $\Delta\mathbf{I}^{bf}$. For linear networks, and using the superposition theorem, we may write

$$\mathbf{Y}_n \Delta\mathbf{V}^n = \mathbf{Q}\,\Delta\mathbf{I}^{bf} = \Delta\mathbf{I}^{nf}, \tag{4.1}$$

where $\Delta\mathbf{I}^{nf}$ represents the faulty nodal currents.

Assumption 4.1 [57]: Node i is faulty if and only if the ith component of $\Delta\mathbf{I}^{nf}$ is nonzero.

For n_f faulty nodes, we may write (4.1) after appropriate rearrangement as

$$\begin{bmatrix} \Delta\mathbf{V}^m \\ \Delta\mathbf{V}^{n-m} \end{bmatrix} = \mathbf{Y}_n^{-1}\Delta\mathbf{I}^{nf} = \begin{bmatrix} \mathbf{Z}_{mn} \\ \mathbf{Z}_{n-m,n} \end{bmatrix} \Delta\mathbf{I}^{nf}, \tag{4.2a}$$

$$= \begin{bmatrix} \mathbf{Z}_{mf} & \mathbf{Z}_{m,n-f} \\ \mathbf{Z}_{n-m,f} & \mathbf{Z}_{n-m,n-f} \end{bmatrix} \begin{bmatrix} \Delta\mathbf{I}^f \\ \mathbf{0} \end{bmatrix}. \tag{4.2b}$$

Hence,

$$\Delta \mathbf{V}^m = \mathbf{Z}_{mf} \Delta \mathbf{I}^f, \tag{4.2c}$$

where $\Delta \mathbf{I}^f$ is the nonzero part of $\Delta \mathbf{I}^{nf}$ and consists of n_f components. Since $n_m > n_f$, (4.2c) is an overdetermined system of equations. The least-squares solution of (4.2c) is given by

$$\Delta \mathbf{I}^f = [\mathbf{Z}_{mf}^T \mathbf{Z}_{mf}]^{-1} \mathbf{Z}_{mf}^T \Delta \mathbf{V}^m. \tag{4.3}$$

Therefore, eliminating $\Delta \mathbf{I}^f$, we get [19]

$$[\mathbf{Z}_{mf}(\mathbf{Z}_{mf}^T \mathbf{Z}_{mf})^{-1} \mathbf{Z}_{mf}^T - \mathbf{1}_{n_m}] \Delta \mathbf{V}^m = \mathbf{0}. \tag{4.4}$$

Equation (4.4) gives us a relationship between the measured voltages when all the nodes of the network are nonfaulty except those corresponding to $\Delta \mathbf{I}^f$. In a network, a node is faulty if any of the network elements incident with it is faulty. Also, (4.4) provides a necessary condition for isolating the faulty nodes. It is independent of the values of the faulty currents $\Delta \mathbf{I}^f$ and depends only on their location.

The faulty nodes can be uniquely located, utilizing the concepts developed by Huang, Lin and Liu in [56], [57] and verified in [154] concerning the testability of the network.

Definition 4.1 [57]: A network is said to be n_f-node fault testable if one will be able to determine from the measurements on accessible nodes:

1) whether or not the network has no more than n_f node faults.

2) if affirmative, whether the faulty nodes can be uniquely located.

The n_f faulty nodes are uniquely located if the following rank test, which is known as the n_f-node-fault testability condition, is satisfied.

$$\text{Rank}[\mathbf{Z}_{mq}] = n_f + 1 \tag{4.5}$$

for all possible q, where q refers to $(n_f + 1)$ columns of $\mathbf{Z}_{mn}$.

For linear passive networks topological conditions exist for checking the satisfaction of (4.5) [57].

Theorem 4.1: The network is n_f-node testable if and only if there exist at least $n_f + 1$ independent paths from any inaccessible node to $n_f + 1$ accessible measurement nodes of the network. (The ground reference node is deleted from the network.)

Two paths are independent if they do not have any common node, except at the terminal node. Theorem 4.1 provides a very simple topological condition. It can be used for designing for testability by adding accessible measurement nodes until the condition in the theorem is satisfied. For active networks, some necessary and almost sufficient topological conditions are given in [145], [146]. The conditions are derived in terms of the Coates flow graph. It is to be noted that the topological conditions are sufficient under the assumption that there is no relation between the elements of the network. For specific values of the network elements they could fail. Therefore, the algebraic conditions are more universal.

If $n_m < n_f$ we could still locate a fault region that is defined as any set of n_w nodes which contains the n_f faulty nodes with $n_m > n_w$. This approach has been followed in [146], where necessary and sufficient conditions as well as a topological algorithm for isolating the fault regions have been presented.

For the simple ladder network of Fig. 21a, if nodes 1 and 3 are the measurement nodes, then $n_m = 2$ and we can at most locate a single faulty node uniquely. Constructing equation (4.2a) using the nominal element values of the network, we get

$$\begin{bmatrix} \Delta V_1^m \\ \Delta V_3^m \\ \Delta V_2^{n-m} \end{bmatrix} = 1/8 \begin{bmatrix} 5 & 2 & 1 \\ 1 & 2 & 5 \\ 2 & 4 & 2 \end{bmatrix} \Delta \mathbf{I}^{nf}.$$

Since every 2 columns of $\mathbf{Z}_{mn}$ are linearly independent, the network is 1-node fault testable.

Now, let us assume that a fault has occurred such that $\Delta V_1{}^m = \Delta V_3{}^m = 1/24$ and it is required to find which of the nodes 1, 2 or 3 is faulty. We construct equation (4.4) for the three possible nodes and check which one will yield $\mathbf{0}$. For node 1 we have

$$\left[\begin{bmatrix} 5 \\ 1 \end{bmatrix}\left[\begin{bmatrix} 5 & 1 \end{bmatrix}\begin{bmatrix} 5 \\ 1 \end{bmatrix}\right]^{-1}\begin{bmatrix} 5 & 1 \end{bmatrix} - \begin{bmatrix} 1 & 0 \\ 0 & 1 \end{bmatrix}\right]\begin{bmatrix} 1/24 \\ 1/24 \end{bmatrix} = \begin{bmatrix} 1/156 \\ -5/156 \end{bmatrix} \neq \mathbf{0}.$$

For node 2 we have

$$\left[\begin{bmatrix}2\\2\end{bmatrix}\begin{bmatrix}2 & 2\end{bmatrix}\begin{bmatrix}2\\2\end{bmatrix}\right]^{-1}\begin{bmatrix}2 & 2\end{bmatrix}-\begin{bmatrix}1 & 0\\0 & 1\end{bmatrix}\left]\begin{bmatrix}1/24\\1/24\end{bmatrix}\right.=\begin{bmatrix}0\\0\end{bmatrix}=\mathbf{0}.$$

For node 3 we get

$$\left[\begin{bmatrix}1\\5\end{bmatrix}\begin{bmatrix}1 & 5\end{bmatrix}\begin{bmatrix}1\\5\end{bmatrix}\right]^{-1}\begin{bmatrix}1 & 5\end{bmatrix}-\begin{bmatrix}1 & 0\\0 & 1\end{bmatrix}\left]\begin{bmatrix}1/24\\1/24\end{bmatrix}\right.=\begin{bmatrix}-5/156\\1/156\end{bmatrix}\neq\mathbf{0}.$$

It is clear that node 2 is the faulty node since (4.4) is only satisfied for node 2 and the algebraic 1-node-fault testability condition (4.5) is satisfied. Solving for ΔI_2^f using (4.3), we get $\Delta I_2^f = 1/6$.

For the network of Fig. 21a, we have just one inaccessible node, and it is clear that there are two separate paths from node 2 to the measurement nodes 1 and 3, respectively. Therefore, Theorem 4.1, which provides us with the topological testability condition, is satisfied.

4.1.2 *Branch-Fault Diagnosis* [66]

It is clear that a faulty two-terminal element affects two nodes, thus we may have some redundancy. This could be addressed by either reducing the number of unknowns as reported in [146] or we may address the more difficult problem of isolating faulty branches [17], [19]. Recalling (4.1), we have

$$\begin{bmatrix}\Delta\mathbf{V}^m\\ \Delta\mathbf{V}^{n-m}\end{bmatrix}=\mathbf{Y}_n^{-1}\mathbf{Q}\,\Delta\mathbf{I}^{bf}=\begin{bmatrix}\mathbf{Z}_{mb}\\ \mathbf{Z}_{n-m,b}\end{bmatrix}\Delta\mathbf{I}^{bf} \tag{4.6}$$

and equations similar to (4.3) and (4.4) for faulty branch currents could be derived [19].

For a linear network, Lin, Huang and Liu [66] developed the condition for uniquely identifying any n_f faulty branches, namely, the n_f-branch-fault testability condition. The network is n_f-branch-fault testable if every $n_f + 1$ columns of $\mathbf{Z}_{mb}$ are linearly independent. Topologically, this implies that if the network contains loops consisting of a number of elements less than or equal to $n_f + 1$, then the network is not n_f-branch-fault testable [148].

More rigorously, necessary conditions have been given in [148] and necessary and almost sufficient conditions for linear passive networks are given in [64]–[66].

Theorem 4.2: Let Q be a set of $(n_f + 1)$ branches and $\mathbf{Z}_{mq}$ be the $n_m x(n_f + 1)$ submatrix of $\mathbf{Z}_{mb}$ whose columns correspond to branches in Q. Then $\mathbf{Z}_{mq}$ has full column rank only if there exists a tree T such that

1) T contains Q,

2) $(T–Q)$ is connected when all accessible nodes are shorted to the ground.

The converse is also true for almost all values of the network parameters ϕ.

Lin et al. [66] have derived topological conditions to check the n_f-branch-fault testability condition.

Theorem 4.3: The network is n_f-branch-fault testable if and only if there exist at least $n_f + 2$ independent paths from any inaccessible node to $n_f + 2$ accessible measurement nodes that could include the ground reference node.

Recalling the simple ladder circuit example of Fig. 21a, we find that the inaccessible node 2 is connected to the measurement nodes 1 and 3, as well as the ground node by three separate paths. Therefore, the network is single-branch-fault testable. Also, constructing (4.6) we get

$$\begin{matrix} & G_1 & G_2 & G_3 & G_4 & G_5 \end{matrix}$$

$$\mathbf{Z}_{mb} = \frac{1}{8}\begin{bmatrix} 5 & 3 & 2 & 1 & 1 \\ 1 & -1 & 2 & -3 & 5 \end{bmatrix},$$

which clearly identifies that every two columns are linearly independent. In fact, if $\Delta V_1^m = 3/8$ and $\Delta V_2^m = -1/8$, we find that the algebraic fault invariant equations, similar to (4.4), are only satisfied for G_2.

The adjoint network approach that is outlined in Section 3.2.2.4 could be utilized to get equations similar to (4.6). Since the theoretical implications would be the same, we do not elaborate further on the adjoint network approach [23], [124], [125], [159], [161], [162], [164].

4.1.3 *Calculation of Faulty Element Values*

Node-fault isolation has been developed to overcome the difficulty in uniquely identifying the faulty branches [19]. Using multiple excitations [57], [147], the faulty branches could easily be identified after isolating the faulty nodes. This is a very efficient way of utilizing the identification technique presented in Section 3.2.2.2, without the need for measuring all voltage nodes; in fact, the inaccessible node voltages are computed using (4.2) and (4.3) as

$$\Delta \mathbf{V}^{n-m} = \mathbf{Z}_{n-m,f}[\mathbf{Z}_{mf}^{T}\,\mathbf{Z}_{mf}]^{-1}\,\mathbf{Z}_{mf}^{T}\,\Delta \mathbf{V}^{m}. \tag{4.7}$$

Topological conditions for identifying remote inaccessible subnetworks using multiple excitations at a subset of the accessible nodes, injection nodes, are given in [147]. Other conditions are given in [56]. From the theory of perturbation, we have

$$\Delta \mathbf{I}^{nf} = -\Delta \mathbf{Y}_{n}[\mathbf{V}^{n} + \Delta \mathbf{V}^{n}] = -\mathbf{Q}\Delta \mathbf{Y}_{b}\,\mathbf{Q}^{T}[\,\mathbf{V}^{n} + \Delta \mathbf{V}^{n}]. \tag{4.8}$$

Consequently, and similar to (3.57a), we have

$$\Delta \mathbf{I}^{f} = -\mathbf{Q}_{f}(\mathbf{V}_{b}^{f} + \Delta \mathbf{V}_{b}^{f})\,\Delta \mathbf{y}^{bf}, \tag{4.9}$$

where $\mathbf{Q}_f$, $\mathbf{V}_b{}^f$ and $\Delta\mathbf{y}^{bf}$ are submatrices of $\mathbf{Q}$, $\mathbf{V}_b$ and $\Delta\mathbf{y}^{b}$ (see (3.57)) that are associated with the faults. For multiple excitations, we can construct a system like (3.58) and solve for $\Delta\mathbf{y}^{bf}$.

The substitution theorem technique is based on checking whether a certain subset of network elements could be faulty or not. Therefore, it is usually referred to as a fault verification technique. The technique has the advantage of reducing the requirements on test points. $n_m = n_f + 1$ measurement nodes are necessary and in many cases sufficient for the unique isolation of n_f faulty nodes or branches. Also, for linear networks, all computations involved are linear and rely only on the nominal network parameters. Moreover, the n_f-testability conditions (to ensure the uniqueness of the identified faults) depend only on the graph of the network, not its element values.

4.2 *Failure Bound Techniques*

For a network with n_Φ elements, n_f of them faulty, the number of different combinations considered by the fault verification technique of Section 4.1.2 will be equal to

$$\binom{n_\Phi}{n_f}.$$

For large networks, this number is enormous and the required computations will be prohibitive.

4.2.1 *Combinatorial Technique* [146]

It is evident from Section 4.1.2 that if we have n_m independent measurements, then the maximum number of faulty elements which we can identify is equal to $n_m - 1$. Based on the assumption that n_f^* is the maximum number of faulty elements, we divide the elements into n_k subsets such that the cardinality of each subset is equal to the integer part of $(n_m - 1)/n_f^*$. Taking a combination of n_f^* subsets, the total number of elements in the resultant set will be less than or equal to $n_m - 1$, and we can apply the fault verification technique of Section 4.1.2 to check whether this set contains the n_f faulty elements. It is clear then, that following this procedure, the number of combinations to be considered is reduced to

$$\binom{n_k}{n_f^*}.$$

4.2.2 *Heuristic Technique*

Wu et al. [177] have introduced a fault diagnosis algorithm under the assumption of a bound on the number of faults n_f^* and Liu's heuristic assumption that the effect of two independent analog failures will never cancel. This is an inherently analog heuristic since two binary failures have a fifty-fifty chance of cancelling one another. In the analog case, however, two independent failures are highly unlikely to cancel one another. Their algorithm, applicable to linear as well as nonlinear networks, has the following structure.

Step 1 Partition the network elements into two subsets. Assume that the subset 1 elements are good. Using the meausrement data and the characteristics of the elements of subset 1, determine the inputs and outputs of the elements of subset 2.

Comment The number of subset 2 elements should be greater than n_f^* and less than the number of measurements n_m.

Step 2 Test each element in subset 2 by determining if the inputs and outputs of the elements are consistent with the nominal characteristics. The elements with inputs and outputs consistent with nominal values are assumed good. No decision is possible for the rest of the subset 2 elements.

Comment If all elements of subset 1 are actually good, then the results for all subset 2 elements should be reliable. Since this is not the case, we invoke the heuristic assumption which leads to the result of Step 2.

Step 3 Repartition the elements, transferring all elements that are found to be good into subset 1. Go to Step 2 and continue the process until the subset 1 elements are entirely good.

The number of steps required is determined by the number of elements which could be tested in one step and the bound on the maximum number of simultaneous faults. Therefore, the procedure yields a natural set of tradeoffs between the number of measurements, simultaneous faults and steps required by the algorithm.

To accelerate the speed of convergence, a coupling table was introduced. This coupling table (generated by sensitivity analysis) indicates whether or not a faulty element of subset 1 will affect the test results on an element of subset 2 (i.e., whether or not they are coupled). If an element in subset 2 is found good, then all elements in subset 1 that are coupled to it are also good.

For linear networks, let the element equations of subset 1 be given by

$$\mathbf{Y}_{b1}\,\mathbf{V}^{b1} = \mathbf{I}^{b1} \tag{4.10a}$$

and those of subset 2 be given by

$$\mathbf{Y}_{b2}\,\mathbf{V}^{b2} = \mathbf{I}^{b2}. \tag{4.10b}$$

We may write KCL and KVL for the network in the form

$$\mathbf{Q}_{m1}\,\mathbf{I}^{b1} + \mathbf{Q}_{m2}\,\mathbf{I}^{b2} = \mathbf{I}^{m}, \tag{4.11a}$$

$$\mathbf{Q}_{n-m,1}\,\mathbf{I}^{b1} + \mathbf{Q}_{n-m,2}\,\mathbf{I}^{b2} = \mathbf{0}, \tag{4.11b}$$

$$\mathbf{Q}^{T}_{m1}\,\mathbf{V}^{m} + \mathbf{Q}^{T}_{n-m,1}\,\mathbf{V}^{n-m} = \mathbf{V}^{b1}, \tag{4.11c}$$

$$\mathbf{Q}^{T}_{m2}\,\mathbf{V}^{m} + \mathbf{Q}^{T}_{n-m,2}\,\mathbf{V}^{n-m} = \mathbf{V}^{b2}, \tag{4.11d}$$

where the incidence matrix $\mathbf{Q}$ is partitioned as

$$\mathbf{Q} = \begin{bmatrix} \mathbf{Q}_{m1} & \mathbf{Q}_{m2} \\ \mathbf{Q}_{n-m,1} & \mathbf{Q}_{n-m,2} \end{bmatrix} \tag{4.12}$$

and subscripts 1 and 2 refer to subset 1 and subset 2 elements, respectively.

Equations (4.10a) and (4.11) can be represented in tableau form as follows.

$$\begin{bmatrix} \mathbf{Q}_{m1}\,\mathbf{Y}_{b1} & \mathbf{0} & \mathbf{Q}_{m2} & \mathbf{0} \\ \mathbf{Q}_{n-m,1}\,\mathbf{Y}_{b1} & \mathbf{0} & \mathbf{Q}_{n-m,2} & \mathbf{0} \\ -\mathbf{1}_{n_{b1}} & \mathbf{Q}^{T}_{n-m,1} & \mathbf{0} & \mathbf{0} \\ \mathbf{0} & \mathbf{Q}^{T}_{n-m,2} & \mathbf{0} & -\mathbf{1}_{n_{b2}} \end{bmatrix} \begin{bmatrix} \mathbf{V}^{b1} \\ \mathbf{V}^{n-m} \\ \mathbf{I}^{b2} \\ \mathbf{V}^{b2} \end{bmatrix} = \begin{bmatrix} \mathbf{I}^{m} \\ \mathbf{0} \\ -\mathbf{Q}^{T}_{m1}\mathbf{V}^{m} \\ -\mathbf{Q}^{T}_{m2}\,\mathbf{V}^{m} \end{bmatrix}. \tag{4.13}$$

One may further eliminate the unknown variables $\mathbf{V}^{b1}$ and $\mathbf{V}^{n-m}$ and solve the resultant equations to get $\mathbf{I}^{b2}$ and $\mathbf{V}^{b2}$. In general, this is possible under the condition of the existence of a left inverse of the matrix $\mathbf{Q}_{m2}$, which in turn determines the allowable element subdivisions. After some mathematical manipulations, we may write

$$\mathbf{I}^{b2} = -\mathbf{Q}^{-L}_{m2}\mathbf{Q}_{m1}\,\mathbf{Y}_{b1}\,\mathbf{Q}^{T}_{n-m,1}\,\mathbf{V}^{n-m} + \mathbf{Q}^{-L}_{m2}[\mathbf{I}^{m} - \mathbf{Q}_{m1}\,\mathbf{Y}_{b1}\mathbf{Q}^{T}_{m1}\,\mathbf{V}^{m}], \tag{4.14a}$$

$$\mathbf{V}^{b2} = \mathbf{Q}^{T}_{m2}\mathbf{V}^{m} + \mathbf{Q}^{T}_{n-m,2}\,\mathbf{V}^{n-m}, \tag{4.14b}$$

where $\mathbf{Q}_{m2}{}^{-L}$ is the desired left inverse and

$$\mathbf{V}^{n-m} = -[\mathbf{Q}_{n-m,1}\,\mathbf{Y}_{b1}\,\mathbf{Q}^{T}_{n-m,1} - \mathbf{Q}_{n-m,2}\mathbf{Q}^{-L}_{m2}\mathbf{Q}_{m1}\mathbf{Y}_{b1}\mathbf{Q}^{T}_{n-m,1}]^{-1}$$

$$\cdot\ [\mathbf{Q}_{n-m,1}\,\mathbf{Y}_{b1}\,\mathbf{Q}_{m1}^{T}\,\mathbf{V}_{m} + \mathbf{Q}_{n-m,2}\,\mathbf{Q}_{m2}^{-L}[\mathbf{I}^{m} - \mathbf{Q}_{m1}\,\mathbf{Y}_{b1}\,\mathbf{Q}_{m1}^{T}\,\mathbf{V}^{m}]] \ . \tag{4.14c}$$

Although the expressions appear to be foreboding, they may all be computed off-line and stored in a database to be retrieved at the time of conducting the testing procedure. Therefore, the only on-line computation required for fault diagnosis of linear networks is the matrix by vector multiplication indicated by (4.14). Using the nominal element values and $\mathbf{V}^{b2}$ of (4.14b), we compute

$$\bar{\mathbf{I}}^{b2} = \mathbf{Y}_{b2}\,\mathbf{V}^{b2} \tag{4.15}$$

and compare $\bar{\mathbf{I}}^{b2}$ with $\mathbf{I}^{b2}$ of (4.14a). If $|\bar{I}_i^{b2} - I_i^{b2}|$ is less than or equal to a predetermined threshold, the ith element is good, otherwise, it is faulty [176].

As an illustration of this technique, we consider the ladder network example of Fig. 21a under the assumption that $n_f^* = 1$ and all nodes are assumed accessible, i.e., $\mathbf{V}^{n-m}$ is empty and $V_1^m = 2/3$, $V_2^m = 1/3$ and $V_3^m = 1/6$. The diagnosis procedure could be summarized in the following steps.

Step 1 Subset 1 contains G_3, G_4 and G_5 and subset 2 contains G_1 and G_2. Therefore,

$$\mathbf{Q}_{m1} = \begin{bmatrix} 0 & 0 & 0 \\ 1 & 1 & 0 \\ 0 & -1 & 1 \end{bmatrix}, \qquad \mathbf{Q}_{m2} = \begin{bmatrix} 1 & 1 \\ 0 & -1 \\ 0 & 0 \end{bmatrix}$$

and

$$\mathbf{Q}_{m2}^{-L} = \begin{bmatrix} 1 & 1 & 0 \\ 0 & -1 & 0 \end{bmatrix}.$$

Substituting in (4.14) with $\mathbf{I}^m = [1\ \ 0\ \ 0]^T$, we get

$$\begin{bmatrix} I_{G_1}^b \\ I_{G_2}^b \end{bmatrix} = \begin{bmatrix} 1/2 \\ 1/2 \end{bmatrix}, \qquad \begin{bmatrix} V_{G_1}^b \\ V_{G_2}^b \end{bmatrix} = \begin{bmatrix} 2/3 \\ 1/3 \end{bmatrix},$$

which implies that both G_1 and G_2 are faulty, but this contradicts the maximum failure bound, therefore we consider them not faulty and place them into subset 1.

Step 2 Subset 1 contains G_1, G_2 and G_4 and subset 2 contains G_3 and G_5. Therefore,

$$\mathbf{Q}_{m1} = \begin{bmatrix} 1 & 1 & 0 \\ 0 & -1 & 1 \\ 0 & 0 & -1 \end{bmatrix}, \qquad \mathbf{Q}_{m2} = \begin{bmatrix} 0 & 0 \\ 1 & 0 \\ 0 & 1 \end{bmatrix}$$

and

$$\mathbf{Q}_{m2}^{-L} = \begin{bmatrix} 0 & 1 & 0 \\ 0 & 0 & 1 \end{bmatrix}.$$

Substituting in (4.14), we get

$$\begin{bmatrix} I^b_{G_3} \\ I^b_{G_5} \end{bmatrix} = \begin{bmatrix} 1/6 \\ 1/6 \end{bmatrix}, \qquad \begin{bmatrix} V^b_{G_3} \\ V^b_{G_5} \end{bmatrix} = \begin{bmatrix} 1/3 \\ 1/6 \end{bmatrix},$$

which implies that G_5 is good element and we do not know whether G_3 is faulty or not since subset 1 contains G_4, which could be faulty.

Step 3 Subset 1 contains G_1, G_2 and G_5 and all are known to be nonfaulty. Therefore, the results of this step are completely reliable. Subset 2 contains G_3 and G_4. Therefore,

$$\mathbf{Q}_{m1} = \begin{bmatrix} 1 & 1 & 0 \\ 0 & -1 & 0 \\ 0 & 0 & 1 \end{bmatrix}, \qquad \mathbf{Q}_{m2} = \begin{bmatrix} 0 & 0 \\ 1 & 1 \\ 0 & -1 \end{bmatrix}$$

and

$$\mathbf{Q}_{m2}^{-L} = \begin{bmatrix} 0 & 1 & 1 \\ 0 & 0 & -1 \end{bmatrix}.$$

Substituting in (4.14), we get

$$\begin{bmatrix} I^b_{G_3} \\ I^b_{G_4} \end{bmatrix} = \begin{bmatrix} 1/6 \\ 1/6 \end{bmatrix}, \qquad \begin{bmatrix} V^b_{G_3} \\ V^b_{G_4} \end{bmatrix} = \begin{bmatrix} 1/3 \\ 1/6 \end{bmatrix},$$

which implies that G_4 is nonfaulty and G_3 is the only faulty element, which is a correct conclusion.

In [38], the failure bound technique is implemented in the tableau context. Also, in [49], the theory of analog system t-fault diagnosability has been developed to provide theoretical characterization of the failure bound technique.

4.3 *Network Decomposition Approach* [126]-[128]

This technique utilizes network decomposition in isolating the fault to within a small subnetwork. A large network could be viewed as a set of mutually uncoupled subnetworks that are connected at the nodes of decomposition. Without loss of generality, we assume that all subnetworks are grounded. The input-output relation of the ith subnetwork S_i is given by

$$\mathbf{I}^{m_i} = \mathbf{h}^{m_i}(\mathbf{V}^{m_i}, \boldsymbol{\phi}_i), \tag{4.16}$$

where $\boldsymbol{\phi}_i$ is the vector of the subnetwork parameters and $\mathbf{I}^{m_i}$ and $\mathbf{V}^{m_i}$ are the currents and voltages of the external nodes of the subnetwork. Let

$$M_i = M_{i\alpha} \cup M_{i\beta} \cup M_{i\gamma} \cup M_{i\delta}, \tag{4.17}$$

where $M_{i\alpha}$ is the set of nodes where both voltages and currents are known, $M_{i\beta}$ is the set of nodes where only voltages are known, $M_{i\gamma}$ is the set of nodes where only currents are known, $M_{i\delta}$ is the set of nodes were neither currents nor voltages are known, and M_i is the set of all external nodes of the subnetwork not including the ground node. Accordingly, we may write (4.16) as

$$\mathbf{I}^{m_{i\alpha}} = \mathbf{h}^{m_{i\alpha}}(\mathbf{V}^{m_{i\alpha}}, \mathbf{V}^{m_{i\beta}}, \mathbf{V}^{m_{i\gamma}}, \mathbf{V}^{m_{i\delta}}, \boldsymbol{\phi}_i), \tag{4.18a}$$

$$\mathbf{I}^{m_{i\beta}} = \mathbf{h}^{m_{i\beta}}(\mathbf{V}^{m_{i\alpha}}, \mathbf{V}^{m_{i\beta}}, \mathbf{V}^{m_{i\gamma}}, \mathbf{V}^{m_{i\delta}}, \boldsymbol{\phi}_i), \tag{4.18b}$$

$$\mathbf{I}^{m_{i\gamma}} = \mathbf{h}^{m_{i\gamma}}(\mathbf{V}^{m_{i\alpha}}, \mathbf{V}^{m_{i\beta}}, \mathbf{V}^{m_{i\gamma}}, \mathbf{V}^{m_{i\delta}}, \boldsymbol{\phi}_i), \tag{4.18c}$$

$$\mathbf{I}^{m_{i\delta}} = \mathbf{h}^{m_{i\delta}}(\mathbf{V}^{m_{i\alpha}}, \mathbf{V}^{m_{i\beta}}, \mathbf{V}^{m_{i\gamma}}, \mathbf{V}^{m_{i\delta}}, \boldsymbol{\phi}_i). \tag{4.18d}$$

4.3.1 *Testing Conditions*

If the cardinality of the set $M_{i\alpha}$ is greater than the cardinality of the set $M_{i\delta}$, a necessary condition for the subnetwork to be faulty free is that (4.18a) and (4.18c) constitute a consistent system of overdetermined equations with $\boldsymbol{\phi}_i$ assuming nominal values $\boldsymbol{\phi}_i^0$. If the external nodes do not decompose the subnetwork further, then the condition is also almost sufficient. This condition is referred to as the internal-self-testing condition (ISTC). In general, the nodes of decomposition are chosen among the set of nodes where voltage

measurements can be performed. When all the voltages of M_i are known and the cardinality of the set M_{ia} is greater than or equal to one, the subnetwork will be fault free if and only if

$$\mathbf{I}^{m_{ia}} - \mathbf{h}^{m_{ia}}(\mathbf{V}^{m_i}, \boldsymbol{\phi}_i^0) = \mathbf{0}. \tag{4.19}$$

This is known as the self-testing condition (STC). Practically, it is difficult to measure the currents $\mathbf{I}^{m_{ia}}$, except when they represent the input excitations to the whole network. The application of KCL and topological relations overcomes this difficulty. The currents are not measured: they are computed using the nominal parameter values together with the measured voltages, then KCL is invoked. Under the assumption that the heuristic assumption holds (the effect of two faults will not cancel), we have the following results.

Lemma 4.1: Mutual-Testing Condition (MTC) [128] A necessary and almost sufficient condition for subnetworks S_i, $i \in J_t$, that are incident on a common node c to be fault-free is that

$$\sum_{i \in J_t} h_c^{m_i}(\mathbf{V}^{m_i}, \boldsymbol{\phi}_i^0) = 0 \ . \tag{4.20}$$

Instead of considering the incidence on a node, we may consider the generalized KCL that involves the incidence on a cut.

Lemma 4.2: Generalized-Mutual-Testing Condition (GMTC) [128] Let $E_i \subset M_i$, $i \in J_t$ denote some external nodes of the subnetwork S_i. Each subnetwork S_i is connected and its external nodes do not decompose it further. If the currents incident to E_i, $i \in J_t$, form a cut set. Then, a necessary and almost sufficient condition for these subnetworks to be fault free is that

$$\sum_{i \in J_t} \sum_{k \in E_i} h_k^{m_i}(\mathbf{V}^{m_i}, \boldsymbol{\phi}_i^0) = 0 \ . \tag{4.21}$$

The ISTC is utilized in identifying faulty region(s) inside a faulty subnetwork that is identified by the application of STC, MTC and GMTC. The application of ISTC starts by partitioning the faulty subnetwork S_i into smaller subnetworks S_j, S_k such that $S_i = S_j \cup S_k$. Utilizing (4.18) we can identify whether S_j or S_k are fault free or not. We utilize the nonfaulty subnetwork to determine the currents and voltages of the common nodes between S_j and S_k.

We continue the binary partitioning process in the identified faulty region until we can not find a partition that satisfies the cardinality condition, namely $|M_{i\alpha}| > |M_{i\delta}|$.

As an example of applying ISTC, we consider the resistive mesh network S shown in Fig. 23 with the nominal values of elements $G_i = 1.0$, $i = 1, 2, \ldots, 20$. All outside nodes $\{1, 2, 3, 6, 7, 10, 11, 12\}$ constitute our measurement nodes where both voltages and currents are known and are given in Table 4.1. Node 12 is taken as the reference ground node. Nodes 4, 5, 8 and 9 are internal nodes where no measurements can be performed. Two faults are assumed in elements G_2 and G_{18}. The process of identifying the faulty elements is summarized in the following steps.

Step 1 S is decomposed as shown in Figs. 24 and 25 into S_1 and S_2.

$$M_{1\alpha} = \{7, 11\}, M_{1\beta} = \{3, 12\}, M_{1\gamma} = \{\varnothing\}, M_{1\delta} = \{8\},$$

$$M_{2\alpha} = \{1, 2, 6, 10\}, M_{2\beta} = \{3, 12\}, M_{2\gamma} = \{\varnothing\}, M_{2\delta} = \{8\}.$$

Applying ISTC, namely, verifying the consistency of (4.18a) and (4.18c), S_1 was found to be faulty free and S_2 was found to be faulty and the following currents and voltages were computed

$$I_3^1 = -I_3^2 = 0.227 \text{ A},$$

$$I_8^1 = -I_8^2 = 0.162 \text{ A},$$

$$I_{12}^1 = -I_{12}^2 = -0.389 \text{ A},$$

$$V_8 = 0.5736 \text{ V}.$$

Step 2 S_2 is decomposed as shown in Figs. 24 and 25 into S_3 and S_4.

$$M_{3\alpha} = \{3, 8, 12\}, M_{3\beta} = \{1, 10\}, M_{3\gamma} = \{\varnothing\}, M_{3\delta} = \{5\},$$

$$M_{4\alpha} = \{2, 6\}, M_{4\beta} = \{1, 10\}, M_{4\gamma} = \{\varnothing\}, M_{4\delta} = \{5\}.$$

Applying ISTC, S_3 was found to be faulty and S_4 to be nonfaulty and the following currents and voltages were computed

$$I_1^4 = -I_1^3 = 0.3785 \text{ A},$$

$$I_5^4 = -I_5^3 = -0.1017 \text{ A},$$

$$I_{10}^{4} = -\ I_{10}^{3} = -\ 0.2754\ \text{A},$$

$$V_5 = 0.7071\ \text{V}.$$

Step 3 S_3 is decomposed as shown in Figs. 24 and 25 into S_5 and S_6.

$M_{5\alpha} = \{1, 3\}, M_{5\beta} = \{\varnothing\}, M_{5\gamma} = \{\varnothing\}, M_{5\delta} = \{4\},$

$M_{6\alpha} = \{5, 8, 10, 12\}, M_{6\beta} = \{\varnothing\}, M_{6\gamma} = \{\varnothing\}, M_{6\delta} = \{4\}.$

Applying ISTC, S_5 and S_6 were found faulty.

Step 4 S_6 is decomposed into S_7 and S_8 as shown in Figs. 24 and 25. S_5 is not decomposable according to the cardinality condition, namely, $|M_{i\alpha}| > |M_{i\delta}|$.

$M_{5\alpha} = \{1, 3\}, M_{5\beta} = \{\varnothing\}, M_{5\gamma} = \{\varnothing\}, M_{5\delta} = \{4\},$

$M_{7\alpha} = \{10, 12\}, M_{7\beta} = \{\varnothing\}, M_{7\gamma} = \{\varnothing\}, M_{7\delta} = \{9\}.$

$M_{8\alpha} = \{5, 8\}, M_{8\beta} = \{\varnothing\}, M_{8\gamma} = \{\varnothing\}, M_{8\delta} = \{4, 9\}.$

Using KCL, we compute the following currents

$$I_4^5 = -\ I_4^8 = -\ 0.3945\ \text{A},$$

$$I_9^8 = -\ I_9^7 = 0.335\ \text{A},$$

and thus, $M_{5\gamma} = \{4\}$, $M_{7\gamma} = \{9\}$ and $M_{8\gamma} = \{4, 9\}$.

Applying ISTC, S_8 was found to be nonfaulty and S_7 to be faulty and the following voltages were computed.

$$V_4 = 0.8579\ \text{V},$$

$$V_9 = 0.4731\ \text{V}.$$

Step 5 For both S_5 and S_7, all external voltages and currents are known. Searching for a single fault in both of them, we found G_2 in S_5 to be faulty and equal 0.5, and G_{18} in S_7 to be faulty and equal 0.5. Hence, we were able to locate the faults in five steps.

4.3.2 *Logical Analysis*

The results of the application of different testing conditions (STC, MTC, GMTC) are analyzed using logical functions to identify the faulty and nonfaulty subnetworks. Every

subnetwork has associated with it a logical variable σ which takes the value 1 if the subnetwork is good and 0 if it is faulty. Every logical testing function (LTF) is equal to the complete product of variables σ_j if all subnetworks involved in the testing condition are fault free

$$LTF_{J_t} \triangleq \sigma_{j_1} \cap \sigma_{j_2} \cap \ldots \cap \sigma_{j_k}, \tag{4.22a}$$

where

$$J_t \triangleq \{j_1, j_2, \ldots, j_k\}, \tag{4.22b}$$

j_i refers to the j_ith subnetwork and k is the number of subnetworks involved in the testing condition, or the complete union of complemented variables σ_j if at least one of the subnetworks is faulty

$$LTF_{J_t} \triangleq \overline{\sigma}_{j_1} \cup \overline{\sigma}_{j_2} \cup \ldots \cup \overline{\sigma}_{j_k}. \tag{4.23}$$

A logical diagnostic function (LDF) is defined as the logical intersection of all LTFs.

$$LDF \triangleq \bigcap_{t=1}^{\ell} LTF_{J_t}, \tag{4.24}$$

where ℓ is the total number of testing conditions. In LDF, the subnetworks that are represented by $\overline{\sigma}_j$ are faulty and those which are represented by σ_j are nonfaulty. If a subnetwork is not represented in the LDF, we assume nothing about its status: more testing conditions are needed to be applied.

Other applications of logical analysis to fault isolation have appeared in [45], [67], [68]. Also, conditions for subnetwork diagnosability are investigated further in [95].

As a simple illustration of the application of the network decomposition technique and logical analysis, the ladder network of Fig. 21a is decomposed into five subnetworks using the measurement nodes 1, 2 and 3 as shown in Fig. 26. Using the measured voltages and the nominal element values, we compute the input currents to these subnetworks as given in Table 4.2. Then we check KCL at the nodes 1, 2 and 3 and form the corresponding LTFs. From Table 4.2, we have

$$LTF_{1\,2} = \sigma_1 \cap \sigma_2,$$

$$LTF_{2\,3\,4} = \overline{\sigma_2} \cup \overline{\sigma_3} \cup \overline{\sigma_4}\,,$$

and

$$LTF_{4\,5} = \sigma_4 \cap \sigma_5\,.$$

Consequently,

$$LDF = (\sigma_1 \cap \sigma_2) \cap (\overline{\sigma_2} \cup \overline{\sigma_3} \cup \overline{\sigma_4}) \cap (\sigma_4 \cap \sigma_5)\,,$$

$$= \sigma_1 \cap \sigma_2 \cap \overline{\sigma_3} \cap \sigma_4 \cap \sigma_5\,,$$

which clearly identifies S_3 as the faulty subnetwork, i.e., G_3 is the only faulty element.

The network decomposition approach has a number of appealing advantages [126]. It is applicable to very large networks as has been demonstrated in [128], with the number of measurement nodes kept within practical acceptable bounds. Subnetwork testing conditions depend on the network topology and KCL, so the technique is applicable to linear and non-linear networks. For linear networks, the on-line computational requirements are similar to the maximum fault bound techniques and the off-line computation involves the analysis of the nominal network only. No upper bound is assumed on the number of faults as in other techniques. Parallel processing techniques could be employed to perform the on-line computations, in particular, when the network is nonlinear, thereby reducing the testing time.

4.4 *Symbolic Function Approach* [48], [113]

We present the application of this approach to the double fault case, i.e., when two circuit elements are faulty. Greater than two faults, the approach does not appear to be practical although it could be applied.

A network function H(s) of a linear active circuit can be expressed as a function of the two faulty parameters ϕ_i and ϕ_j in the form

$$H(\phi_i, \phi_j) = \frac{a_0 + a_1\phi_i + a_2\phi_j + a_3\phi_i\phi_j}{b_0 + b_1\phi_i + b_2\phi_j + b_3\phi_i\phi_j}\,, \tag{4.25}$$

where the coefficients a_i, b_i are functions of the complex frequency s and the nominal parameters of the nonfaulty elements. The function $H(\phi_i, \phi_j)$ is obtained by direct measurements at a certain frequency s_ℓ. Assuming that a_3 or $b_3 \neq 0$, and considering $\phi_i \phi_j$ as an independent unknown variable, we construct a system of linear equations in the unknown variables ϕ_i, ϕ_j and $\phi_i \phi_j$ by measuring H(s) and computing the coefficients a_i, b_i at three independent frequencies (two could be enough). If the parameters are all real and if from the solution we find that the value of $\phi_i \phi_j$ equals the product of ϕ_i by ϕ_j we conclude that the fault is localized in the parameters ϕ_i and ϕ_j. Or, utilizing the measurements at three independent frequencies, we construct two systems of equations in the parameters ϕ_i, ϕ_j and $\phi_i \phi_j$ and solve for these unknowns and check the consistency of the two solutions. For the linear frequency dependent circuit of Fig. 4, we have

$$\frac{V_{out}}{V_{in}}(s) = \frac{a_0 + a_2 C_1}{b_0 + b_1 R_4 + b_2 C_1 + b_3 R_4 C_1},$$

where the coefficients are given by

$$a_0 = R_2,$$

$$a_2 = s R_1 R_2,$$

$$b_0 = (R_1 + R_2) + s(C_2 + C_3)(R_2 R_3 + R_1 R_3 + R_1 R_2),$$

$$b_1 = s C_3(R_1 + R_2) + s^2 C_2 C_3(R_1 R_2 + R_3 R_2 + R_3 R_1),$$

$$b_2 = s R_1 R_2 + s^2 R_1 R_2 R_3(C_2 + C_3),$$

$$b_3 = s^2 R_1 R_2 C_3 + s^3 R_1 R_2 R_3 C_2 C_3$$

and are computed using the nominal parameter values. Assuming that at $\omega = 200$ and 800 rad/sec V_{out}/V_{in} is measured and is given by (.0958, –.3961), (–.0431, –0.0687), respectively. We form a real linear system of equations to solve for the variables C_1, R_4 and $R_4 C_1$. We get $C_1 = 10^{-9}$ F, $R_4 = 5 \times 10^6\ \Omega$ and $R_4 C_1 = 0.005$, which implies that C_1 and R_4 are the actual faulty elements.

4.5 *Fault Verification in Nonlinear Systems* [172]

Recalling (3.1), we may write

$$\mathbf{V}^m = \mathbf{h}(\mathbf{I}^m, \boldsymbol{\phi}^0, \Delta\boldsymbol{\phi}^f)\,, \tag{4.26}$$

where $\Delta\boldsymbol{\phi}^f$ represents the change of the network elements from nominal. Based on the assumption that $n_f < n_m$, $\Delta\boldsymbol{\phi}^f$ will have only n_f nonzero components and (4.26) is an overdetermined system of equations. A search procedure is implemented to find the faulty elements by assuming that a certain set of n_f elements is faulty and minimizing

$$\|\mathbf{V}^m - \mathbf{h}(\mathbf{I}^m, \boldsymbol{\phi}^0, \Delta\boldsymbol{\phi}^f)\|\,, \tag{4.27}$$

with respect to $\Delta\boldsymbol{\phi}^f$, for all possible different combinations of n_f network elements. If the actual values of all nonfaulty elements are nominal, the value of (4.27) will be zero only if the correct faulty parameters are chosen in $\Delta\boldsymbol{\phi}^f$.

The problem of the diagnosability of a network from a set of nonlinear equations is related to the rank of the test matrix $\mathbf{R}$. Visvanathan and Sangiovanni-Vincentelli have given the conditions for single fault diagnosability [172]. The network is n_f-fault diagnosable if we can locally identify the n_f-faulty elements uniquely, for all possible n_f element combinations. This is similar to the concept of n_f fault-testability introduced for linear systems. Let $Q \subset I_\phi$ be the set of (n_f+1) indices and $\mathbf{R}_{qq}$ be the qxq submatrix of the test matrix $\mathbf{R}$ corresponding to Q, then we have the following theorem.

Theorem 4.4 [172]: If for all possible $Q \subset I_\phi$, the matrix $\mathbf{R}_{qq}(\boldsymbol{\phi}^0)$ is positive definite and the rank of $\mathbf{R}_{qq}(\boldsymbol{\phi}^0)$ is generic, then the network is n_f-fault diagnosable.

V. APPROXIMATION TECHNIQUES

Approximation techniques address the problem of fault isolation with a limited number of measurements. They identify the most likely faulty elements that satisfy a prespecified testing criterion. These techniques are characterized by the need of extensive on-line computations. Two techniques are discussed; the probabilistic techniques [22], [61], and the optimization based techniques [4], [50], [85], [107]. The probabilistic techniques could be classified under the simulation-before-test techniques since all simulations are performed before testing and also due to their great similarity, in principle, to the fault dictionary approach.

We consider here three techniques that utilize optimization in finding the most likely faulty elements. The ℓ_2 approximation technique [50], [107] utilizes the weighted-least-squares criterion. The changes in network elements are obtained by solving a system of linear equations. The quadratic optimization technique [85] and ℓ_1 approximation techniques [4] utilize the ℓ_1 norm in identifying the elements which have exhibited large changes from nominal. These elements are considered to be the faulty elements. All techniques assume that all good elements are within their tolerance bounds.

5.1 *Inverse Probability Technique* [22], [61]

This technique is quite similar to the fault dictionary techniques. It is primarily applied to locate single faults. In the pre-test stage the possible faults are characterized statistically. At the time of testing, the probability for each individual element to be faulty is computed using a limited number of measurements and the pre-stored statistical diagnostic data base. Since all network simulations are done before actual testing, this technique is classified as a simulation-before-test approach. In contrast to the fault dictionary techniques, the on-line computation requires extensive calculations.

Recalling (2.34), the conditional probability of obtaining $\mathbf{V}^m$ measurements when the fth network element changes by $\Delta\phi_f$ is given by

$$\text{Prob}(\mathbf{V}^m | \Delta\phi_f) = \frac{\exp\{-\frac{1}{2}(\mathbf{V}^m - \mathbf{V}^f)^T(\Lambda^f_{mm})^{-1}(\mathbf{V}^m - \mathbf{V}^f)\}}{(2\pi)^{1/2}|\Lambda^f_{mm}|^{1/2}} . \tag{5.1}$$

The actual value of the failed component is not desired. The only quantity of interest is the probability that each element has failed.

This is obtained using Bayes' theorem (2.35), and by integrating over all possible values of $\Delta\phi_f$

$$\text{Prob}(\phi_f | \mathbf{V}^m) = k \int \text{Prob}(\mathbf{V}^m | \Delta\phi_f)\,\text{Prob}(\Delta\phi_f)\,d\Delta\phi_f, \tag{5.2}$$

where k is a normalization factor determined by setting the sum of the probabilities of all possible failures equal to one. The element which corresponds to the greatest value of (5.2) is the one most likely to have failed.

It is to be noted that in (5.1) both $\mathbf{V}^f$ and Λ^f_{mm} will vary with the change in the parameter $\Delta\phi_f$. Therefore, the computer implementation of the technique requires a library of inverted covariance matrices and associated values of the network response $\mathbf{V}^f$ at different values of $\Delta\phi_f$. The integration (5.2) is performed numerically using any efficient integration rule (e.g., Simpson's rule). Obviously, infinite changes of $\Delta\phi_f$ are not considered. Therefore, some catastrophic faults are considered only in the limiting sense.

The generation of the covariance matrix elements is achieved by a Monte-Carlo simulation of the variations from nominal of the in-tolerance elements. For the $\Delta\phi_f$ change in the fth element, ℓ circuits are randomly generated, while the remaining circuit element values are constrained within their tolerance bounds.

Each of the ℓ circuits is then simulated to compute the correspnding responses $\mathbf{V}_i^m$. The fault represented by $\Delta\phi_f$ is now characterized statistically on the basis of the responses $\mathbf{V}_i^m$, $i = 1,2,\ldots,\ell$. The $n_m \times n_m$ covariance matrix is given by

$$\Lambda^f_{mm} = \frac{1}{(\ell-1)} \sum_{i=1}^{\ell} (\mathbf{V}_i^m - \mathbf{V}^f)(\mathbf{V}_i^m - \mathbf{V}^f)^T , \tag{5.3a}$$

where $\mathbf{V}^f$ in (5.3a) is given by

$$\mathbf{V}^f \triangleq \frac{1}{\ell} \sum_{i=1}^{\ell} \mathbf{V}_i^m \,. \tag{5.3b}$$

As indicated above the pre-test preparation is cumbersome due to both the large amount of data to be stored and the amount of necessary computation. If every network parameter is discretized at n_x points the number of values to be stored is equal to

$$(n_m^2 + n_m + 2)\, n_x\, n_\phi, \tag{5.4}$$

which is enormous for very large networks.

5.2 *ℓ_2 Approximation Technique*

This technique is based on the assumption that the catastrophic faults have been eliminated and the circuit failure is due to components drifting out of tolerance (as from age, temperature changes, etc.) [107]. A limited number of measurements, insufficient to identify all network elements, are utilized to estimate the most likely element values. The least-squares criterion is employed to find the changes in the network elements from nominal.

For linear networks, the changes in measurements are related to auxiliary current sources as follows from (4.2), namely,

$$\Delta\mathbf{V}^m = \mathbf{Z}_{mb}\, \Delta\mathbf{I}^{bf} \,. \tag{5.5}$$

Equation (5.5) is an underdetermined system of linear equations in the components of the vector $\Delta\mathbf{I}^{bf}$. Utilizing (3.59) every component of $\Delta\mathbf{I}^{bf}$ could be expressed in the form

$$\Delta I_i^{bf} = (V_i^b + \Delta V_i^b)\Delta y_i = (V_i^b + \Delta V_i^b)(j\omega)^{\alpha_i} \Delta\phi_i \,. \tag{5.6}$$

It is clear that $\Delta\mathbf{I}^{bf}$ is directly dependent on the changes in the network elements. In general, (5.5) is a set of complex equations which could be modified into real form as follows.

$$\begin{bmatrix} \mathrm{Re}\,[\Delta\mathbf{V}^m] \\ \mathrm{Im}\,[\Delta\mathbf{V}^m] \end{bmatrix} = \begin{bmatrix} \mathrm{Re}\,[\mathbf{Z}_{mb}] & -\mathrm{Im}\,[\mathbf{Z}_{mb}] \\ \mathrm{Im}\,[\mathbf{Z}_{mb}] & \mathrm{Re}\,[\mathbf{Z}_{mb}] \end{bmatrix} \begin{bmatrix} \mathrm{Re}\,[\Delta\mathbf{I}^{bf}] \\ \mathrm{Im}\,[\Delta\mathbf{I}^{bf}] \end{bmatrix} \,. \tag{5.7}$$

We utilize the ℓ_2 criterion, namely, to minimize

$$\sum_{i=1}^{n_b} \left(w_{i1} \left[\mathrm{Re}\,[\Delta I_i^{bf}] \right]^2 + w_{i2} \left[\mathrm{Im}\,[\Delta I_i^{bf}] \right]^2 \right) \tag{5.8}$$

subject to (5.7) to get an estimate of ΔI^{bf}. w_{i1} and w_{i2} are positive weighting functions. The weighting functions could be chosen such that (5.8) approximates

$$\sum_{i=1}^{n_b} \Delta\phi_i^2 \tag{5.9}$$

under the condition that the changes $\Delta\phi_i$ are quite small. An appropriate choice of w_{i1} and w_{i2} could be

$$w_{i1} = 1/(2\,[\mathrm{Re}[(j\omega)^{a_i} V_i^b]]^2)\ , \tag{5.10a}$$

$$w_{i2} = 1/(2\,[\mathrm{Im}[(j\omega)^{a_i} V_i^b]]^2)\ . \tag{5.10b}$$

The solution of the linear ℓ_2 problem is directly obtained in terms of the generalized inverse of the matrix of equation (5.7).

For the ladder circuit example of Fig. 21a let $G_1 = 1.02$, $G_2 = 0.5$, $G_3 = 0.98$, $G_4 = 0.98$ and $G_5 = 0.95$. The voltages at the measurement nodes 1, 2 and 3 are given by $V_1 = 0.718$V, $V_2 = 0.183$V and $V_3 = 0.093$V, respectively. Therefore, we have only three measurements; not enough to identify all network elements. Since all branch voltages are known we minimize

$$\sum_{i=1}^{5} (\Delta I_i^{bf}/V_i^b)^2$$

subject to

$$\begin{bmatrix} 5 & 3 & 2 & 1 & 1 \\ 2 & -2 & 4 & 2 & 2 \\ 1 & -1 & 2 & -3 & 5 \end{bmatrix} \begin{bmatrix} \Delta I_1^{bf} \\ \Delta I_2^{bf} \\ \Delta I_3^{bf} \\ \Delta I_4^{bf} \\ \Delta I_5^{bf} \end{bmatrix} = \begin{bmatrix} 0.093 \\ -0.067 \\ -0.032 \end{bmatrix}\ ,$$

where the RHS is the change of the nodal voltages from nominal. The solution is given by

$$\Delta \mathbf{I}^{bf} = \begin{bmatrix} -.0049 \\ .2140 \\ -.0217 \\ -.0043 \\ -.0014 \end{bmatrix},$$

from which we get $\Delta G_1 = .0068$, $\Delta G_2 = -.398$, $\Delta G_3 = .119$, $\Delta G_4 = .047$ and $\Delta G_5 = .0148$ which are the expected deviations in the conductances from the nominal value of unity.

5.3 *Quadratic Optimization Technique* [85]

Contrary to the ℓ_2 approximation technique, the main assumption here is that the difference between the actual and the nominal values for a few elements, which correspond to the faulty elements, is much greater than for the remaining network elements that are nonfaulty.

An optimization technique is employed that utilizes an objective criterion of the form

$$\left(\sum_{i=1}^{n_\phi} \sqrt{|\Delta\phi_i| + c_1} \right) + c_2 \|\Delta \mathbf{V}^m - \mathbf{Z}_{mb} \Delta \mathbf{I}^{bf}\|, \tag{5.11}$$

where the first term penalizes the nonzero element values and the second term implies that the result should satisfy (5.5). c_1 and c_2 are constants. c_1 is included in (5.11) to eliminate differential problems when $\Delta\phi_i = 0$. Merrill [85] considered a sequence of quadratic approximations to (5.11). This led to solving a sequence of quadratic programming problems.

The reported results of this approach [85] were in complete agreement with the hypothesis of a few faulty elements. The hypothesis agrees with most practical observations.

5.4 *ℓ_1 Approximation Techniques*

Instead of solving a sequence of quadratic optimization problems, a linear programming formulation has been proposed in [3],[4]. This technique takes advantage of the nature of the ℓ_1 norm as well as the linearity of (5.5). The linear optimization problem is defined as follows.

$$\text{Minimize} \sum_{i=1}^{n_b} \left(w_{i1} |\text{Re}[\Delta I_i^{bf}]| + w_{i2} |\text{Im}[\Delta I_i^{bf}]| \right), \tag{5.12}$$

subject to the linear equality constraints (5.7). This linear optimization problem can be easily converted to the regular linear programming form by an appropriate transformation of the variables.

The least-one objective function tends to satisfy the equality constraints (5.7) with the minimum number of parameters different from zero. This is consistent with the assumption that a few elements are actually faulty.

The results of the linear programming problem provides us with $\Delta \mathbf{I}^{bf}$. The network is then simulated using $\Delta \mathbf{I}^{bf}$ to find $\Delta \mathbf{V}^{b}$. The changes in every network parameter can then be easily computed using (5.6). Comparing the change in every component with its allowed tolerance, the most likely faulty components could be isolated.

We consider here the same example that has been considered for the ℓ_2 approximation technique. We minimized

$$\sum_{i=1}^{5} |\Delta I_i^{bf}|$$

subject to the same set of equality constraints. The solution of the linear programming problem provided us with ΔI_i^{bf}, $i = 1,2,...,5$, which gave the following values for the changes in the elements: $\Delta G_1 = 0.0$, $\Delta G_2 = -0.473$, $\Delta G_3 = 0.0331$, $\Delta G_4 = 0.03$ and $\Delta G_5 = 0.0$. Clearly, the ℓ_1 approximation technique provides sharper results as compared to the ℓ_2 approximation technique.

Practically, we would like to have (5.7) less underdetermined. This is achieved without increasing the number of accessible nodes by exciting the network more than once using different excitations, e.g., a different frequency or different input signals. We then consider $\Delta \boldsymbol{\phi}$ instead of $\Delta \mathbf{I}^{bf}$ as the error parameters.

Equation (5.5) can be written as

$$\Delta \mathbf{V}^{m} = \mathbf{Z}_{mb} \boldsymbol{\Omega}_b (\mathbf{V}_b + \Delta \mathbf{V}_b) \Delta \boldsymbol{\phi}, \tag{5.13a}$$

where

$$\boldsymbol{\Omega}_b = \text{diag}\,\{(j\omega)^{a_1}, (j\omega)^{a_2}, \ldots, (j\omega)^{a_{n_\phi}}\}. \tag{5.13b}$$

To preserve the linearity of (5.13a) $\Delta \mathbf{V}_b$, is initially assumed. This is a linearization of (5.13a). An iterative procedure is applied to update $\Delta \mathbf{V}_b$ and at the same time compute the changes $\Delta\, \boldsymbol{\phi}$.

For k different excitations applied to the faulty network, we consider the following optimization problem.

$$\underset{\Delta\boldsymbol{\phi}}{\text{Minimize}} \sum_{i=1}^{n_\phi} |\Delta\phi_i/\phi_i^0| \tag{5.14a}$$

subject to

$$\begin{bmatrix} \Delta \mathbf{V}_1^m \\ \Delta \mathbf{V}_2^m \\ . \\ . \\ . \\ \Delta \mathbf{V}_k^m \end{bmatrix} = \begin{bmatrix} \mathbf{Z}_{mb1}\, \boldsymbol{\Omega}_{b1}\, (\mathbf{V}_b + \Delta \mathbf{V}_b)_1 \\ \mathbf{Z}_{mb2}\, \boldsymbol{\Omega}_{b2}\, (\mathbf{V}_b + \Delta \mathbf{V}_b)_2 \\ . \\ . \\ . \\ \mathbf{Z}_{mbk}\, \boldsymbol{\Omega}_{bk}\, (\mathbf{V}_b + \Delta \mathbf{V}_b)_k \end{bmatrix} \Delta\boldsymbol{\phi}\ . \tag{5.14b}$$

The solution of (5.14) provides the changes $\Delta\boldsymbol{\phi}$ that are utilized together with the input excitations to the network to update $(\mathbf{V}_b + \Delta \mathbf{V}_b)$ as well as $\mathbf{Z}_{mb}$. This iterative procedure is repeated until convergence is achieved [4].

VI. DISCUSSION AND COMPARISON

6.1 *Artificial Intelligence Technique*

Recently, there has been an attempt to apply artificial intelligence (AI) concepts to the problem of fault location [27],[28]. As pointed out in [27], the AI approach depends on the use of circuit understanding in developing test programs. The approach, in general, will work well in circuits designed in, more or less, a modular form. The AI testing approach could be summarized in the following steps.

1) Decompose the circuit into functional entities,

2) Apply a test signal and do signal tracing to isolate the fault to one or more subcircuits,

3) Apply a diagnosis model to isolate the fault to one element within the subcircuit.

Clearly, the approach is quite similar to the decomposition approach described in Section 4.3, with the exception that functional decomposition is utilized instead of nodal decomposition. Nodal decomposition, which could include functional decomposition, is much more powerful and, as described in [128], a hierarchical decomposition technique could be employed during testing to reduce testing time and provide an efficient and systematic testing procedure.

6.2 *Comparison*

A number of different points are very important regarding the practical application of any fault location technique. We consider the following criteria: on-line computational requirements, off-line computational requirements, test points, robustness, type of faults, network types, network models, diagnosis resolution and in-situ testing. In what follows we consider in some detail the goals for a practical algorithm together with the degree to which the various techniques of Sections II-V achieve these goals.

6.2.1 *On-Line Computational Requirements*

The optimum technique should have minimal on-line computational requirements. This implies that the after-test simulation is fast and the computations needed are simple. This is directly related to the cost and the speed of testing.

Fault dictionary techniques usually implement a very simple isolation criterion, e.g., the nearest-neighbor rule, and the required computations involve only simple mathematical operations. Therefore, they satisfy the on-line computational requirements. For a very large network the dictionary size could be large, such that many entries are processed before isolating the fault, i.e., the testing time could be long. An appropriate approach is to use the decomposition concept in dictionary construction [130] and in the isolation procedure. The advantage of having a minimal on-line computational requirement has made the fault dictionary approach the most logical for practical considerations. Nevertheless, the other inherent deficiencies forced the researchers to search for other more promising approaches.

We have considered two classes of techniques for the parameter identification approach. The nonlinear techniques, while providing us with strong theoretical results, need a nonlinear equation solver. This implies that the ATE should possess sophisticated computational facilities. Moreover, the computation time, in general, will be more than needed for the fault dictionary approach. This usually renders these techniques impractical in an on-line environment under the demand of fast testing time. In contrast to the nonlinear techniques, the linear techniques require solutions of systems of linear equations. Consequently, the on-line computational requirements are moderate and, with rapid advances in the microprocessor technology, the ATE could easily have the simple capability of solving linear systems of equations. In that respect the linear techniques for the parameter identification approach are very close to the practical goal. But, unfortunately, the improvement in on-line computational requirements is usually achieved at the expense of increasing the number of test nodes.

Fault verification techniques have been proposed to achieve the goals of minimal computational requirements without the need of accessing all network nodes. The combinatorial, heuristic and network decomposition techniques have been proposed to reduce the number of combinations considered, i.e., testing time. For linear networks the on-line computations are reduced to matrix by vector multiplications. For nonlinear networks a nonlinear network solver is still required. Using the parallel processing capabilities of modern ATE, the testing time could be further reduced to approach the practical goal.

The approximation techniques utilize a limited number of measurements to essentially perform parameter identification. The on-line computational requirements for the technique that employs quadratic programming could be impractical for on-line implementation. The techniques that only utilize linear programming require less computational power, but they could still be beyond the capability of on-line ATE. The inverse probability technique requires the usage of numerical integration, which is quite feasible for practical implementation and we may consider it to need only moderate computational requirements. Definitely the ℓ_2 approximation technique is the best approximation technique concerning the required computational power since it only requires a matrix by vector multiplication under the assumption that the required pseudo-inverse matrix is obtained beforehand. The problem with the ℓ_2 technique is that the choice of the objective function weights is very crucial to achieving a good approximate solution.

6.2.2 *Off-Line Computational Requirements*

Since the off-line computations are done before performing the actual test, the optimum technique should have moderate off-line computational requirements. The purpose is to reduce, as much as possible, the on-line computations.

The problem with the fault dictionary techniques is that the off-line computations could be excessive due to the need of considering a large number of hypothesized fault cases. Three factors could reduce the off-line computations, namely, the use of network

decomposition in dictionary construction, the use of efficient before-test simulation procedures, e.g., the Householder formula and the complementary pivot theory, and the use of fault models that resemble the corresponding fault conditions and do not cause any ill-conditioning problems during the before-test simulation.

For the parameter identification techniques the before-test simulation is usually done to identify the testing signals and to select the test nodes to achieve a desired degree of test-ability. This is considered a minimal activity compared with the on-line activities, as we indicated earlier.

The fault verification techniques utilize the nominal network parameters in constructing most of the information needed at the time of testing. In particular, for linear networks the matrices that describe the performance of the network are computed and stored before carrying out the actual testing. These computations, though minimal compared with those carried out in the fault dictionary techniques, reduce the on-line computational requirements considerably. Therefore, these techniques closely approach the practical goal.

The on-line implementation of the approximation techniques requires the availability of much test data that could be obtained beforehand either using the nominal or the fault models of the circuit under test. The inverse probability technique is quite similar to the fault dictionary techniques, where most of the computations are done off-line and could be considered reasonably high. For the quadratic programming technique and the ℓ_1 approximation techniques, much valuable information is obtained off-line using the nominal parameters. But, compared with their on-line requirements, the off-line requirements could be considered minimal. For the ℓ_2 approximation technique the pseudo-inverse matrix is usually computed off-line to reduce the on-line requirements to matrix by vector multiplication. Therefore, the off-line requirements for the ℓ_2 approximation technique could be considered moderate.

6.2.3 *Test Nodes*

Due to the practical restriction that there are usually only a few nodes accessible for measurements and testing, the number of required test nodes has to be as small as possible. Some researchers have suggested the upper limit of $\sqrt{n_\phi}$ [121].

Except for the linear techniques of the parameter identification approach, which require all network nodes to be accessible, all other techniques utilize a limited number of test nodes. Nevertheless, the correct isolation and speed of testing usually increase with the increase of the number of test nodes. Also, some techniques utilize fewer test nodes than the others. More specifically, the fault dictionary approach usually needs a very limited number of test nodes. In many cases the fault dictionary is constructed using only input-output measurements.

The nonlinear identification techniques usually need a greater number of test nodes than the fault dictionary approach to achieve full diagnosability of all network parameters. But, as we indicated in Section III, time-domain testing needs fewer test points compared with dc testing.

In the fault verification techniques there is usually a compromise between the number of test nodes, the testing time and the degree of diagnosability. For example, in the network decomposition approach using a very limited number of test nodes, the network could be decomposed into very few large subnetworks connected through these test nodes. Isolation of the faulty subnetwork would be fast, but the location of the sources of fault inside the faulty subnetwork would be relatively slow. The case of the combinatorial technique and the heuristic technique would be similar.

The approximation techniques are proposed to cope with the practical restriction of a limited number of test nodes. Since they are approximate, any increase of accessibility improves their diagnostic results.

6.2.4 *Robustness*

The optimum approach should be robust against the deviations of the nonfaulty elements inside their tolerance region. In analog circuits, unlike digital circuits, the actual values of circuit parameters always deviate from the nominal values. Therefore, any analog testing program has to face the tolerance problem.

The parameter identification techniques solve the robustness problem by evaluating all network elements. But, the testing requirements of the techniques, namely, the large number of test nodes and the on-line computational power could be impractical.

For fault dictionary techniques the effect of tolerances on degrading the degree of diagnosability is the major deficiency of the approach. The degree of diagnosability could be maintained by increasing the size of the dictionary, which, in general, is an impractical solution. In Fig. 27 we illustrate the effect of increasing the tolerances on the nonfaulty elements on the correct diagnosability of the 14 fault cases of Fig. 4 [170]. The nearest-neighbor rule criterion was utilized in isolating the faults. Clearly, a decrease in the degree of diagnosability results.

Fault verification techniques are developed based on the concept that the nonfaulty elements will be at their nominal values. Therefore, the tolerance problem has to be tackled. Several ideas [3], [19], [65], [70], [128] have been proposed with that in mind.

For linear networks, recalling (4.4), the consistency relations are not satisfied, in the presence of tolerances, to the required degree of accuracy. Taking tolerances into consideration and utilizing a first-order approximation (4.4) can be expressed as

$$\mathbf{H}(\boldsymbol{\phi}^0)\,\Delta\mathbf{V}^m = \left[\sum_{i=1}^{n_\phi} \frac{\partial \mathbf{H}}{\partial \phi_i}\,\Delta\phi_i\right]\Delta\mathbf{V}^m + \mathbf{H}\left[\sum_{i=1}^{n_\phi} \frac{\partial \Delta\mathbf{V}^m}{\partial \phi_i}\,\Delta\phi_i\right] = \overline{\mathbf{e}}\,, \tag{6.1a}$$

where

$$\mathbf{H}(\boldsymbol{\phi}^0) = [\mathbf{Z}_{mf}\,(\mathbf{Z}_{mf}^T\,\mathbf{Z}_{mf})^{-1}\,\mathbf{Z}_{mf}^T - \mathbf{1}_{n_m}]\,. \tag{6.1b}$$

All derivatives in (6.1a) are evaluated with respect to the nominal point. From (6.1a) the norm of $\bar{\mathbf{e}}$, namely $\|\bar{\mathbf{e}}\|$, could be evaluated, thereby a possible bound on the inconsistency due to tolerances, or fuzzy consistency, can be estimated [19].

(6.1a) is, usually, an underdetermined system of equations in the deviations $\Delta\boldsymbol{\phi}$. Similarly to the ℓ_2 approximation technique the weighted-least-squares solution provides an estimate of the deviations $\Delta\boldsymbol{\phi}$ (the expected value of $\Delta\boldsymbol{\phi}$ given $\Delta\mathbf{V}^m$). If any component of the computed vector $\Delta\boldsymbol{\phi}$ significantly exceeds its tolerance value, the equation's inconsistency is considered not to be due to tolerance variations of the nonfaulty elements. This technique has been utilized in conjunction with the network decomposition technique [126]-[128] for testing nonlinear networks. Satisfactory results were obtained.

Tolerances make the location of the fault more difficult, exactly as noise makes the recovery of an original signal a difficult task. A high signal/noise ratio is usually desired and similarly the performance of many fault location algorithms will depend on the fault/tolerance ratio, in a certain sense. The ℓ_2 approximation technique assumes that all elements could be changed from nominal with the changes assumed small. For very large changes in certain elements (faults) the performance of the algorithm is extremely unreliable. In contrast, the ℓ_1 approximation techniques assume that few elements have been changed significantly. The increase in the deviations in the remaining elements (due to tolerances) will affect the reliability of the techniques. The inverse probability method is built around the idea of extracting the original signal from a noisy signal. Therefore, for reasonable deviations of the nonfaulty elements the method behaves well [61].

6.2.5 *Types of Faults*

The ideal approach should be able to handle single or multiple faults, whether they are catastrophic or deviation faults.

Most fault dictionary techniques are suited to single fault location, in particular, single catastrophic and large deviation faults. It has been observed that this covers more

than 70% of the actual faults [53]. By adding certain specific faults that are unique to the tested circuit, the percentage of fault coverage could reach 85%.

The parameter identification techniques can handle easily all types of faults, although numerically some catastrophic faults could cause ill-conditioning and difficulty in the convergence of the numerical solution may result.

Fault verification techniques are, in general, very efficient in locating single faults. The use of the decomposition technique, the heuristic technique, and the combinatorial technique made it possible to practically locate multiple faults.

Except for the ℓ_2 approximation technique, all other approximation techniques assume very few faulty elements, e.g., a single fault in the inverse probability technique.

6.2.6 *Network Types*

The objective is to handle all types of analog networks, especially, linear and nonlinear networks. Most techniques have been applied to linear or nonlinear networks.

The advantage in applying the dictionary approach to nonlinear networks is that the on-line computational requirements will be almost the same as in the linear case. For all other techniques the on-line computational requirements are higher than in the linear case. Nevertheless, the availability of parallel processing could substantially remedy this difficulty. We also should note that some techniques are only suited to linear networks. We have indicated this for every technique in Table 6.1.

6.2.7 *Network Models*

The ideal technique should be able to utilize both the nominal models and the fault models of the network elements. As indicated in Section 2.4.4, many fault models for network elements and devices should be developed.

The use of the correct fault model is essential to the success of fault dictionary techniques. All other techniques, which are analytically based, primarily depend on the use of the nominal network model which is known and is quite reliable. The use of an exact fault model may be essential in achieving full diagnosability using parameter identification techniques, or speeding up the performance of fault verification techniques. For example, after locating the faulty subnetwork, the fault model could be used to identify the source of fault inside the network [126].

6.2.8 *Diagnosis Level*

Isolation to the element level could be impractical. It has been noted that a module oriented algorithm is preferred over a parameter oriented algorithm if it can be formulated without compromising other factors [121]. This is evidently true in the age of integrated circuits.

Most fault dictionary techniques achieve a very high degree of diagnosability when diagnosis is limited to the ambiguity set level. For example, if fault cases R_3^-, C_2^- and C_3^- of the circuit of Fig. 4 are in one ambiguity set, the diagnosability will reach 100% for this ambiguity set [170].

The parameter identification techniques and the approximation techniques, though described as parameter oriented techniques, could equally well be applicable as module oriented techniques. This could reduce the size of the identification problem (the number of unknown parameters in the module oriented description) and result in the saving of testing time [111].

The use of the network decomposition technique has the advantage that the method is initially modular, during which the faulty subnetwork is isolated. Subsequently, it is element oriented, when the faulty elements inside the faulty subnetwork are identified. In that respect the fault verification techniques are very close to achieving the required goal.

6.2.9 *In-Situ Testing*

The ideal algorithm should allow for in-situ testing. Such an algorithm should work with an arbitrary input signal rather than a fixed set of test inputs.

Fault dictionary techniques and parameter identification techniques, in general, require specific sets of test inputs. From that point they are not suitable for in-situ testing.

Fault verification techniques and approximation techniques utilize a limited number of measurements that could be obtained using the normal input signal to the circuit under test. Therefore, they are more amenable to in-situ testing.

In Table 6.1 the goals for a practical algorithm are summarized and the degree to which the various techniques achieve these goals is indicated.

6.3 *Testability Measures*

In order to ascertain the effectiveness of an analog test technique, it is usually necessary to establish a measure of testability. A number of measures of testability based on sensitivity matrices, graph theory and circuit understanding has been proposed [31], [74]. In particular, in Section 2.2.1 the D-optimal criterion [104] could be utilized as a measure of testability as well as test complexity. In Section III, the rank of the test matrix is utilized in defining a measure of testability [122], [134], [172] and in Section IV we have introduced concepts of n_f-node-fault testability [56], [57], n_f-branch-fault testability [66] and subnetwork testing conditions [128].

Some examples of simple measures could be [31] the number of circuit elements, the number of inputs per output, the average number of ambiguity groups, the ratio of the total number of elements that can be sensed from the test nodes to the total number of network elements [151], as well as some other heuristic measures [74].

The analog test program should be verified to ensure that it performs as expected. This verification can be performed by checking the test program on randomly selected

network samples, against the theoretic measure of testability and against another well recognized independently developed test program [31].

Test complexity affects testing costs and it is well recognized that testability is the key to future cost savings with the increasing complexity and sheer density of VLSI boards.

VII. CONCLUSIONS

We have considered in detail the theory and techniques for the analog fault diagnosis problem. Naturally, we have selected the most widely accepted techniques. Some other techniques, which either address specific analog circuits or contribute essentially similar practical and theoretical concepts [29], [52], [71]-[73], [75], [80], [84], [90], [96], [106], [109], [137], [152], [160], [178], have not been considered here.

The recent theoretical developments in parameter identification techniques and fault verification techniques have suggested regarding network diagnosis as a third branch of network theory. Early fault dictionary and statistical techniques have emphasized the heuristic nature of the subject.

A successful practical technique for fault isolation is still the objective of many current researchers, but the recently developed techniques have been incorporated in some automatic test program generation (AATPG) schemes [41], [105], [153].

ACKNOWLEDGEMENTS

The authors thank Dr. R.-W. Liu of the University of Notre Dame, Indiana, for his personal recommendation to write this review paper. The authors are grateful to Dr. T. Ozawa of Kyoto University, Japan, for his careful reading of the manuscript. The authors must acknowledge useful early discussions with Dr. R.M. Biernacki of the Technical University of Warsaw, Poland, who introduced the subject of fault analysis to the second author. Continuous interaction with Dr. J.A. Starzyk of Ohio University, Athens, while he was at McMaster University, has benefited the authors in their understanding of the subject. Much of the material in this paper is drawn from lectures given by the second author to staff and graduate students at McMaster University during the academic year 1983-1984. In particular, the authors should single out Mr. S.H. Chen, Mr. M.A. El-Gamal and Mr. Q.J. Zhang, who verified the numerical results of most of the examples given in this manuscript.

REFERENCES

[1] R.J. Allen, "Failure prediction employing continuous monitoring techniques", IEEE Trans. Aerospace-Support Conf. Procedures, vol. AS-1, pp. 924-930, 1963.

[2] J.W. Bandler and R.M. Biernacki, "Postproduction parameter identification and tuning of analog circuits", Proc. European Conf. Circuit Theory and Design (Warsaw, Poland), vol. 2, pp. 205-220, 1980.

[3] J.W. Bandler, R.M. Biernacki and A.E. Salama, "A linear programming approach to fault location in analog circuits", Proc. IEEE Int. Symp. Circuits and Systems (Chicago, IL), pp. 256-260, 1981.

[4] J.W. Bandler, R.M. Biernacki, A.E. Salama and J.A. Starzyk, "Fault isolation in linear analog circuits using the L_1 norm", Proc. IEEE Int. Symp. Circuits and Systems (Rome, Italy), pp. 1140-1143, 1982.

[5] J.W. Bandler and A.E. Salama, "Recent advances in fault location of analog networks", Proc. IEEE Int. Symp. Circuits and Systems (Montreal, Canada), pp. 660-663, 1984.

[6] J.D. Bastian, "Detection and isolation of faults within analog circuits", IEEE Semiconductor Test Conf. Digest (Cherry Hill, NJ), pp. 143-145, 1979.

[7] P.W. Becker and J.E. Thamdrup, "Pattern recognition applied to automated testing", Inst. Elect. Eng. Conf. Publ. No. 91, The Automation of Testing, pp. 82-86, 1972.

[8] S.D. Bedrosian, "Converse of the star-mesh transformation", IRE Trans. Circuit Theory, vol. CT-8, pp. 491-493, 1961.

[9] S.D. Bedrosian, "A simplified explicit solution of networks with two internal nodes", IEEE Trans. Communication and Electronics, vol. 71, pp. 219-224, 1964.

[10] S.D. Bedrosian and R.S. Berkowitz, "Solution procedure for single-element-kind networks", IRE Int. Convention Record, vol. 10, part 2, pp. 16-24, 1962.

[11] S.D. Bedrosian and J.H. Lee, "Automatic fault test generation for nonlinear analog circuits using the fuzzy concept", Proc. 21st Midwest Symp. Circuits and Systems (Ames, IA), pp. 399-403, 1978.

[12] S.D. Bedrosian and J.H. Lee, "An application of fuzzy measure for analog fault isolation", Proc. IEEE Int. Automatic Testing Conf. AUTOTESTCON '79 (Minneapolis, MN), pp. 276-280, 1979.

[13] S.D. Bedrosian and D.W.C. Shen, "Adaptive learning model for optimization of analog tests", Proc. 20th Midwest Symp. Circuits and Systems (Lubbock, TX), pp. 206-210, 1977.

[14] R.S. Berkowitz, "Conditions for network-element-value solvability", IRE Trans. Circuit Theory, vol. CT-9, pp. 24-29, 1962.

[15] R.S. Berkowitz and P.B. Krishnaswamy, "Computer techniques for solving electric circuits for fault isolation", IEEE Trans. Aerospace-Support Conf. Procedures, vol. AS-1, pp. 1090-1099, 1963.

[16] R.S. Berkowitz and R.L. Wexelblat, "Statistical considerations in element value solutions", IRE Trans. Military Electronics, vol. MIL-6, pp. 282-288, 1962.

[17] R.M. Biernacki and J.W. Bandler, "Fault location of analog circuits", Proc. IEEE Int. Symp. Circuits and Systems (Houston, TX), pp. 1078-1081, 1980.

[18] R.M. Biernacki and J.W. Bandler, "Postproduction parameter identification of analog circuits", Proc. IEEE Int. Symp. Circuits and Systems (Houston, TX), pp. 1082-1086, 1980.

[19] R.M. Biernacki and J.W. Bandler, "Multiple-fault location of analog circuits", IEEE Trans. Circuits and Systems, vol. CAS-28, pp. 361-367, 1981.

[20] R.M. Biernacki and J.A. Starzyk, "Sufficient test conditions for parameter identification of analog circuits based on voltage measurements", Proc. European Conf. Circuit Theory and Design (Warsaw, Poland), vol. 2, pp. 233-241, 1980.

[21] R.M. Biernacki and J.A. Starzyk, "A test generation algorithm for parameter identification of analog circuits", Proc. European Conf. Circuit Theory and Design (The Hague, Netherlands), pp. 993-997, 1981.

[22] F.D. Brown, N.F. McAllister and R.P. Perry, "An application of inverse probability to fault isolation", IRE Trans. Military Electronics, vol. MIL-6, pp. 260-267, 1962.

[23] J.L. Brown, Jr., E. Plotkin, L. Roytman and A. Zayezdny, "Fault diagnosis in non-reciprocal networks", Proc. European Conf. Circuit Theory and Design (The Hague, Netherlands), pp. 998-1002, 1981.

[24] J.M. Brown, D.R. Towill and P.A. Payne, "Predicting servo-mechanism dynamic errors from frequency response measurements", The Radio and Electronic Engineer, vol. 42, pp. 7-20, 1972.

[25] P.H. Capitain, "Complementary signal sensitivity to component tolerance", Proc. IEEE Int. Automatic Testing Conf. AUTOTESTCON '82 (Dayton, OH), pp. 223-227, 1982.

[26] H.S.M. Chen and R. Saeks, "A search algorithm for the solution of the multifrequency fault diagnosis equations", IEEE Trans. Circuits and Systems, vol. CAS-26, pp. 589-594, 1979.

[27] R.T. Chien, R.J. Fletcher, W.P.-C. Ho and L.J. Peterson, "On the use of procedural models for generation of test programs", IEEE Trans. Circuits and Systems, vol. CAS-26, pp. 555-557, 1979.

[28] R.T. Chien and W.P.-C. Ho, "Strategy for automatic testing by circuit understanding", Proc. IEEE Int. Automatic Testing Conf. AUTOTESTCON '79 (Minneapolis, MN), pp. 254-260, 1979.

[29] M. Collier, "Pinpointing stripline mismatches", Microwave J., vol. 18, no. 9, p. 49, 1975.

[30] R. DeCarlo and C. Gordon, "Tableau approach to ac-multifrequency fault diagnosis", Proc. IEEE Int. Symp. Circuits and Systems (Chicago, IL), pp. 270-273, 1981.

[31] W.J. Dejka, "A review of measures of testability for analog systems", Proc. IEEE Int. Automatic Testing Conf. AUTOTESTCON '77 (Hyannis, MA), pp. 279-284, 1977.

[32] P. Duhamel and J.-C. Rault, "Automatic test generation techniques for analog circuits and systems: a review", IEEE Trans. Circuits and Systems, vol. CAS-26, pp. 411-440, 1979.

[33] F.M. El-Turky and S. He, "Efficient generation of fault dictionaries", Proc. 25th Midwest Symp. Circuits and Systems (Houghton, MI), pp. 267-270, 1982.

[34] F.M. El-Turky and J. Vlach, "Calculation of element values from node voltage measurements", Proc. IEEE Int. Symp. Circuits and Systems (Houston, TX), pp. 170-172, 1980.

[35] S. Even and A. Lempel, "On a problem of diagnosis", IEEE Trans. Circuit Theory, vol. CT-14, pp. 361-364, 1967.

[36] J.K. Fidler and R.J. Mack, "Fault diagnosis using similar dependence", Proc. European Conf. Circuit Theory and Design (Warsaw, Poland), vol. 2, pp. 221-232, 1980.

[37] E. Flecha and R. DeCarlo, "Time domain tableau approach to the fault diagnosis of analog nonlinear circuits", Proc. IEEE Int. Symp. Circuits and Systems (Newport Beach, CA), pp. 1110-1113, 1983.

[38] E. Flecha and R. DeCarlo, "The nonlinear analog fault diagnosis scheme of Wu, Nakajima, Wey and Saeks in the tableau context", IEEE Trans. Circuits and Systems, vol. CAS-31, pp. 828-830, 1984.

[39] S. Freeman, "Optimum fault isolation by statistical inference", IEEE Trans. Circuits and Systems, vol. CAS-26, pp. 505-512, 1979.

[40] S. Freeman, "Critical path analysis for analog circuits", Proc. IEEE Int. Automatic Testing Conf. AUTOTESTCON '80 (Washington, DC), pp. 301-304, 1980.

[41] S. Freeman, "Automatic test program generation for analog circuits: initial success in demonstrating a new approach", Proc. IEEE Int. Conf. Circuits and Computers (Port Chester, NY), pp. 937-940, 1980.

[42] S. Freeman, "How to generate a small-signal test program set: an information theory", Proc. IEEE Int. Automatic Testing Conf. AUTOTESTCON '81 (Orlando, FL), pp. 347-353, 1981.

[43] S. Freeman, "Statistical inference algorithms for automated testing of analog circuits", Proc. IEEE Int. Symp. Large Scale Systems (Virginia Beach, VA), pp. 32-39, 1982.

[44] S. Freeman, "Modelling ATE/CUT interactions when an analog circuit is diagnosed by ATE", Proc. IEEE Int. Automatic Testing Conf. AUTOTESTCON '82 (Dayton, OH), pp. 190-198, 1982.

[45] T. Fukui and Y. Nakanishi, "A method of designing output sensors for equipment diagnosis based on information content of output sensors", Electronics and Communications in Japan, vol. 51-C, no. 1, pp. 113-121, 1968.

[46] R.F. Garzia, "Fault isolation computer methods", NASA Contractor Report, NASA CR-1758, Marshall Space Flight Centre, Hunstville, AL, 1971.

[47] L. Gefferth, "Fault identification in resistive and reactive networks", Int. J. Circuit Theory and Applications, vol. 2, pp. 273-277, 1974.

[48] L. Gefferth, "Diagnosis of linear electronic circuits with two faulty elements", Proc. 4th Symp. Reliability in Electronics (Budapest, Hungary), pp 115-122, 1977.

[49] S.L. Hakimi and K. Nakajima, "On a theory of t-fault diagnosable analog systems", IEEE Trans. Circuits and Systems, vol. CAS-31, pp. 946-951, 1984.

[50] W.J. Hankley and H.M. Merrill, "A pattern recognition technique for system error analysis", IEEE Trans. Reliability, vol. R-20, pp. 148-153, 1971.

[51] S. Hayashi, Y. Hattori and T. Sasaki, "Considerations on network-element-value evaluation", Electronics and Communications in Japan, vol. 50, no. 12, pp. 118-127, 1967.

[52] E.Y. Ho, "An efficient analog pack fault diagnosis algorithm", Proc. IEEE Int. Automatic Testing Conf. AUTOTESTCON '80 (Washington, DC), pp. 295-300, 1980.

[53] W. Hochwald and J.D. Bastian, "A dc approach for analog fault dictionary determination", IEEE Trans. Circuits and Systems, vol. CAS-26, pp. 523-529, 1979.

[54] J. Huanca and R. Spence, "A statistical fault isolation algorithm for linear and nonlinear toleranced analogue systems", Proc. IEEE Int. Symp. Circuits and Systems (Rome, Italy), pp. 1148-1151, 1982.

[55] J. Huanca and R. Spence, "New statistical algorithm for fault location in toleranced analogue circuits", IEE Proceedings, vol. 130, pt. G, pp. 243-251, 1983.

[56] Z.F. Huang, C.-S. Lin and R.-W. Liu, "Topological conditions on multiple fault testability of analog circuits", Proc. IEEE Int. Symp. Circuits and Systems (Rome, Italy), pp. 1152-1155, 1982.

[57] Z.F. Huang, C.-S. Lin and R.-W. Liu, "Node-fault diagnosis and a design of testability", IEEE Trans. Circuits and Systems, vol. CAS-30, pp. 257-265, 1983.

[58] J.E. Jagodnik and M.S. Wolfson, "Systematic fault simulation in an analog circuit simulator", IEEE Trans. Circuits and Systems, vol. CAS-26, pp. 549-554, 1979.

[59] A.T. Johnson, Jr., "Efficient fault analysis in linear analog circuits", IEEE Trans. Circuits and Systems, vol. CAS-26, pp. 475-484, 1979.

[60] S. Katz, R.M.H. Cheng and V. Aula, "Locating a single shunt fault in resistor ladder networks", Int. J. Circuit Theory and Applications, vol. 7, pp. 399-412, 1979.

[61] J. Kranton and A. Libenson, "A pattern recognition approach to fault isolation", IEEE Trans. Aerospace-Support Conf. Procedures, vol. AS-1, pp. 1320-1326, 1963.

[62] J.H. Lee and S.D. Bedrosian, "Fault isolation algorithm for analog electronic systems using the fuzzy concept", IEEE Trans. Circuit and Systems, vol. CAS-26, pp. 518-522, 1979.

[63] S.R. Liberty, L. Tung and R. Saeks, "Fault prediction – toward a mathematical theory", in Rational Fault Analysis. New York: Marcel Dekker, pp. 135-142, 1977.

[64] C.-S. Lin, "A study on fault diagnosis", Tech. Rep. 82-2, Univ. of Notre Dame, Notre Dame, IN, 1982.

[65] C.-S. Lin, Z.F. Huang and R.-W. Liu, "Fault diagnosis of linear analog networks: a theory and its implementation", Proc. IEEE Int. Symp. Circuits and Systems (Newport Beach, CA), pp. 1090-1093, 1983.

[66] C.-S. Lin, Z.F. Huang and R.-W. Liu, "Topological conditions for single-branch-fault", IEEE Trans. Circuits and Systems, vol. CAS-30, pp. 376-381, 1983.

[67] C.-S. Lin and R.-W. Liu, "Fault directory approach – a case study", Proc. IEEE Int. Symp. Circuits and Systems (Chicago, IL), pp. 239-242, 1981.

[68] M.F.-S. Lin and S.P. Chan, "Fault diagnosis of linear systems", Proc. 7th Annual Allerton Conf. on Circuit and System Theory (Monticello, IL), pp. 503-510, 1969.

[69] P.-M. Lin, "DC fault diagnosis using complementary pivot theory", Proc. IEEE Int. Symp. Circuits and Systems (Rome, Italy), pp. 1132-1135, 1982.

[70] R.-W. Liu, C.-S. Lin, Z.-F. Huang and L.-Z. Hu, "Analog fault diagnosis: a new circuit theory", Proc. IEEE Int. Symp. Circuits and Systems (Newport Beach, CA), pp. 931-939, 1983.

[71] R.-W. Liu and V. Visvanathan, "Diagnosability of large-scale dynamical systems", Proc. 20th Midwest Symp. Circuits and Systems (Lubbock, TX), pp. 585-589, 1977.

[72] R.-W. Liu and V. Visvanathan, "Sequentially linear fault diagnosis: part I – theory", IEEE Trans. Circuits and Systems, vol. CAS-26, pp. 490-495, 1979.

[73] R.-W. Liu, V. Visvanathan and C. Lin, "Tearing in fault diagnosis", Proc. IEEE Int. Symp. Circuits and Systems (Tokyo, Japan), pp. 874-877, 1979.

[74] B.A. Longendorfer, "Computer-aided testability analysis of analog circuitry", Proc. IEEE Int. Automatic Testing Conf. AUTOTESTCON '81 (Orlando, FL), pp. 122-127, 1981.

[75] P.A. Lux and K.W. Drake, "Fault detection with a simple adaptive mechanism", IEEE Trans. Industrial Electronics and Control Instrumentation, vol. IECI-14, pp. 80-85, 1967.

[76] C.J. Macleod, "Parameter estimation using pseudorandom binary sequences", Electronics Letters, vol. 5, pp. 35-36, 1969.

[77] C.J. Macleod, "System identification using time-weighted pseudorandom sequences", Int. J. Control, vol. 14, pp. 97-109, 1971.

[78] C.J. Macleod, "Comparison of methods of parameter estimation using pseudorandom sequences", Electronics Letters, vol. 9, pp. 342-343, 1973.

[79] J.H. Maenpaa, C.J. Stehman and W.J. Stahl, "Fault isolation in conventional linear systems: a progress report", IEEE Trans. Reliability, vol. R-18, pp. 12-14, 1969.

[80] Y.V. Malyshenko, "Algorithm of construction of diagnostic test for linear dc networks", Automation and Remote Control, vol. 39, pp. 734-738, 1978.

[81] G.O. Martens and J.D. Dyck, "Fault identification in electronic circuits with the aid of bilinear transformation", IEEE Trans. Reliability, vol. R-21, pp. 99-104, 1972.

[82] W. Mayeda and G. Peponides, "Determination of component values in passive networks under limited measurements", Proc. 12th Asilomar Conf. on Circuits, Systems and Computers (Pacific Grove, CA), pp. 761-764, 1978.

[83] D.A. McCalister and L.L. Bickford, "Frequency response determination using white noise excitation", J. Spacecraft, vol. 5, pp. 872-874, 1968.

[84] W.R. McCormack and C. Michel, "Diagnostic maintenance, a technique using a computer", IEEE Trans. Aerospace - Support Conf. Procedures, vol. AS-1, pp. 931-941, 1963.

[85] H.M. Merrill, "Failure diagnosis using quadratic programming", IEEE Trans. Reliability, vol. R-22, pp. 207-213, 1973.

[86] D.F. Mix and J.G. Sheppard, "Average correlation functions in on-line testing of linear systems", IEEE Trans. Aerospace Electronic Systems, vol. AES-9, pp. 665-669, 1973.

[87] C. Morgan, V.Y. Tawfik and D.R. Towill, "Fault location in a noisy multiple-nonlinearity servosystem", IEEE Trans. Circuits and Systems, vol. CAS-26, pp. 586-589, 1979.

[88] C. Morgan and D.R. Towill, "Application of the multiharmonic Fourier filter to nonlinear system fault location", IEEE Trans. Instrumentation and Measurement, vol. IM-26, pp. 164-169, 1977.

[89] K. Nadesalingam and D.R. Towill, "Frequency domain fault detection and diagnosis in hybrid control systems: a feasibility study", IEEE Trans. Instrumentation and Measurement, vol. IM-27, 193-199, 1978.

[90] J.J. Narraway, "Accessibility in systems", Inst. Elect. Eng. Conf. Publ. no. 91, The Automation of Testing, pp. 1-6, 1972.

[91] N. Navid and A.N. Willson, Jr., "Fault diagnosis for resistive analog circuits", Proc. IEEE Int. Symp. Circuits and Systems (Tokyo, Japan), pp. 882-885, 1979.

[92] N. Navid and A.N. Willson, Jr., "A theory and an algorithm for analog circuit fault diagnosis", IEEE Trans. Circuits and Systems, vol. CAS-26, pp. 440-457, 1979.

[93] E.C. Neu, "A new n-port network theorem", Proc. 13th Midwest Symp. Circuit Theory (Minneapolis, MN), pp. IV.5.1 - IV.5.10, 1970.

[94] T. Ozawa, "A concept concerning the independence of voltages and currents in electrical networks", Proc. IEEE Int. Symp. Circuits and Systems (Newport Beach, CA), pp. 331-334, 1983.

[95] T. Ozawa, J.W. Bandler and A.E. Salama, "Diagnosability in the decomposition approach for fault location in large analog networks", IEEE Trans. Circuits and Systems, vol. CAS-32, pp. 415-416, 1985.

[96] T. Ozawa and Y. Kajitani, "Diagnosability of linear active networks", IEEE Trans. Circuits and Systems, vol. CAS-26, pp. 485-489, 1979.

[97] T. Ozawa, S. Shinoda and M. Yamada, "An equivalent-circuit transformation and its application to network-element-value calculation", IEEE Trans. Circuits and Systems, vol. CAS-30, pp. 432-441, 1983.

[98] T. Ozawa and M. Yamada, "Conditions for determining parameter values in a linear active network from node voltage measurements", Proc. IEEE Int. Symp. Circuits and Systems (Chicago, IL), pp. 274-277, 1981.

[99] T. Ozawa and M. Yamada, "Conditions for network-element-value determination by multifrequency measurements", Proc. IEEE Int. Symp. Circuits and Systems (Rome, Italy), pp. 1156-1159, 1982.

[100] A. Pahwa and R.A. Rohrer, "Band faults: efficient approximations to fault bands for the simulation before fault diagnosis of linear circuits", IEEE Trans. Circuits and Systems, vol. CAS-29, pp. 81-88, 1982.

[101] S.C. Pinault, "Automated test frequency selection for hybrid filters", Proc. IEEE Int. Symp. Circuits and Systems (Newport Beach, CA), pp. 777-780, 1983.

[102] W.A. Plice, "Overview of current automated analog test design", Proc. IEEE Test Semiconductor Conference (Cherry Hill, NJ), pp. 128-136, 1979.

[103] W.A. Plice, "UUT modeling", Proc. IEEE Int. Automatic Testing Conf. AUTOTESTCON '81 (Orlando, FL), pp. 106-113, 1981.

[104] R.W. Priester and J.B. Clary, "New measures of testability and test complexity for linear analog failure analysis", IEEE Trans. Circuits and Systems, vol. CAS-28, pp. 1088-1092, 1981.

[105] N.S. Prywes, "Software and analog test technology", Proc. IEEE Int. Symp. Large Scale Systems (Virginia Beach, VA), pp. 40-41, 1982.

[106] M.N. Ransom and R. Saeks, "Fault isolation via term expansion", Proc. 3rd Pittsburgh Symp. on Modelling and Simulation (Pittsburgh, PA), pp. 224-228, 1973.

[107] M.N. Ransom and R. Saeks, "Fault isolation with insufficient measurements", IEEE Trans. Circuit Theory, vol. CT-20, pp. 416-417, 1973.

[108] M.N. Ransom and R. Saeks, "The connection function – theory and application", Int. J. Circuit Theory and Applications, vol. 3, pp. 5-21, 1975.

[109] L. Rapisarda and R. DeCarlo, "Fault diagnosis for interconnected systems: algorithm improvement", Proc. IEEE Int. Symp. Large Scale Systems (Virginia Beach, VA), pp. 308-313, 1982.

[110] L. Rapisarda and R. DeCarlo, "Analog multifrequency fault diagnosis", IEEE Trans. Circuits and Systems, vol. CAS-30, pp. 223-234, 1983.

[111] L. Rapisarda, R. DeCarlo and J. Peczkowski, "Fault diagnosis for interconnected systems: functional group versus component analysis", Proc. 25th Midwest Symp. Circuits and Systems (Houghton, MI), pp. 263-266, 1982.

[112] S.C.D. Roy, "Single shunt fault diagnosis in a resistive ladder", IEEE Trans. Instrumentation and Measurement, vol. IM-30, pp. 143-146, 1981.

[113] L.M. Roytman, E. Plotkin and M.N.S. Swamy, "Multifrequency method of fault diagnosis in analogue circuits", Proc. IEEE Int. Symp. Circuits and Systems (Rome, Italy), pp. 1144-1147, 1982.

[114] L.M. Roytman and M.N.S. Swamy, "Some properties of orthonormal excitations of the circuit and the calculation of the circuit elements", Proc. IEEE Int. Symp. Circuits and Systems (Chicago, IL), pp. 289-291, 1981.

[115] L.M. Roytman and M.N.S. Swamy, "Multiple-fault diagnosis in analogue circuits", Int. J. Electronics, vol. 50, pp. 289-297, 1981.

[116] L.M. Roytman and M.N.S. Swamy, "One method of the circuit diagnosis", Proc. IEEE, vol. 69, pp. 661-662, 1981.

[117] L.M. Roytman and M.N.S. Swamy, "Diagnosis of passive networks", Proc. IEEE Int. Symp. Circuits and Systems (Chicago, IL), pp. 292-294, 1981.

[118] L.M. Roytman and M.N.S. Swamy, "Parameter identification in linear networks", Int. J. Electronics, vol. 50, pp. 137-140, 1981.

[119] R. Saeks, "An experiment in fault prediction II", Proc. IEEE Int. Automatic Testing Conf. AUTOTESTCON '76 (Arlington, TX), p. 53, 1976.

[120] R. Saeks, "An approach to built-in testing", IEEE Trans. Aerospace and Electronic Systems, vol. AES-14, pp. 813-818, 1978.

[121] R. Saeks, "Criteria for analog fault diagnosis", Proc. European Conf. Circuit Theory and Design (The Hague, Netherlands), pp. 75-78, 1981.

[122] R. Saeks, A. Sangiovanni-Vincentelli and V. Visvanathan, "Diagnosability of non-linear circuits and systems – part II: dynamical systems", IEEE Trans. Circuits and Systems, vol. CAS-28, pp. 1103-1108, 1981.

[123] R. Saeks, S.P. Singh and R.-W. Liu, "Fault isolation via component simulation", IEEE Trans. Circuit Theory, vol. CT-19, pp. 634-640, 1972.

[124] A.A. Sakla, "Fault analysis in analog circuits", Ph.D. Dissertation, University of Illinois at Urbana-Champaign, IL, 1979.

[125] A.A. Sakla, E.I. El-Masry and T.N. Trick, "A sensitivity algorithm for fault location in large analog circuits", Proc. IEEE Int. Symp. Circuit and Systems (Houston, TX), pp. 1075-1077, 1980.

[126] A.E. Salama "Fault analysis and parameter tuning in analog circuits", Ph.D. Thesis, McMaster University, Hamilton, Canada, 1983.

[127] A.E. Salama, J.A. Starzyk and J.W. Bandler, "A unified decomposition approach for fault location in large analog circuits", Proc. European Conf. Circuit Theory and Design (Stuttgart, West Germany), pp. 125-127, 1983.

[128] A.E. Salama, J.A. Starzyk and J.W. Bandler, "A unified decomposition approach for fault location in large analog circuits", IEEE Trans. Circuits and Systems, vol. CAS-31, pp. 602-622, 1984.

[129] H.H. Schreiber, "A state space approach to analog fault signature generation", Proc. 20th Midwest Symp. Circuits and Systems (Lubbock, TX), pp. 200-205, 1977.

[130] H.H. Schreiber, "A review of analog automatic test generation", Proc. IEEE Int. Automatic Testing Conf. AUTOTESTCON '78 (San Diego, CA), pp. 1-8, 1978.

[131] H.H. Schreiber, "Fault dictionary based upon stimulus design", IEEE Trans. Circuits and Systems, vol. CAS-26, pp. 529-537, 1979.

[132] H.H. Schreiber and F.-L. Wang, "Fault isolation in analog systems using go-no-go testing", Proc. IEEE Semiconductor Test Conf. (Cherry Hill, NJ), pp. 146-154, 1979.

[133] N. Sen and R. Saeks, "A measure of testability and its application to test point selection - Theory", Proc. 20th Midwest Symp. Circuits and Systems (Lubbock, TX), pp. 576-583, 1977.

[134] N. Sen and R. Saeks, "Fault diagnosis for linear systems via multifrequency measurements", IEEE Trans. Circuits and Systems, vol. CAS-26, pp. 457-465, 1979.

[135] S. Seshu and R. Waxman, "Fault isolation in conventional linear systems - a feasibility study", IEEE Trans. Reliability, vol. R-15, pp. 11-16, 1966.

[136] S. Shinoda and S.P. Chan, "Element-value solvability of a linear passive resistive network with internal nodes", Proc. 14th Asilomar Conf. on Circuits, Systems and Computers (Pacific Grove, CA), pp. 29-34, 1980.

[137] S. Shinoda, K. Onaga and W. Mayeda, "Graph theoretic properties of pseudo-incidence matrix with an application to network diagnosis", Proc. 12th Asilomar Conf. on Circuits, Systems and Computers (Pacific Grove, CA), pp. 749-753, 1978.

[138] S. Shinoda and I. Yamaguchi, "Parameter-value determination of linear active networks with inaccessible nodes", Proc. IEEE Int. Symp. Circuits and Systems (Newport Beach, CA), pp. 1114-1117, 1983.

[139] S. Shinoda and I. Yamaguchi, "Element-value determination of LCR networks with inaccessible nodes", Proc. IEEE Int. Symp. Circuits and Systems (Newport Beach, CA), pp. 1118-1120, 1983.

[140] J.V. Shumovich and R.E. Tucker, "Advanced concepts for component failure isolation", Proc. ELECTRO '78 (Boston, MA), pp. 19-24, 1978.

[141] H. Sriyanada and D.R. Towill, "Fault diagnosis via automatic dynamic testing: a voting technique", Inst. Elec. Eng. Conf. Publ. no. 91, The Automation of Testing, pp. 196-201, 1972.

[142] H. Sriyanada and D.R. Towill, "Fault diagnosis using time domain measurements", The Radio and Electronic Engineer, vol. 43, pp. 523-533, 1973.

[143] H. Sriyanada, D.R. Towill and J.H. Williams, "Voting techniques for fault diagnosis for frequency-domain test-data", IEEE Trans. Reliability, vol. R-24, pp. 260-267, 1975.

[144] W.J. Stahl, J.H. Maenpaa and C.J. Stehman, "Computer-aided design: part 13, defining faults with a dictionary", Electronics, vol. 41, no. 2, pp. 64-68, 1968.

[145] J.A. Starzyk and J.W. Bandler, "Location of fault regions in analog circuits", Simulation Optimization Systems Research Laboratory, McMaster University, Hamilton, Canada, Report SOS-81-17-R, 1981.

[146] J.A. Starzyk and J.W. Bandler, "Nodal approach to multiple-fault location in analog circuits", Proc. IEEE Int. Symp. Circuits and Systems (Rome, Italy), pp. 1136-1139, 1982.

[147] J.A. Starzyk and J.W. Bandler, "Design of tests for parameter evaluation within remote inaccessible faulty subnetworks", Proc. IEEE Int. Symp. Circuits and Systems (Newport Beach, CA), pp. 1106-1109, 1983.

[148] J.A. Starzyk and J.W. Bandler, "Multiport approach to multiple-fault location in analog circuits", IEEE Trans. Circuits and Systems, vol. CAS-30, pp. 762-765, 1983.

[149] J.A. Starzyk, R.M. Biernacki and J.W. Bandler, "Evaluation of faulty elements within linear subnetworks", Int. J. Circuit Theory and Applications, vol. 12, pp. 23-27, 1984.

[150] F.Y. Sui and S.G. Ming, "The fault diagnosis and the approach to preventing chain-fault", Proc. IEEE Int. Symp. Circuits and Systems (Houston, TX), pp. 1068-1071, 1980.

[151] G.C. Temes, "Efficient methods of fault simulation", Proc. 20th Midwest Symp. Circuits and Systems (Lubbock, TX), pp. 191-194, 1977.

[152] J.F.M. Theeuwen and J.A.G. Jess, "A new approach to the biasing problem and the fault localization of nonlinear electronic circuits", IEEE Trans. Circuits and Systems, vol. CAS-29, pp. 125-135, 1982.

153] C. Tinaztepe and N.S. Prywes, "Generation of software for computer controlled test equipment for testing analog circuits", IEEE Trans. Circuits and Systems, vol. CAS-26, pp. 537-548, 1979.

[154] Y. Togawa and T. Matsumoto, "On the topological testability conjecture for analog fault diagnosis problems", IEEE Trans. Circuits and Systems, vol. CAS-31, pp. 147-158, 1984.

[155] K.Y. Tong, "Single fault location in a linear analogue system with variable sensitivity matrix", Electronics Letters, vol. 16, pp. 221-222, 1980.

[156] D.R. Towill, "Dynamic testing of control systems", The Radio and Electronic Engineer, vol. 47, pp. 505-521, 1977.

[157] D.R. Towill and P.A. Payne, "Frequency domain approach to automatic testing of control systems", The Radio and Electronic Engineer, vol. 41, pp. 51-60, 1971.

[158] T.N. Trick, "A note on parameter value determination from node voltage measurements", IEEE Trans. Circuits and Systems, vol. CAS-27, pp. 1269-1270, 1981.

[159] T.N. Trick and C.J. Alajajian, "Fault analysis of analog circuits", Proc. 20th Midwest Symp. Circuits and Systems (Lubbock, TX), pp. 211-215, 1977.

[160] T.N. Trick and R.T. Chien, "A note on single fault detection in positive resistor circuits", IEEE Trans. Circuits and Systems, vol. CAS-25, pp. 46-48, 1978.

[161] T.N. Trick, E.I. El-Masry, A.A. Sakla and B.L. Inn, "Single fault detection in analog circuit", IEEE Semiconductor Test Conf. Digest (Cherry Hill, NJ), pp. 137-142, 1979.

[162] T.N. Trick and Y. Li, "A sensitivity based algorithm for fault isolation in analog circuits", Proc. IEEE Int. Symp. Circuits and Systems (Newport Beach, CA), pp. 1098-1101, 1983.

[163] T.N. Trick, W. Mayeda and A.A. Sakla, "Calculation of parameter values from node voltage measurements", IEEE Trans. Circuits and Systems, vol. CAS-26, pp. 466-474, 1979.

[164] T.N. Trick and A.A. Sakla, "A new algorithm for the fault analysis and tuning of analog circuits", Proc. IEEE Int. Symp. Circuits and Systems (New York, NY), pp. 156-160, 1978.

[165] R.E. Tucker and L.P. McNamee, "Computer-aided design application to S-3A analog test programs", Proc. IEEE Int. Automatic Testing Conf. AUTOTESTCON '76 (Arlington, TX), pp. 172-179, 1976.

[166] R.E. Tucker and L.P. McNamee, "Computer-aided design application to fault detection and isolation techniques", Proc. IEEE Int. Symp. Circuits and Systems (Phoenix, AZ), pp. 684-687, 1977.

[167] L. Tung and R. Saeks, "An experiment in fault prediction", Proc. 4th Symp. Reliability in Electronics (Budapest, Hungary), pp.249-257, 1977.

[168] K.C. Varghese, D.R. Towill and J.H. Williams, "ATPG for an aerospace analog compensation unit using only input-output frequency domain measurements", Proc. IEEE Int. Automatic Testing Conf. AUTOTESTCON '79 (Minneapolis, MN), pp. 261-267, 1979.

[169] K.C. Varghese, J.H. Williams and D.R. Towill, "Computer-aided feature selection for enhanced analogue system fault location", Pattern Recognition, vol. 10, pp. 265-280, 1978.

[170] K.C. Varghese, J.H. Williams and D.R. Towill, "Simplified ATPG and analog fault location via a clustering and separability technique", IEEE Trans. Circuits and Systems, vol. CAS-26, pp. 496-505, 1979.

[171] V. Visvanathan and A. Sangiovanni-Vincentelli, "Fault diagnosis of nonlinear memoryless systems", Proc. IEEE Int. Symp. Circuits and Systems (Houston, TX), pp. 1087-1091, 1980.

[172] V. Visvanathan and A. Sangiovanni-Vincentelli, "Diagnosability of nonlinear circuits and systems – part I: the dc case", IEEE Trans. Circuits and Systems, vol. CAS-28, pp. 1093-1102, 1981.

[173] V. Visvanathan and A. Sangiovanni-Vincentelli, "A computational approach for the diagnosability of dynamical circuits", IEEE Trans. Computer-Aided Design, vol. CAD-3, pp. 165-171, 1984.

[174] C.-L. Wang, "Polygon to star transformations", IRE Trans. Circuit Theory, vol. CT-8, pp. 489-491, 1961.

[175] F.-L. Wang and H.H. Schreiber, "A pragmatic approach to automatic test generation and failure isolation of analog systems", IEEE Trans. Circuits and Systems, vol. CAS-26, pp. 584-585, 1979.

[176] C.-L. Wey, D. Holder and R. Saeks, "On the implementation of an analog ATPG", Proc. IEEE Int. Symp. Circuits and Systems (Newport Beach, CA), pp. 1102-1105, 1983.

[177] C.-C. Wu, K. Nakajima, C.-L. Wey and R. Saeks, "Analog fault diagnosis with failure bounds", IEEE Trans. Circuits and Systems, vol. CAS-29, pp. 277-284, 1982.

[178] C.-C. Wu, A. Sangiovanni-Vincentelli and R. Saeks, "A differential-interpolation approach to analog fault simulation", Proc. IEEE Int. Symp. Circuits and Systems (Chicago, IL), pp. 266-269, 1981.

TABLE 2.1

FAULT DEFINITION OF THE VIDEO AMPLIFIER EXAMPLE

FAULTS	
NUMBER	DESCRIPTION
1	Q1BES
2	Q2CES
3	Q2BO
4	Q3BES
5	Q3BO
6	Q4BES
7	Q4BO
8	Q5BES
9	Q5BO
10	Q6BES
11	Q6BCS
12	Q6BO
13	DZ1O
14	DZ1S
15	DZ2O
16	DZ2S
17	DZ3O
18	DZ3S
19	DZ4O
20	DZ4S

S indicates short condition.
O indicates open condition.

TABLE 2.2

THE DC FAULT DICTIONARY FOR SPECIFIC FAULTS

Measurement Nodes	Input Stimuli	Faults		
		Q3BES	Q6BES	DZ1S
Node 2	−30V +30V	6.95 6.95	0.12 6.91	0.12 6.95
Node 5	−30V +30V	0.09 0.09	5.93 0.09	5.92 0.09
Node 8	−30V +30V	5.99 5.99	0.09 5.97	0.08 6.0
Node 11	−30V +30V	5.32 0.15	5.93 0.2	1.7 0.13
Node 16	−30V +30V	0.02 0.03	3.07 4.22	3.11 0.03

TABLE 2.3

SIGNATURE CODES OF THE DEVIATION OF THE AMPLITUDE RESPONSE FROM NOMINAL

Signature Code	Interpretation
0	within 0.5 dB of nominal
1	0.5 to 1 dB less than nominal
2	1 to 2 dB less than nominal
3	2 to 5 dB less than nominal
4	greater than 5 dB less than nominal
5	0.5 dB to 1 dB higher than nominal
6	1 to 2 dB higher than nominal
7	2 to 5 dB higher than nominal
8	greater than 5 dB higher than nominal

TABLE 2.4

SIGNATURE CODES FOR SPECIFIC FAULT CASES

Code	Fault Case	Code	Fault Case
10000	R_1^+	56000	R_1^-
50000	R_2^+	21000	R_2^-
02434	R_3^+	06788	R_3^-
00214	R_4^+	00578	R_4^-
05050	C_1^+	01210	C_1^-
02334	C_2^+	06778	C_2^-
02434	C_3^+	06788	C_3^-

+ indicates +50% change in the corresponding element.
− indicates −50% change in the corresponding element.

TABLE 2.5

SPARSE FAULT DICTIONARY CONSTRUCTED USING QUANTIZATION

Measurements	Faults													
	R_1^+	R_1^-	R_2^+	R_2^-	R_3^+	R_3^-	R_4^+	R_4^-	C_1^+	C_1^-	C_2^+	C_2^-	C_3^+	C_3^-
Gain at 10 rad/sec	1	−1	−1	1										
Gain at 200 rad/sec					1	−1			−1	1	1	−1	1	−1
Gain at 800 rad/sec					1	−1	1	−1			1	−1	1	−1
Phase at 2000 rad/sec						−1	1	−1			1	−1	1	−1
Phase at 8000 rad/sec								−1				−1		−1

no entry means zero.

TABLE 2.6

SPARSE FAULT DICTIONARY CONSTRUCTED USING NONDIMENSIONALIZATION AND NORMALIZATION

Measurements	Faults													
	R_1^+	R_1^-	R_2^+	R_2^-	R_3^+	R_3^-	R_4^+	R_4^-	C_1^+	C_1^-	C_2^+	C_2^-	C_3^+	C_3^-
Gain at 10 rad/sec	.99	−.96	−.98	.98										
Gain at 200 rad/sec		−.25	−.14	.16	.81	−.57	.29	−.15	−.99	.97	.71	−.53	.80	−.63
Gain at 800 rad/sec					.56	−.76	.38	−.22	−.08	.16	.48	−.45	.52	−.62
Phase at 2000 rad/sec					.15	−.26	.79	−.77	.09	−.14	.45	−.59	.25	−.39
Phase at 8000 rad/sec							.35	−.57			.2	−.39		−.21

no entry means zero.

TABLE 2.7

THE AMBIGUITY SETS FOR EACH TEST NODE OF
OF THE VIDEO AMPLIFIER CIRCUIT

Measurement Nodes	Input Stimuli	Ambiguity Sets				
		Set 1	Set 2	Set 3	Set 4	Set 5
Node 2	−30 V	2,4,5,8,9,13,17	nominal*			
	30 V	3,6,7,15	19	20	nominal	
Node 5	−30 V	2,4,5,13	9	17	18	nominal
	30 V	3,6,7,15	nominal			
Node 8	−30 V	2,4,5,13	nominal			
	30 V	3	7	15	16	nominal
Node 11	−30 V	2	5	13	14	nominal
	30 V	3,6,7,15,19	nominal			
Node 16	−30 V	2,4,5,8,9,15,17	11	nominal		
	30 V	3,6,7,10,12,15,19	nominal			
Node 26	−30 V	2,4,5,8,9,13,17	nominal			
	30 V	3,6,7,15,19	nominal			
Node 27	−30 V	2,4,5,8,9,13,17	nominal			
	30 V	3,6,7,15,19	nominal			
Node 33	−30 V	2,4,5,8,9,15,17	nominal			
	30 V	3,6,7,15,19	nominal			

* the nominal set contains the rest of the 20 faults given in Table 2.1.

TABLE 2.8

SELECTED MEASUREMENTS AND THEIR CONFIDENCE LEVEL

Sequence Number	Number of Measurements	Measurements		Confidence Level
		Gain at	Phase at	
1	1		100 rad/sec	50*
2	2	10 rad/sec	100	68.25
3	3	10	100,600	85.55
4	4	10	100,600,10000	87.31
5	4	10	100,600,9000	87.55
6	4	10	100,600,8000	87.84
7	4	10	100,600,7000	87.24
8	6	10,80,1000	100,600,6000	87.95
9	7	10,80,500,900	100,600,6000	88.07
10	9	10,80,200,400,700	100,600,5000,9000	89.33
11	9	10,70,200,400,700	100,600,5000,9000	89.27
12	9	10,70,200,400,700	100,600,4000,8000	89.52
13	10	10,70,200,400,700	100,200,600,4000,7000	89.03
14	11	10,70,200,400,600, 1000	100,200,600,4000,7000	88.95
15	12	10,60,200,400,600, 1000	100,200,600,3000,6000, 9000	89.22

* in percentage

TABLE 2.9

FAULT ISOLATION RESULTS USING THE NEAREST-NEIGHBOR RULE CRITERION FOR THREE INDUCED FAULTS IN THE VIDEO AMPLIFIER EXAMPLE

Induced Fault	Nearest-Neighbour Rule Criterion For Different Faults																			
	1	2	3	4	5	6	7	8	9	10	11	12	13	14	15	16	17	18	19	20
Q3 BES Fault No. 4	130	29	299	0.6*	7	231	228	69	109	146	119	146	93	141	306	151	264	96	215	148
Q6 BES Fault No. 10	17	179	155	144	148	88	86	69	73	1.2*	14	1.2*	143	36	161	39	142	39	69	36
DZ1S Fault No. 14	18	129	189	139	167	120	117	70	74	35	21	35	300	1.2*	196	40	143	40	104	36

* identifies the minimum distance measure.

TABLE 3.1

RESULTS OF THE DC TESTING OF THE INVERTER CIRCUIT

Input	Output	μ*
V_{in}	V_{out1}	4
V_{in}	V_{out1}, V_{out2}	2
V_{in}	V_{out1}, V_{out2}, I_{cc}	0

TABLE 3.2

RESULTS OF THE DYNAMICAL TESTING OF THE INVERTER CIRCUIT

Input	Output	μ*
$v_{in}(t)$	$v_{out1}(t)$	3
$v_{in}(t)$	$v_{out1(t)}$, $v_{out2(t)}$	0

TABLE 4.1

VOLTAGES AND CURRENTS OF MEASUREMENT NODES OF THE MESH NETWORK

Node No.	Voltage (V)	Current (A)
1	1.246	1.0
2	0.8675	0.0
3	0.8222	0.0
6	0.6494	0.0
7	0.5952	0.0
10	0.3740	0.0
11	0.3896	0.0

TABLE 4.2

DIAGNOSIS OF THE LADDER NETWORK USING NETWORK DECOMPOSITION AND LOGICAL ANALYSIS

Measurements	Computed Currents	Diagnosis	Test
$V_1^m = 2/3$ V	Subnetwork S_1	$I_1^1 + I_1^2 = 0$	LTF_{12}
$V_2^m = 1/3$ V	$I_1^1 = -1/3$ A	$I_2^2 + I_2^3 + I_2^4 \neq 0$	LTF_{234}
$V_3^m = 1/6$ V	Subnetwork S_2	$I_3^4 + I_3^5 = 0$	LTF_{45}
$I_{in} = 1$ A	$I_1^2 = 1/3$ A		
	$I_2^2 = -1/3$ A		
	Subnetwork S_3		
	$I_2^3 = 1/3$ A		
	Subnetwork S_4		
	$I_2^4 = 1/6$ A		
	$I_3^4 = -1/6$ A		
	Subnetwork S_5		
	$I_3^5 = 1/6$ A		

TABLE 6.1

COMPARISON OF THE FAULT LOCATION TECHNIQUES WITH THE PRACTICAL GOALS

	On-Line Computation	Off-Line Computation	Test Nodes	Robustness	Types of Faults	Network Types	Network Models	Diagnosis Level	In-Situ Testing
Fault Dictionary	Minimal	High	Limited	No	Single	Linear/ Nonlinear	Fault	Set	No
Nonlinear Parameter Identification	High	Minimal	Limited	Yes	Multiple	Linear/ Nonlinear	Nominal	Element	No
Linear Parameter Identification	Minimal	Moderate	Almost All Nodes	Yes	Multiple	Mostly Linear	Nominal	Element	No
Combinatorial Fault Verification	Moderate	Minimal	Limited	Yes/No	Multiple	Linear/ Nonlinear	Nominal	Element	Yes
Failure Bounds	Moderate	Minimal	Limited	Yes/No	Multiple	Linear/ Nonlinear	Nominal	Element	Yes
Network Decomposition	Minimal	Minimal	Limited	Yes	Multiple	Linear/ Nonlinear	Nominal	Subnetwork	Yes
Inverse Probability	Moderate	High	Limited	Yes/No	Single	Linear	Nominal	Element	Yes
ℓ_2 Approximation	Minimal	Moderate	Limited	No	Multiple	Linear/ Nonlinear	Nominal	Element	Yes
ℓ_1 Approximation	High	Minimal	Limited	Yes/No	Mostly Single	Linear/ Nonlinear	Nominal	Element	Yes
Goals	Minimal	Moderate	Limited	Yes	Multiple	General	Fault/ Nominal	Module/ Parameter	Yes

Figure Captions

Fig. 1 Classification of the fault location techniques according to the stage in the testing process at which simulation of the tested circuit occurs.

Fig. 2 The block diagram of the dc approach for the construction of a fault dictionary as proposed by Hochwald and Bastian [53].

Fig. 3 The video amplifier circuit example which is utilized by Hochwald and Bastian [53] to illustrate their dc fault dictionary approach.

Fig. 4 The passive circuit example which has been taken from Varghese et al. [169]. We utilize it to illustrate the application of various fault location techniques.

Fig. 5 The loci of the changes in the transfer function of the circuit of Fig. 4 with respect to the changes in the seven different elements of the network at the test frequency $\omega = 200$ rad/sec.

Fig. 6 The use of the pseudo-noise signal to generate the impulse response function of the circuit under test. The output samples provide signatures which describe the condition of the circuit.

Fig. 7a The two-pole Butterworth filter example which has been taken from Schreiber [129], to illustrate the application of the complementary signal method. The nominal parameter values are given by $R_1 = 100\Omega$, $L_1 = \sqrt{2} \times 10^2$H, $C_2 = \sqrt{2} \times 10^{-2}$F and $R_2 = 100\Omega$.

Fig. 7b The response of the circuit of Fig. 7a to the nominal complementary signal. Curve a indicates the case when all parameters are kept at nominal. Curve b indicates the case when C_2 changes by -50% of its nominal value. For the complementary signal we have $\alpha_0 = 1, \alpha_1 = -1.318, \alpha_2 = 0.493$ and $\tau = 0.5$ sec.

Fig. 8 Grouping faults using heuristic as well as fault bands techniques. Profile (a) represents the fault bands profile, profile (b) represents the nominal fault profile and profile (c) represents the heuristic fault profile. F_i represents an ambiguity faulty set.

Fig. 9 The flow diagram of the iterative procedure of optimum measurement selection utilizing the heuristic technique which has been proposed by Varghese et al. [169].

Fig. 10a A simple RLC passive circuit utilized to illustrate the application of the D-criterion in obtaining the optimum measurements.

Fig. 10b The dependency of the determinant of Λ_{mm} on the choice of test frequency. The dashed curve a is for the case when $|V_{out1}|$ is the output and the solid curve b for the case when $|V_{out2}|$ is the output.

Fig. 11 Comparison of fault isolation using two different criteria as reported by Huanca and Spence [55].

Fig. 12 The representation of fault conditions by switches as proposed by Lin [69]. (a) represents an open circuit fault condition, (b) represents short circuit fault condition and (c) represents a fixed resistance change fault condition.

Fig. 13 Multiport representation of a faulty network obtained by extracting n_d ideal diodes, n_m measurement ports and n_s switches from the original network [69].

Fig. 14 A fault model of the transistor which has been proposed by Tucker et al. [165], that can be used in conjunction with any computer-aided analysis program. The normal unfaulted resistor values are given by $R_1 = R_2 = R_3 = 0.01\ \Omega$ and $R_4 = R_5 = R_6 = 100\ M\Omega$. The different realizable fault conditions are given as follows.

Fault Condition	Resistor Value
Collector Open	$R_1 = 100\ M\Omega$
Base Open	$R_2 = 100\ M\Omega$
Emitter Open	$R_3 = 100\ M\Omega$
Collector-Base Short	$R_4 = 0.01\ \Omega$
Collector-Emitter Short	$R_5 = 0.01\ \Omega$
Emitter-Base Short	$R_6 = 0.01\ \Omega$

Fig. 15 A simple nonlinear resistive circuit example that has been utilized to illustrate the application of the nonlinear dc testing theory which has been developed by Visvanathan and Sangiovanni-Vincentelli [172].

Fig. 16 A simple illustrative example that has been utilized by Saeks et al. [122] to illustrate the application of the theory of nonlinear dynamic network testing.

Fig. 17a The transistor inverter circuit that has been utilized by Visvanathan and Sangiovanni-Vincentelli [173] to illustrate the practical application of the time domain testing theory. The nominal element values are given by $R_1 = 4k\Omega$, $R_2 = 1.6\ k\Omega$, $R_3 = 130\ \Omega$, $R_4 = 1\ k\Omega$ and $I_{sd} = 1.0x10^{-14}$ A.

Fig. 17b The transistor model that is utilized in the simulation of the transistor inverter circuit. The nominal element and parameter values are given by $r_{cc}' = 75\ \Omega$, $r_{bb}' = 200\ \Omega$, $r_{ee}' = 2\ \Omega$, $C_{bc} = C_{be} = 1$ pF, $\beta_F = 200$, $\beta_R = 2$ and $I_s = 1.5x10^{-15}$ A.

Fig. 18 A simple RC passive network.

Fig.19 A linear passive resistive network that has been proposed by Navid and Willson [91] to illustrate the application of their linear resistive network testing theory.

Fig. 20a The resistive network of Fig. 19 after eliminating node 5.

Fig. 20b The resistive network of Fig. 19 after eliminating nodes 5 and 6. All elements of the resultant network could be obtained by direct measurements.

Fig. 20c The graph representation of the equations that are used in reviving node 6. The graph is a connected dendroid.

Fig. 20d The graph representation of the equations that are used in reviving node 5.

Fig. 21a The ladder network example which is used to illustrate the application of different fault location techniques.

Fig. 21b The proper tree of the ladder network is indicated by solid lines.

Fig. 22a The adjoint network that is used for identifying the changes in G_1 and G_2 from their nominal values.

Fig. 22b The adjoint network that is used for identifying the changes in G_4 and G_5 from their nominal values.

Fig. 22c The adjoint network that is used for identifying the changes in G_2, G_3 and G_4 from their nominal values.

Fig. 23 The resistive network that is utilized to illustrate the application of the internal-self-testing condition in identifying faulty regions.

Fig. 24 The tree of decomposition obtained during testing using ISTC.

Fig. 25 The subnetworks obtained during testing of the network of Fig. 23.

Fig. 26 Decomposition of the ladder network of Fig. 21a into five subnetworks using measurement nodes 1, 2 and 3.

Fig. 27 The effect of increasing tolerances on the degree of diagnosability. This figure is constructed using data that has been published in [170]. Curve a indicates the case when the tolerances on the nonfaulty elements are $\pm 3\%$, curve b for $\pm 6\%$ tolerances, and curve c for $\pm 9\%$ tolerances.

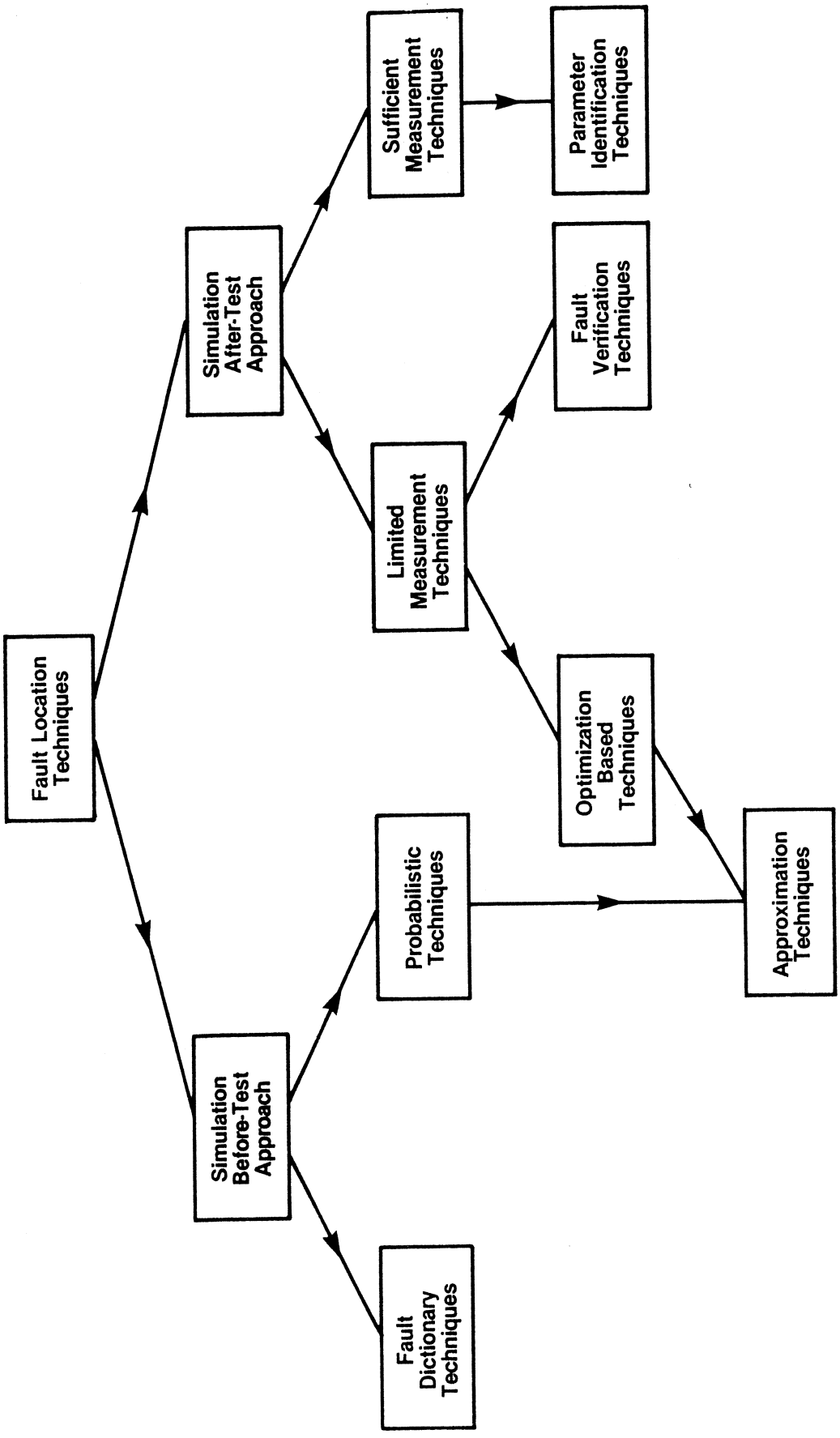
Fault Location Techniques
Simulation After-Test Approach
Simulation Before-Test Approach
Sufficient Measurement Techniques
Parameter Identification Techniques
Limited Measurement Techniques
Fault Verification Techniques
Optimization Based Techniques
Probabilistic Techniques
Approximation Techniques
Fault Dictionary Techniques

Fig. 1

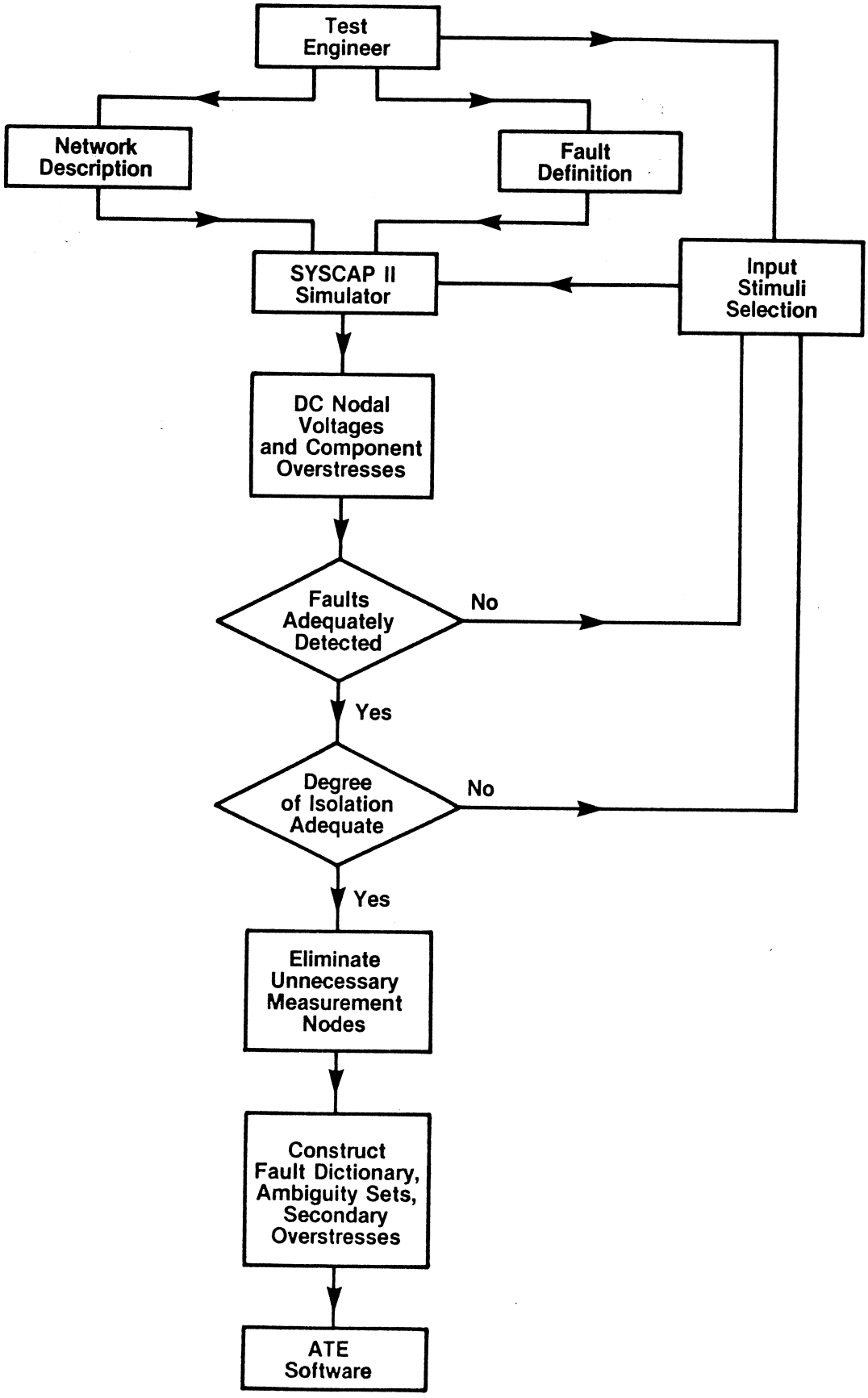
Test Engineer
Network Description
Fault Definition
SYSCAP II Simulator
Input Stimuli Selection
DC Nodal Voltages and Component Overstresses
Faults Adequately Detected
No
Yes
Degree of Isolation Adequate
No
Yes
Eliminate Unnecessary Measurement Nodes
Construct Fault Dictionary, Ambiguity Sets, Secondary Overstresses
ATE Software

Fig. 2

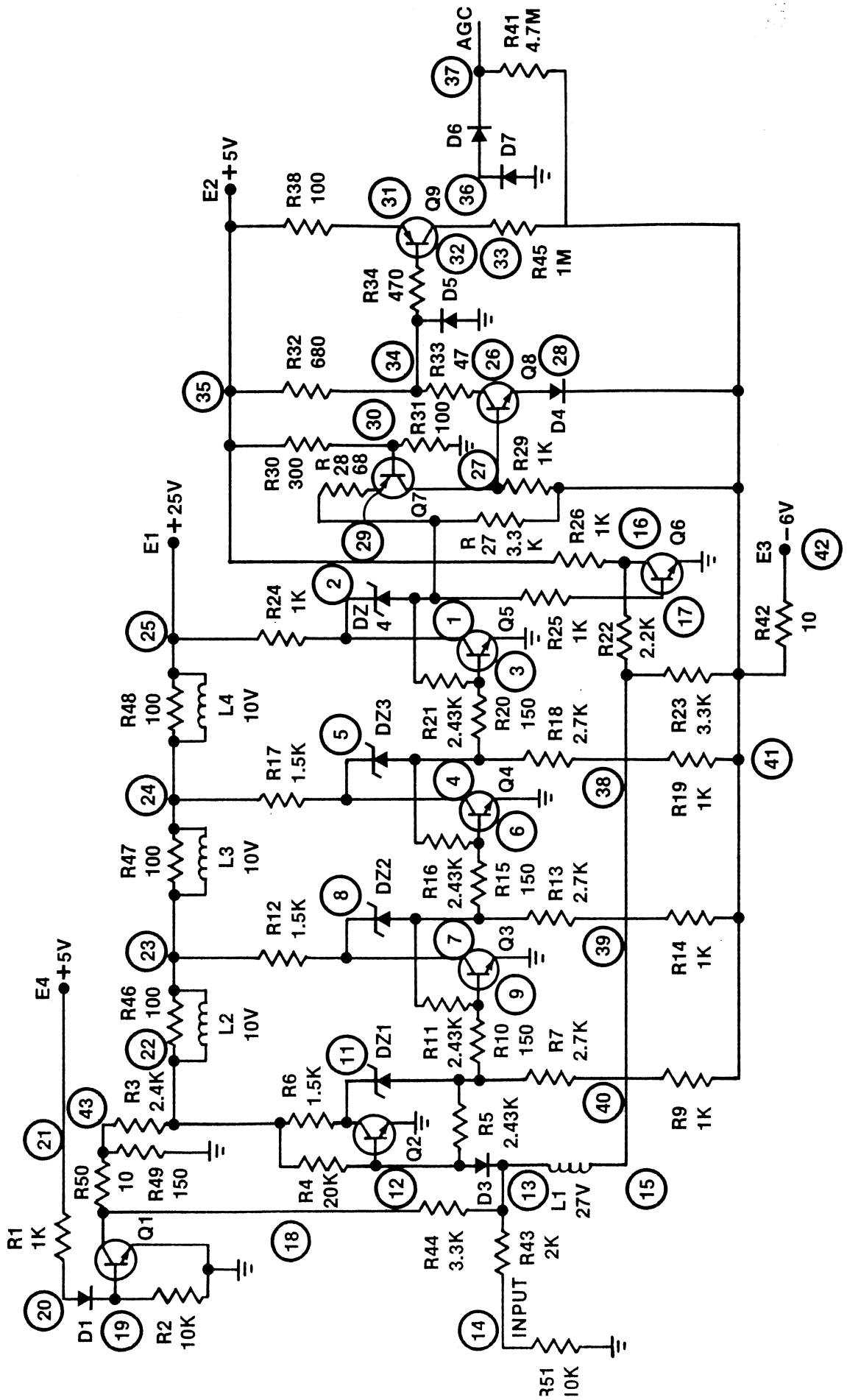
E4 +5V
E1 +25V
E2 +5V
E3 -6V
AGC
INPUT
R1 1K
R2 10K
R3 2.4K
R4 20K
R5 2.43K
R6 1.5K
R7 2.7K
R9 1K
R10 150
R11 2.43K
R12 1.5K
R13 2.7K
R14 1K
R15 150
R16 2.43K
R17 1.5K
R18 2.7K
R19 1K
R20 150
R21 2.43K
R22 2.2K
R23 3.3K
R24 1K
R25 1K
R26 1K
R27 3.3K
R28 68
R29 1K
R30 300
R31 100
R32 680
R33 47
R34 470
R38 100
R41 4.7M
R42 10
R43 2K
R44 3.3K
R45 1M
R46 100
R47 100
R48 100
R49 150
R50 10
R51 10K
L1 27V
L2 10V
L3 10V
L4 10V
DZ1
DZ2
DZ3
DZ 4
D1
D3
D4
D5
D6
D7
Q1
Q2
Q3
Q4
Q5
Q6
Q7
Q8
Q9

Fig. 3

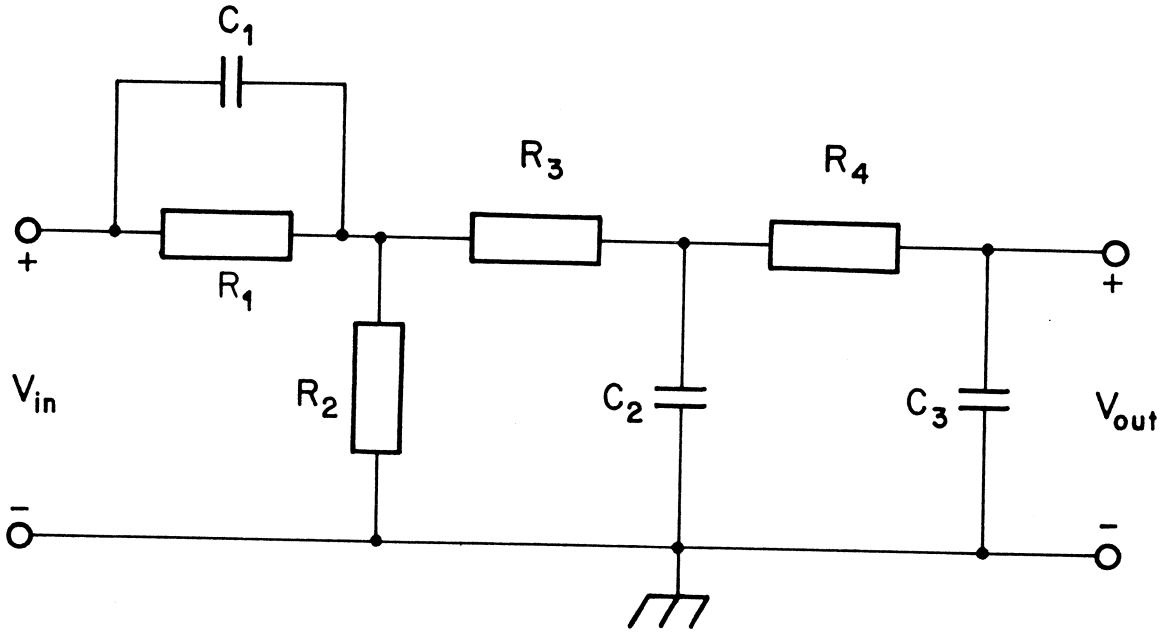

Fig. 4

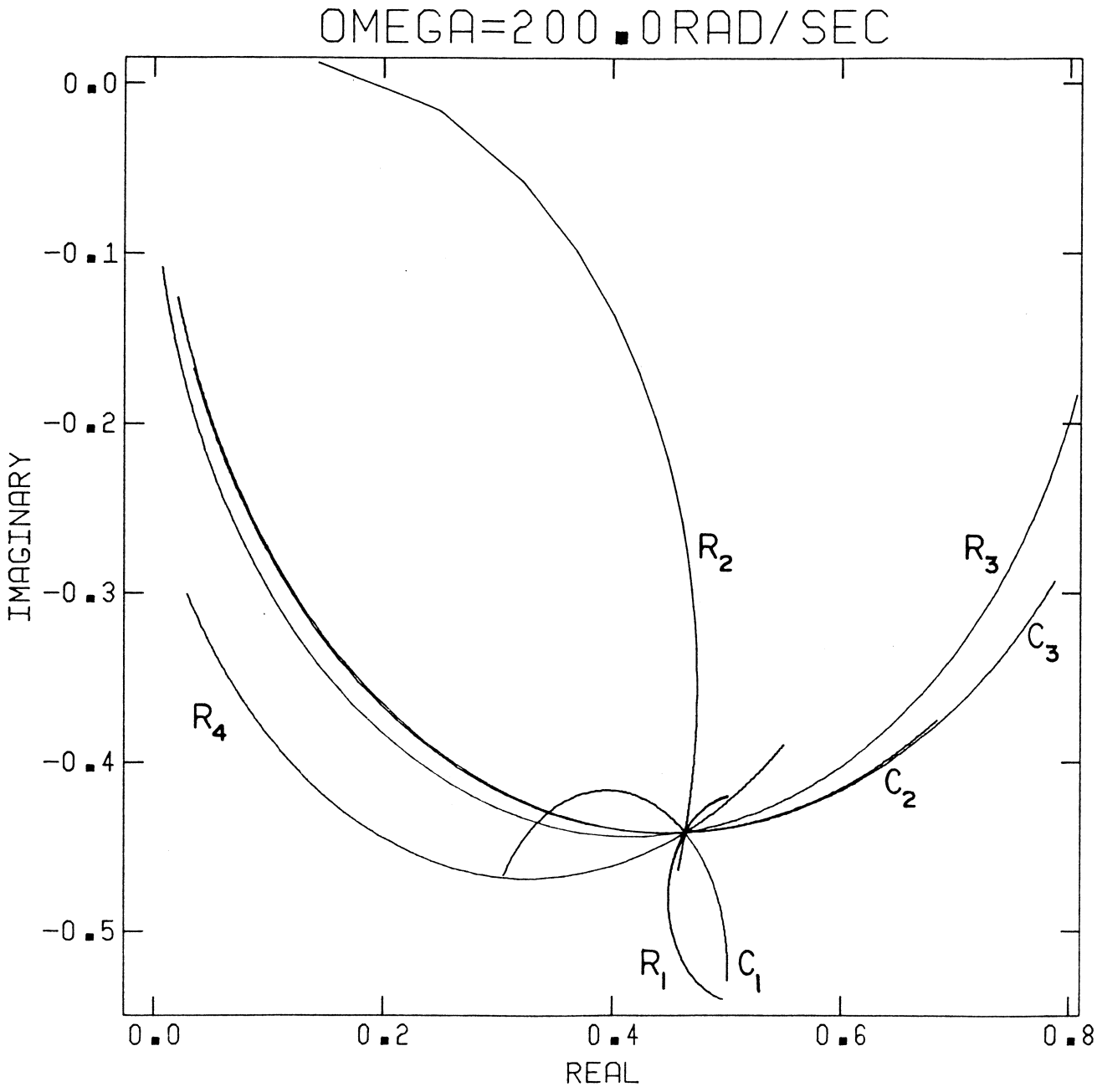
OMEGA=200.0RAD/SEC
0.0
-0.1
-0.2
-0.3
-0.4
-0.5
IMAGINARY
0.0
0.2
0.4
0.6
0.8
REAL
R1
R2
R3
R4
C1
C2
C3

Fig. 5

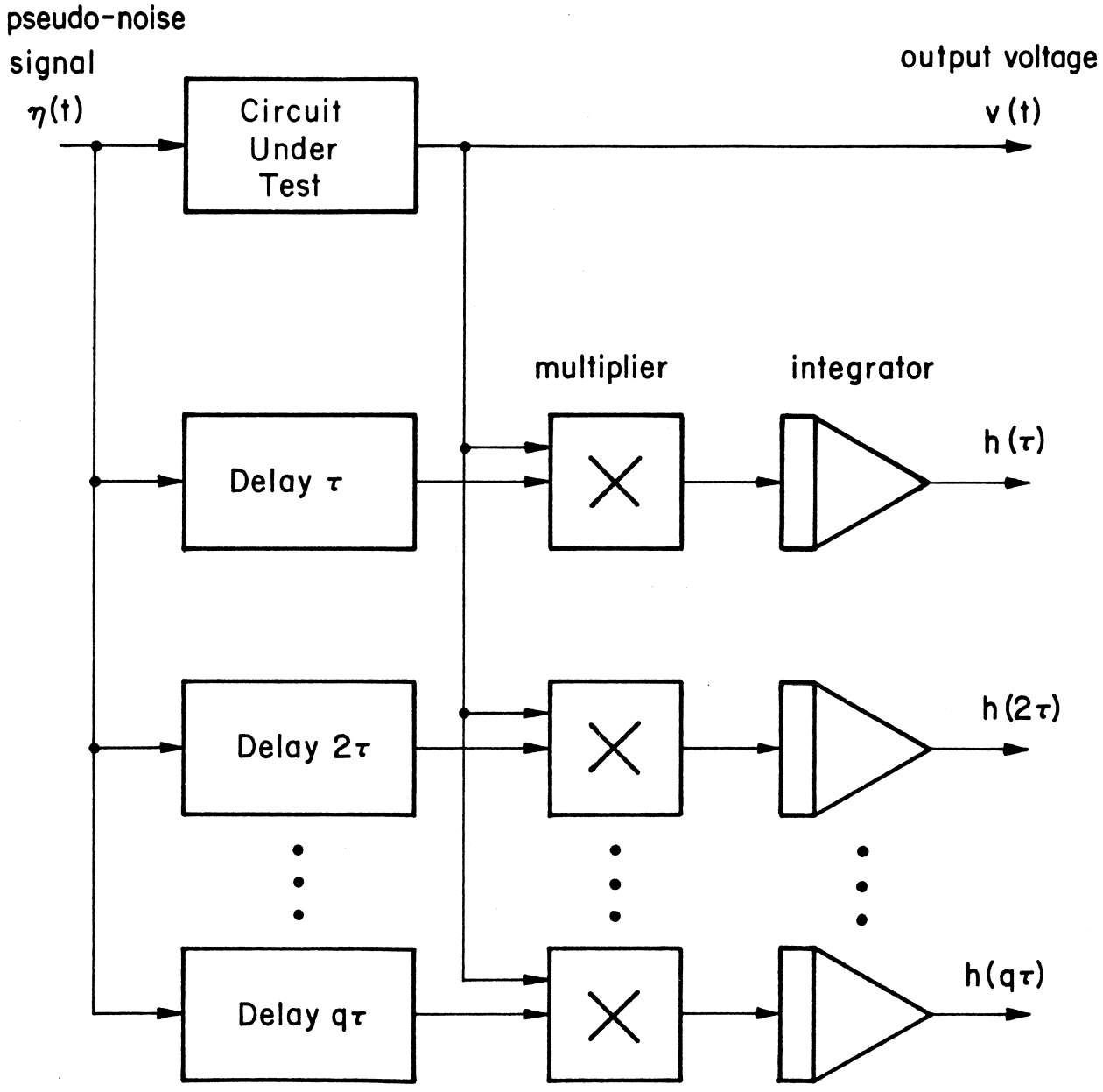
pseudo-noise
signal
η(t)
Circuit
Under
Test
output voltage
v(t)
multiplier
integrator
Delay τ
h(τ)
Delay 2τ
h(2τ)
Delay qτ
h(qτ)

Fig. 6

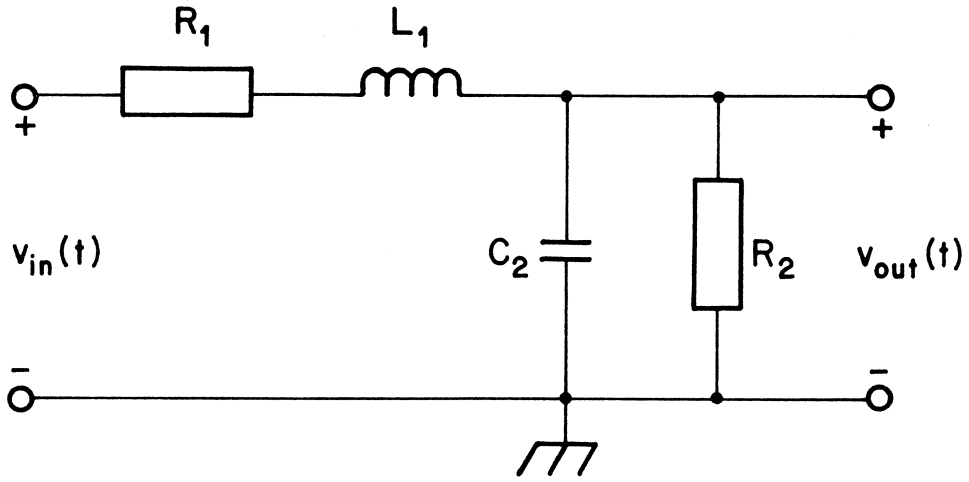

Fig. 7a

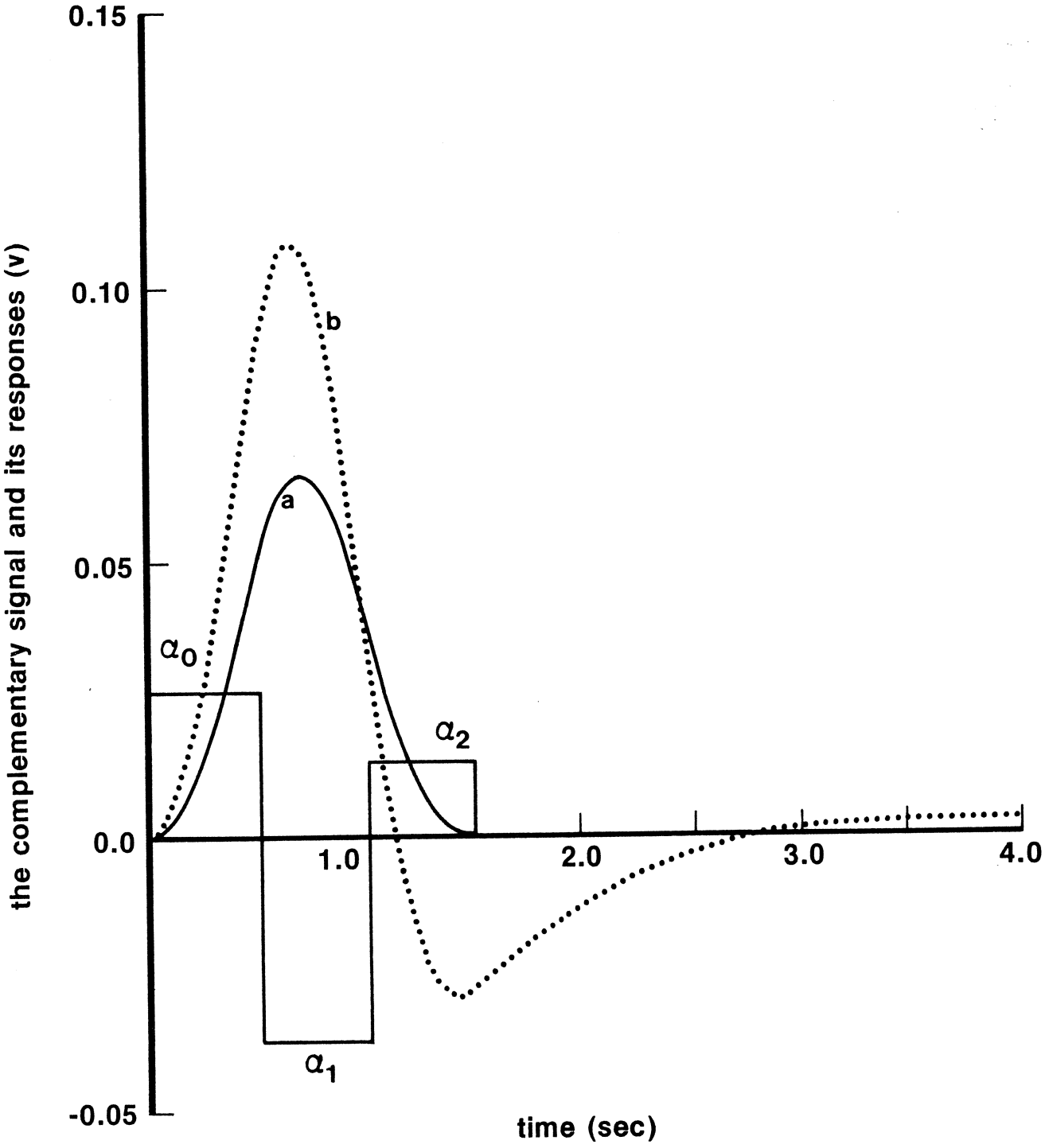
0.15
0.10
0.05
0.0
-0.05
the complementary signal and its responses (v)
b
a
α_0
α_2
α_1
1.0
2.0
3.0
4.0
time (sec)

Fig. 7b

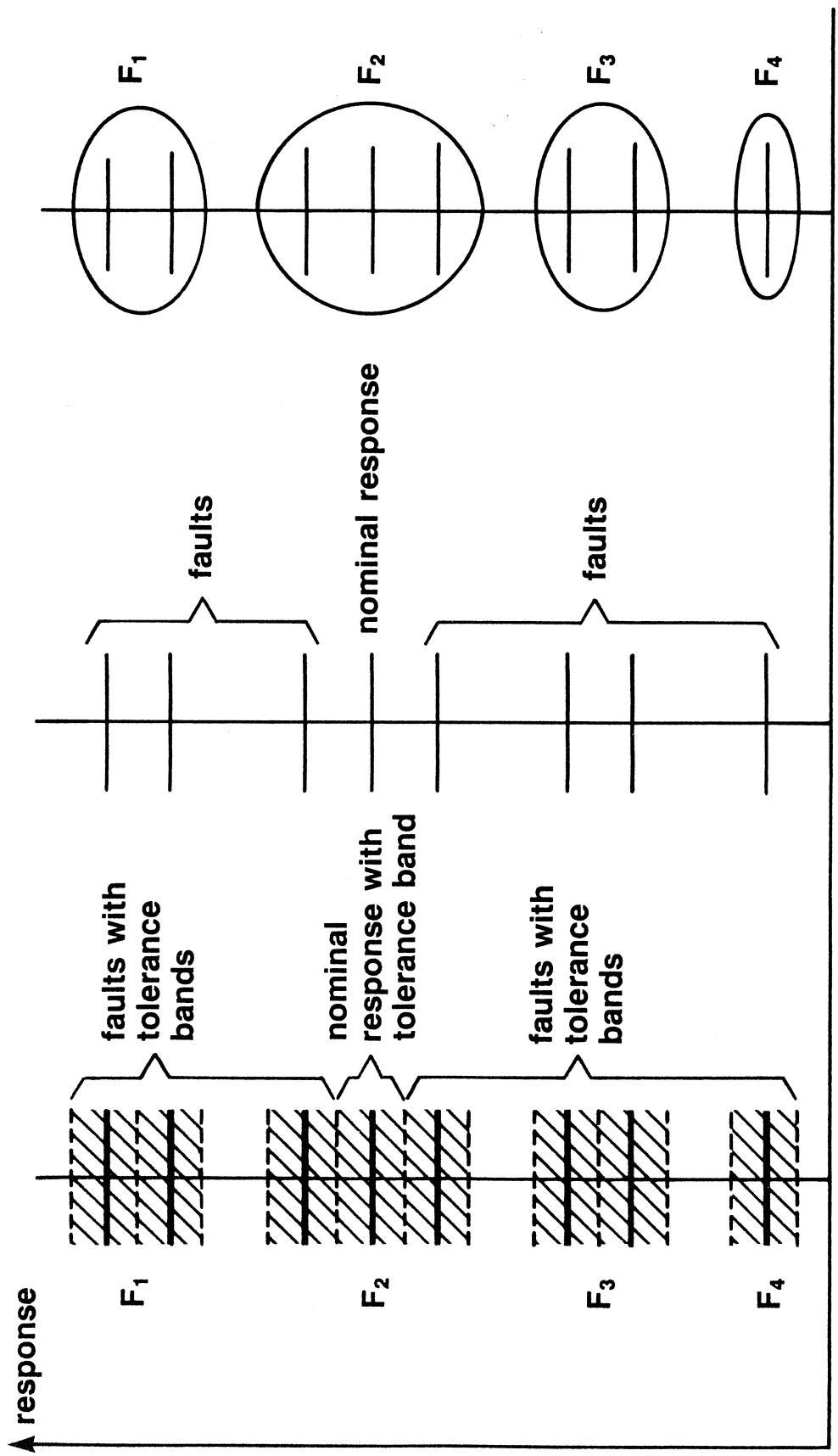
response
faults with tolerance bands
nominal response with tolerance band
faults with tolerance bands
F1
F2
F3
F4
(a)
faults
nominal response
faults
(b)
F1
F2
F3
F4
(c)

Fig. 8

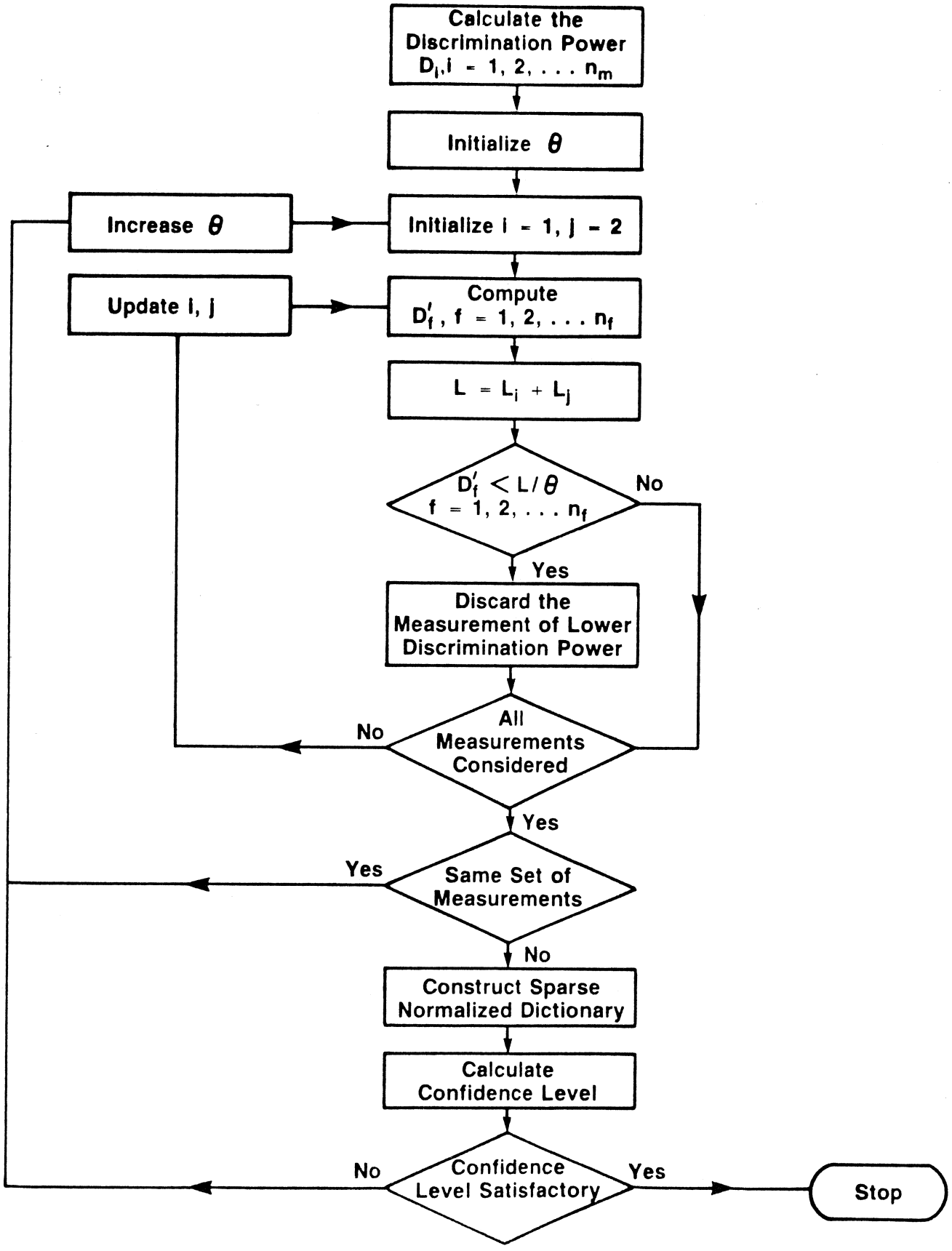
Calculate the Discrimination Power $D_i, i = 1, 2, \ldots n_m$
Initialize θ
Increase θ
Initialize i = 1, j = 2
Update i, j
Compute D'_f, $f = 1, 2, \ldots n_f$
$L = L_i + L_j$
$D'_f < L/\theta$ $f = 1, 2, \ldots n_f$
No
Yes
Discard the Measurement of Lower Discrimination Power
All Measurements Considered
No
Yes
Same Set of Measurements
Yes
No
Construct Sparse Normalized Dictionary
Calculate Confidence Level
Confidence Level Satisfactory
No
Yes
Stop

Fig. 9

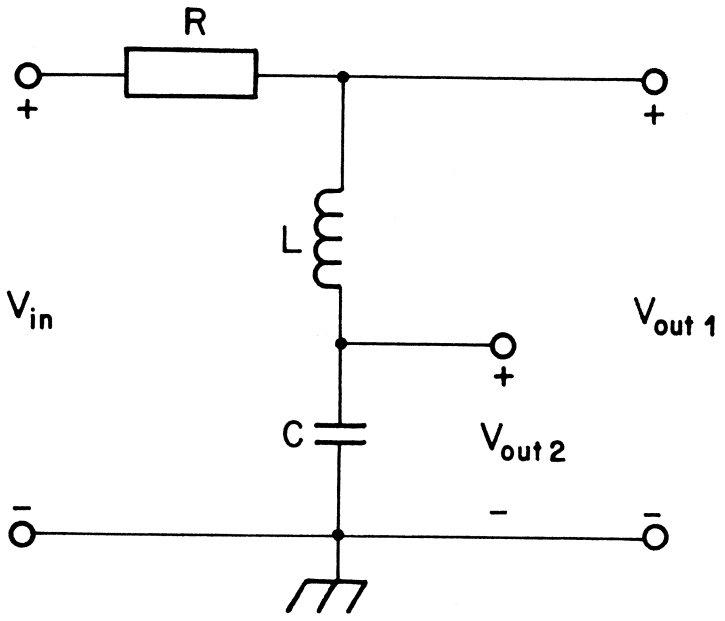

Fig. 10a

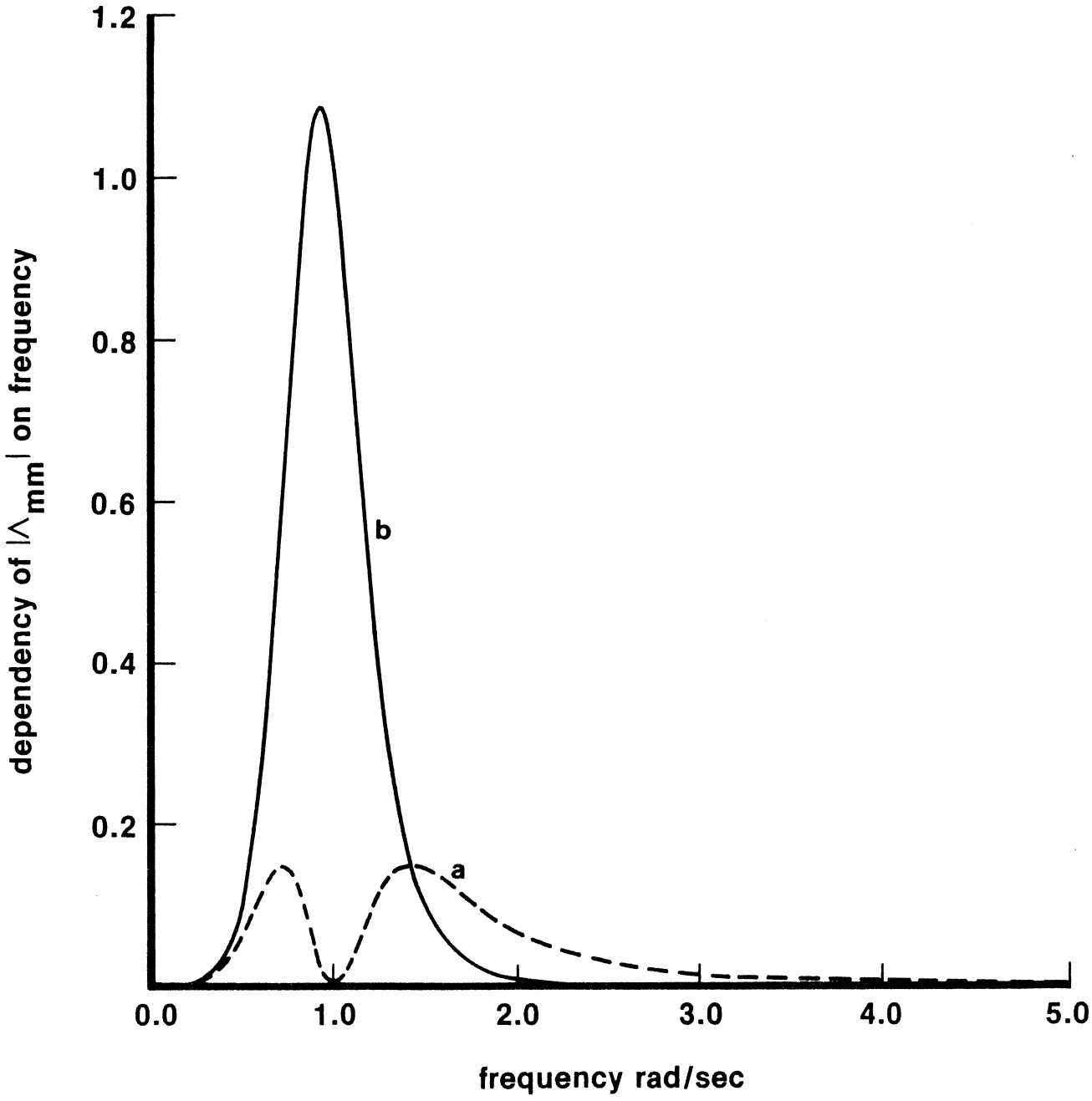
1.2
1.0
0.8
0.6
0.4
0.2
dependency of $|\Lambda_{mm}|$ on frequency
b
a
0.0
1.0
2.0
3.0
4.0
5.0
frequency rad/sec

Fig. 10b

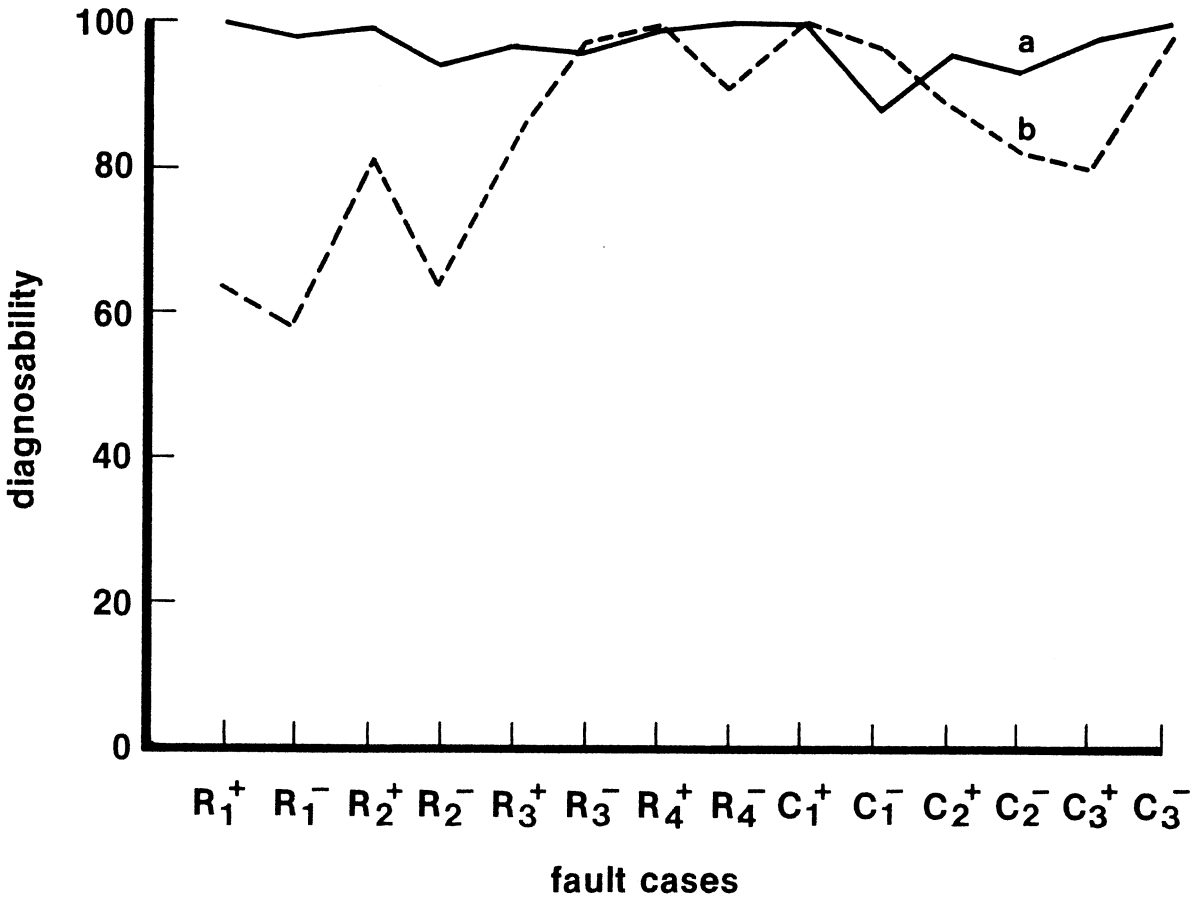
100
80
60
40
20
0
diagnosability
a
b
R_1^+ R_1^- R_2^+ R_2^- R_3^+ R_3^- R_4^+ R_4^- C_1^+ C_1^- C_2^+ C_2^- C_3^+ C_3^-
fault cases

Fig. 11

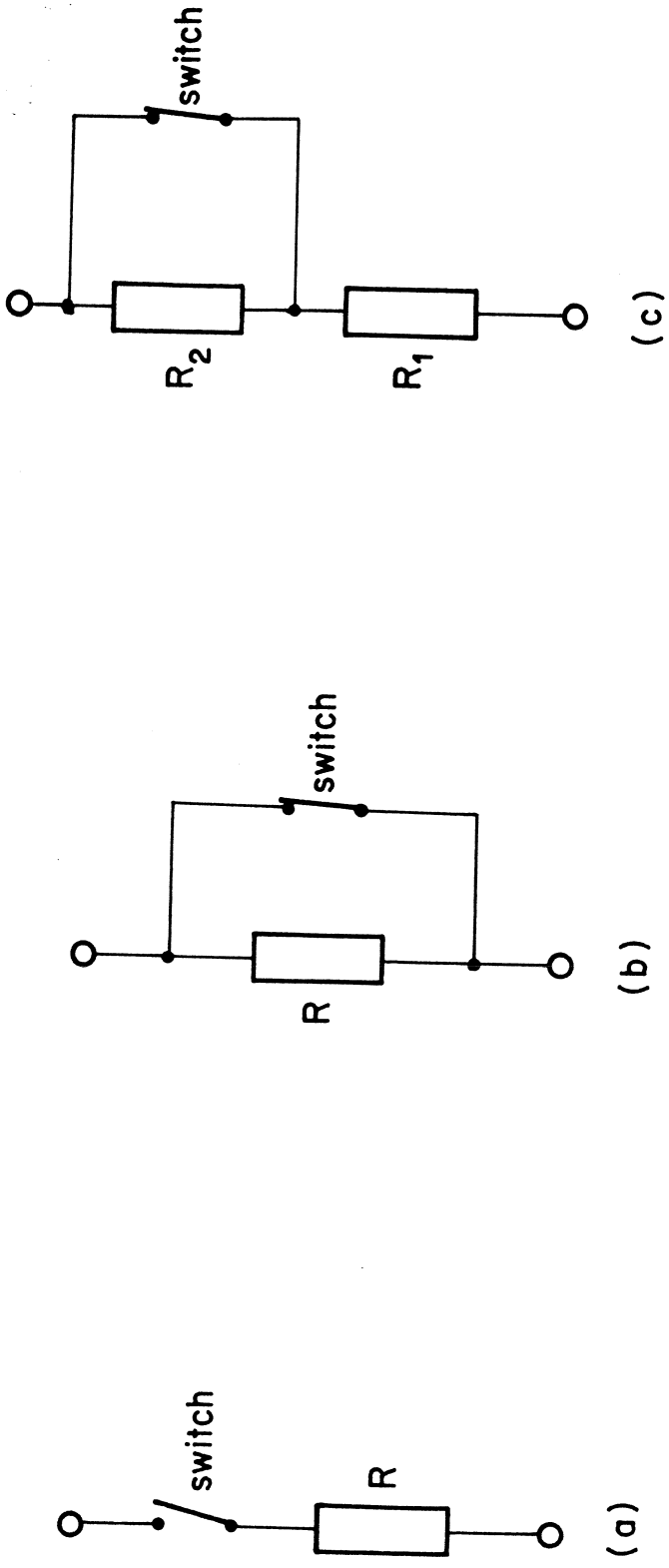

Fig. 12

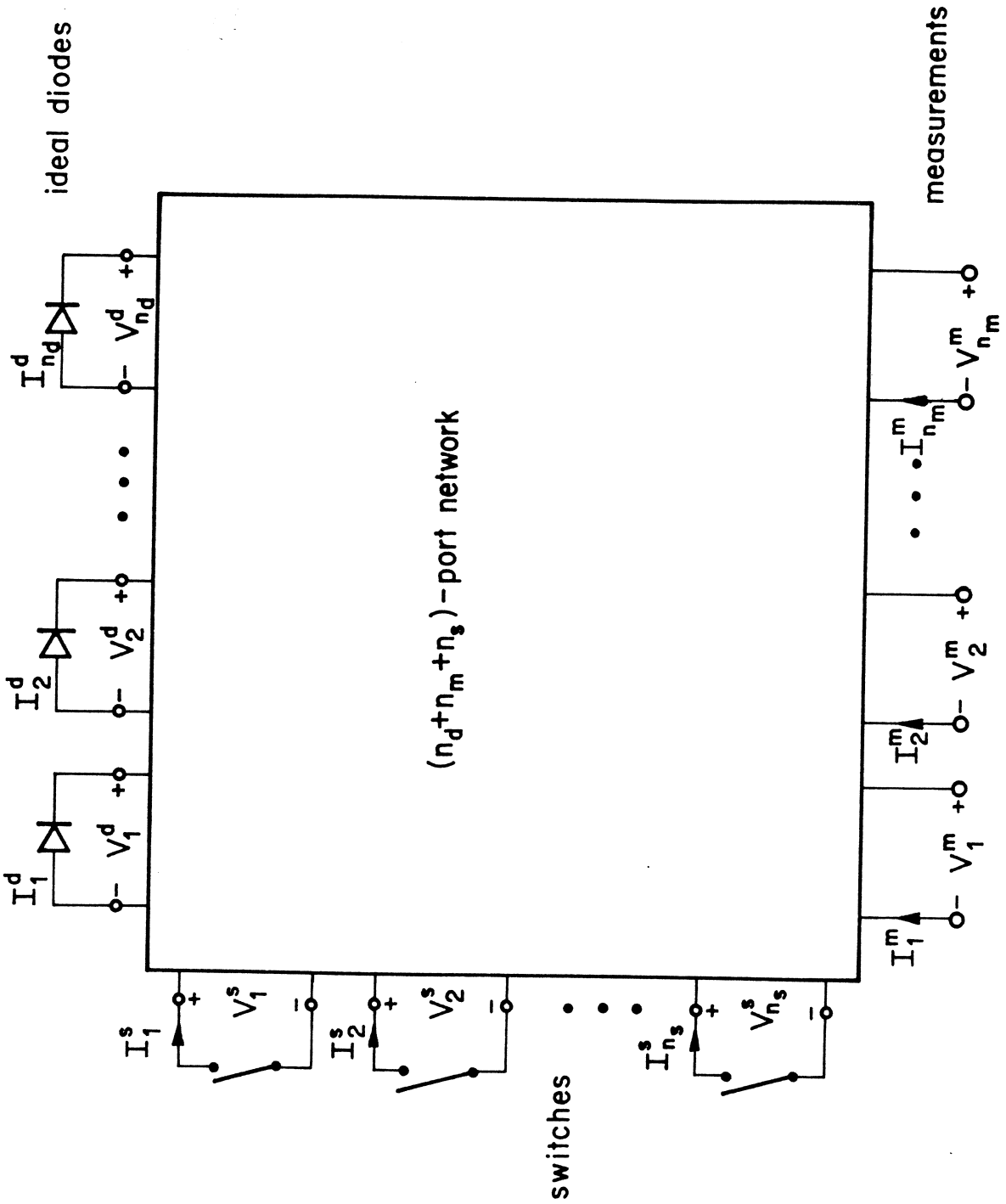
ideal diodes
measurements
switches
$(n_d+n_m+n_s)$-port network
I^d_1
V^d_1
I^d_2
V^d_2
$I^d_{n_d}$
$V^d_{n_d}$
I^m_1
V^m_1
I^m_2
V^m_2
$I^m_{n_m}$
$V^m_{n_m}$
I^s_1
V^s_1
I^s_2
V^s_2
$I^s_{n_s}$
$V^s_{n_s}$

Fig. 13

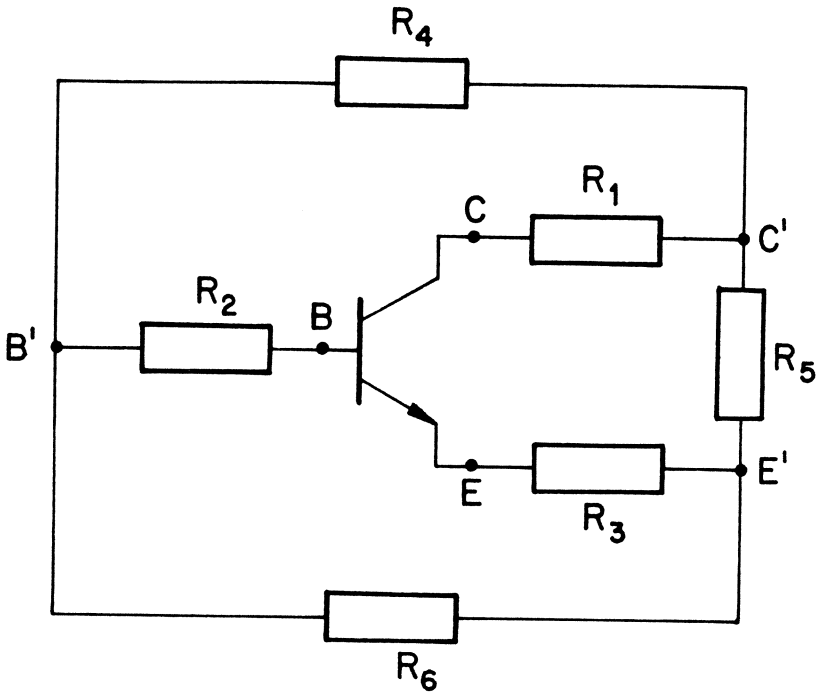

Fig. 14

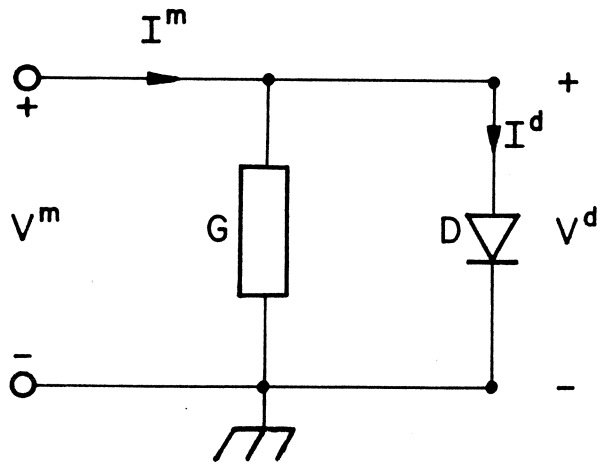

Fig. 15

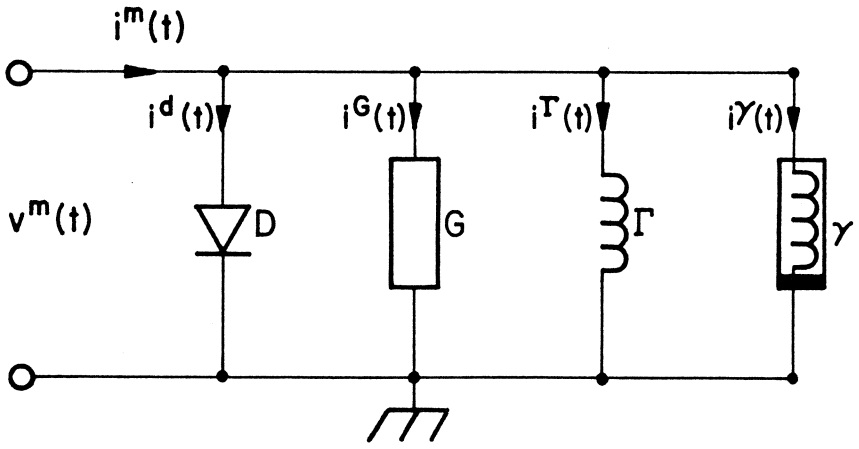

Fig. 16

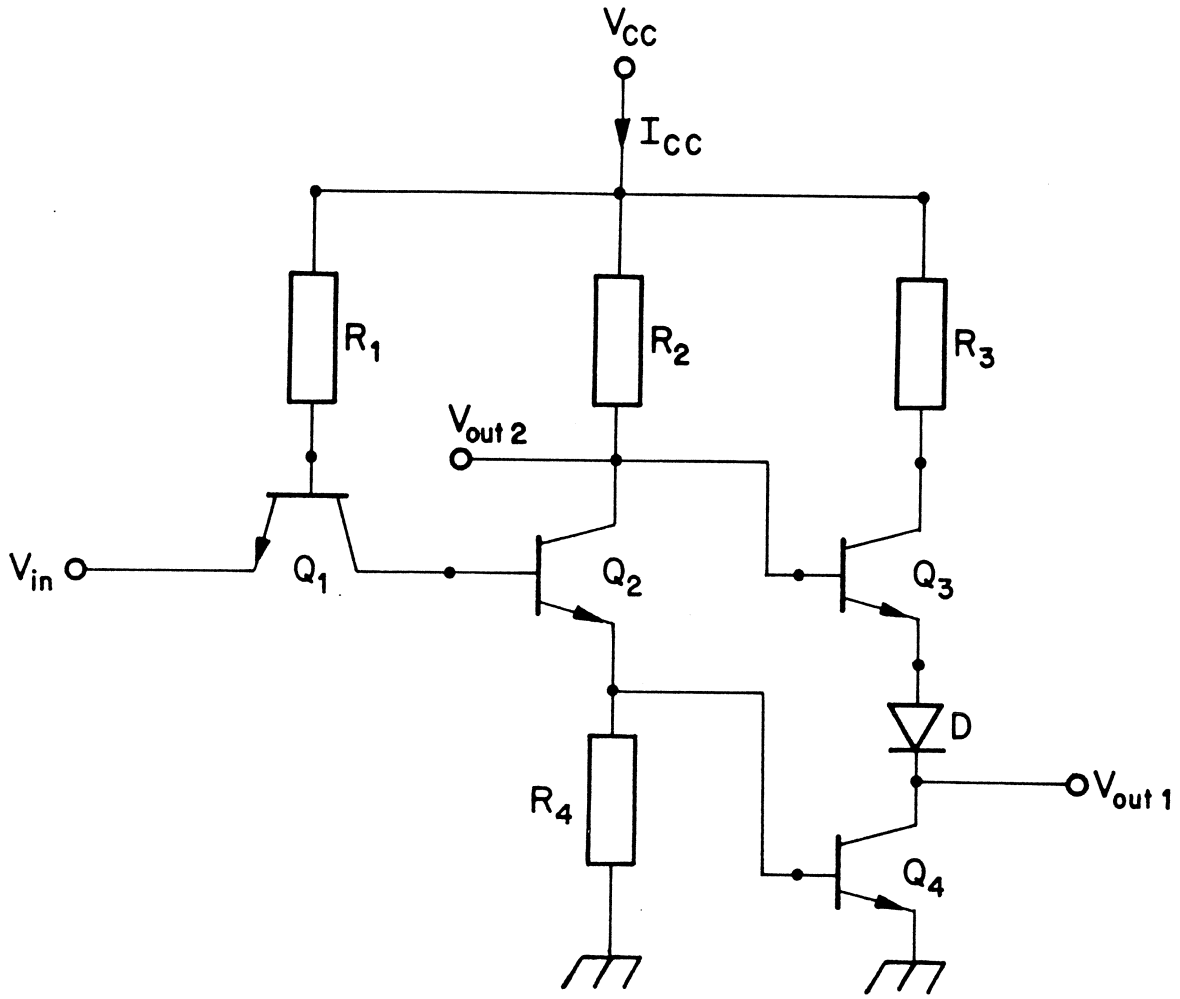

Fig. 17a

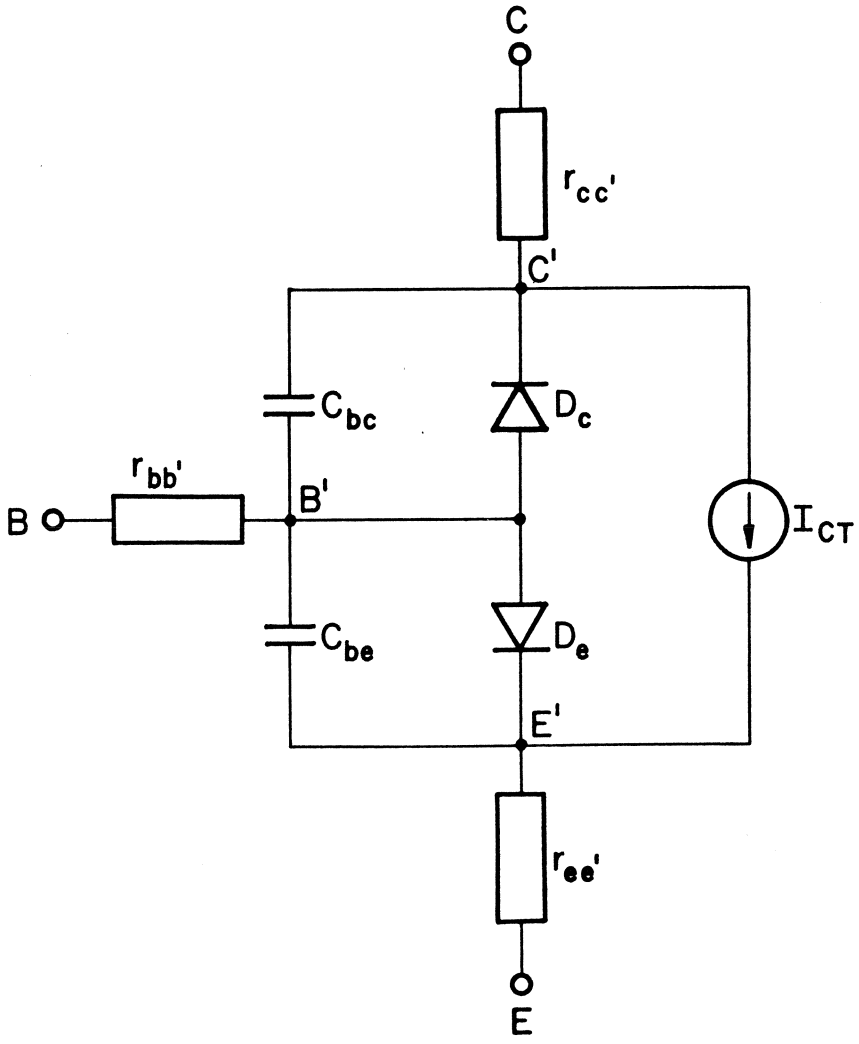

Fig. 17b

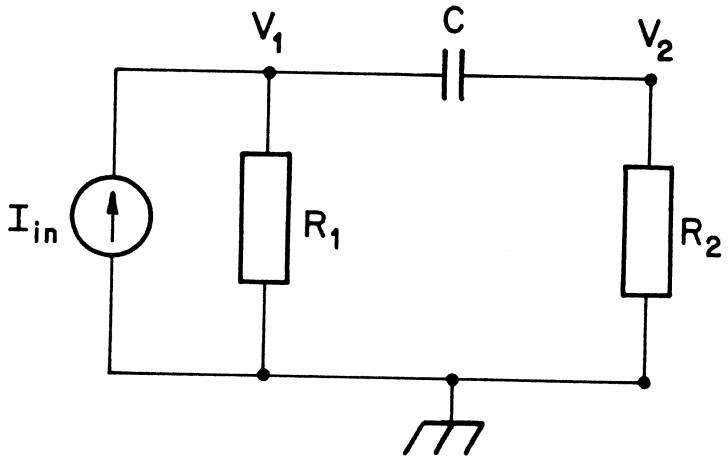

Fig. 18

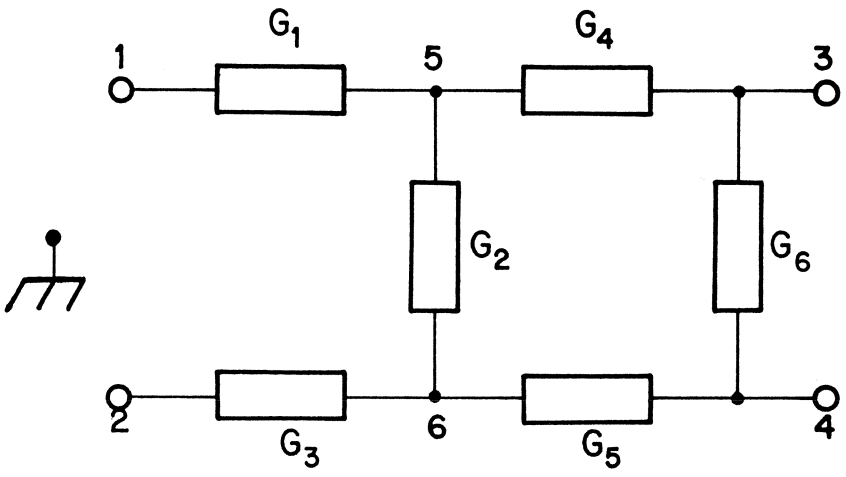

Fig. 19

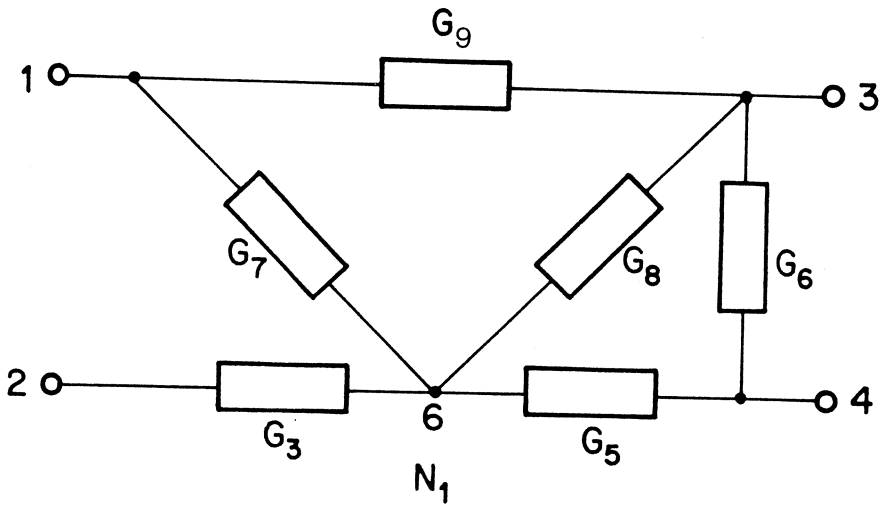

Fig. 20a

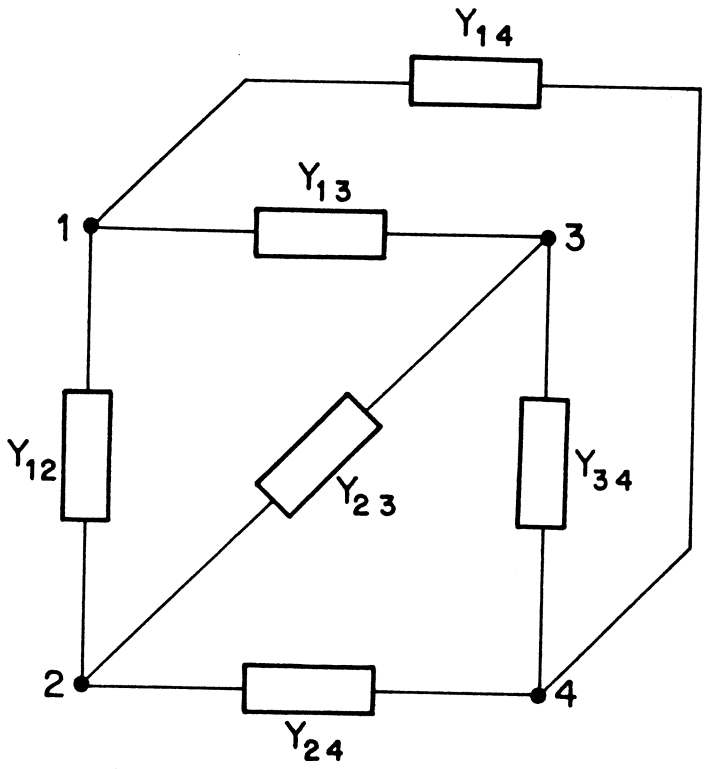

Fig. 20b

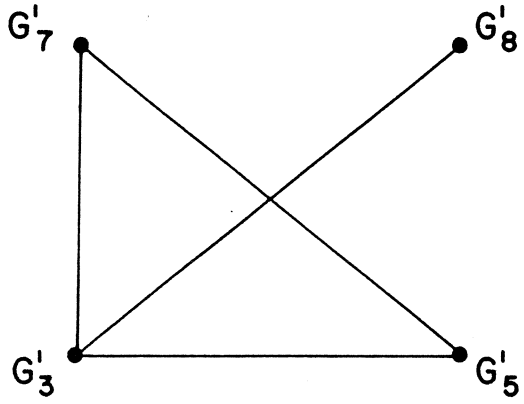

Fig. 20c

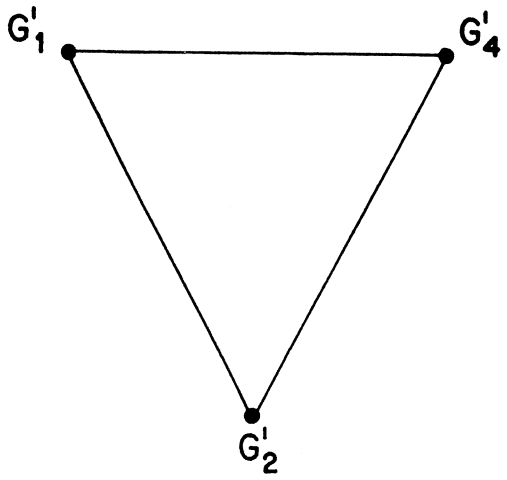

Fig. 20d

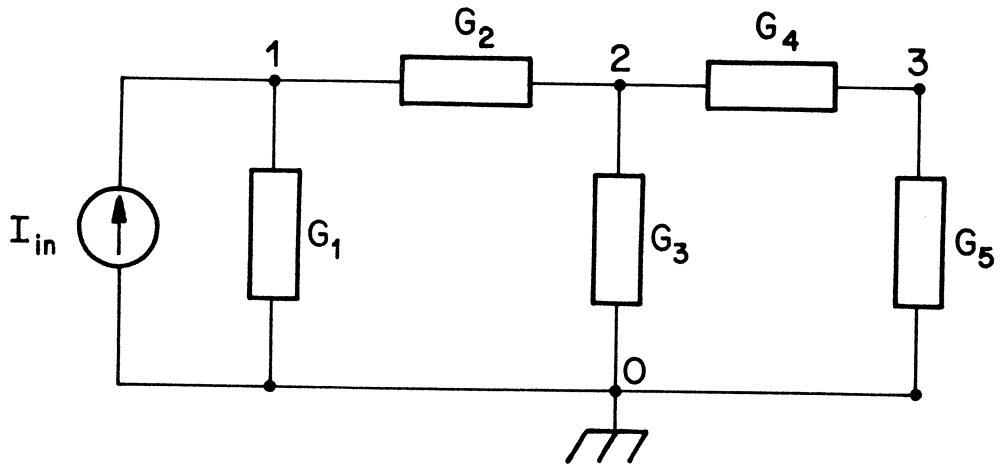

Fig. 21a

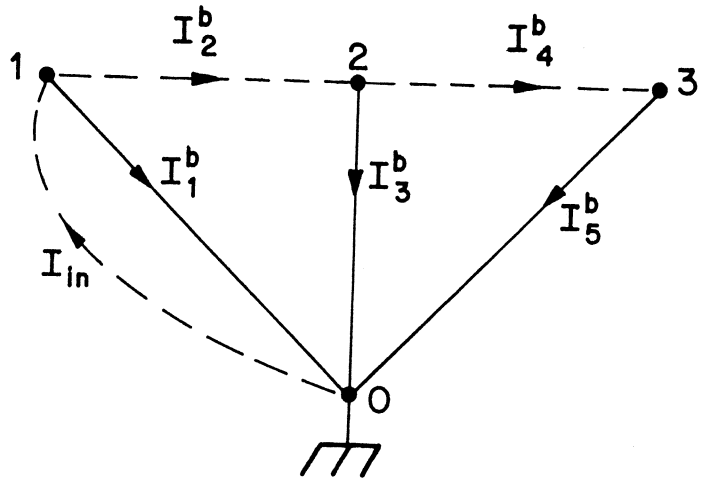

Fig. 21b

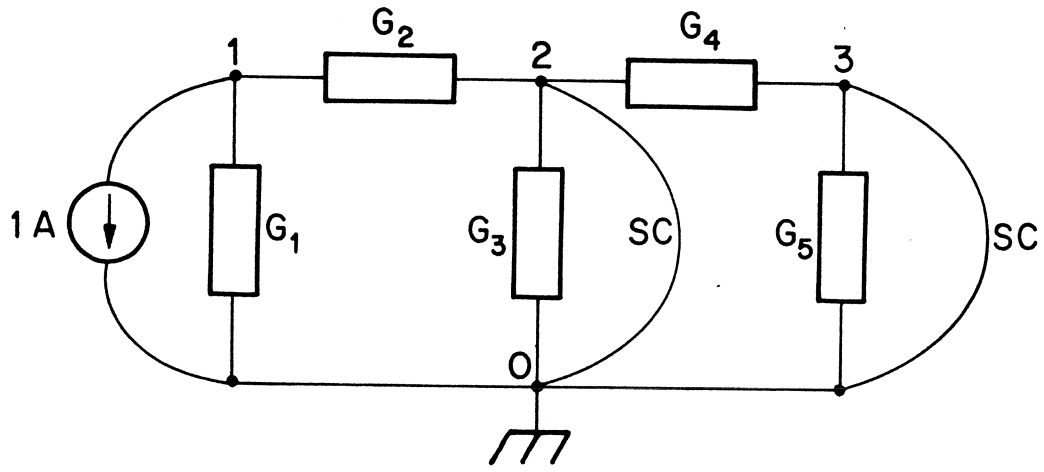

Fig. 22a

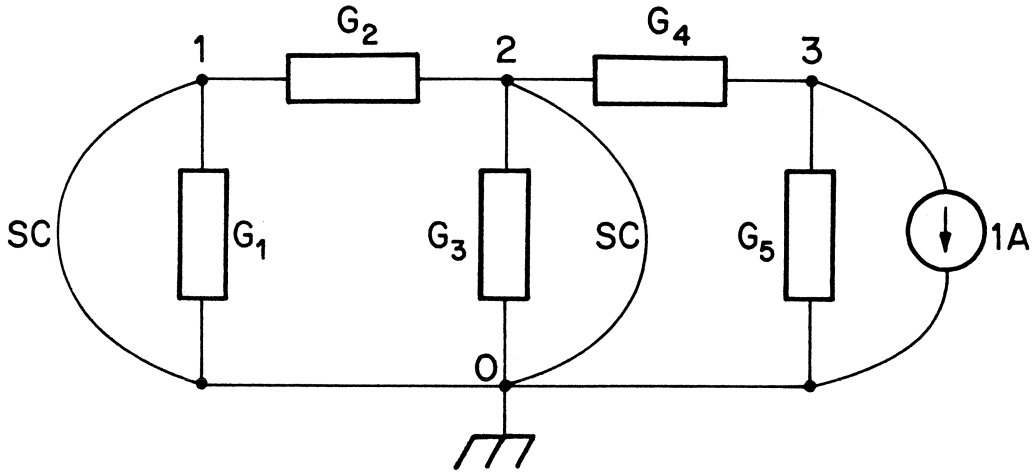

Fig. 22b

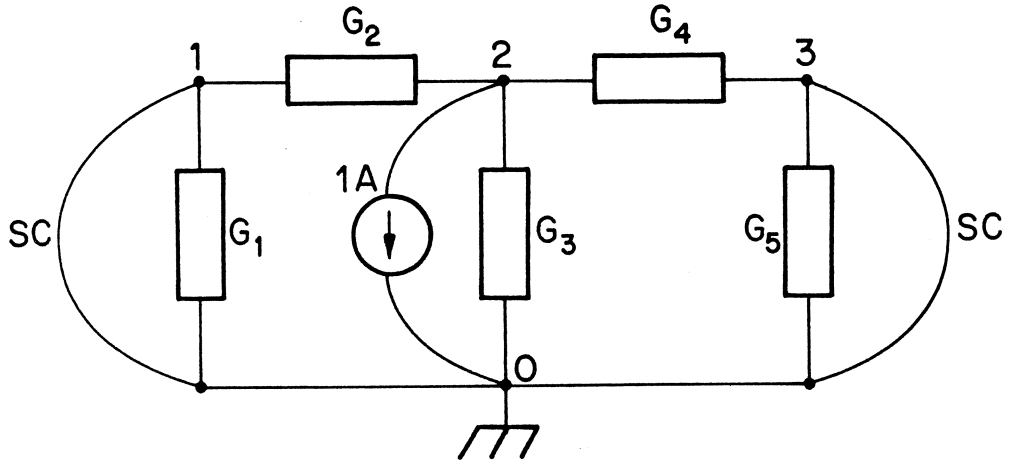

Fig. 22c

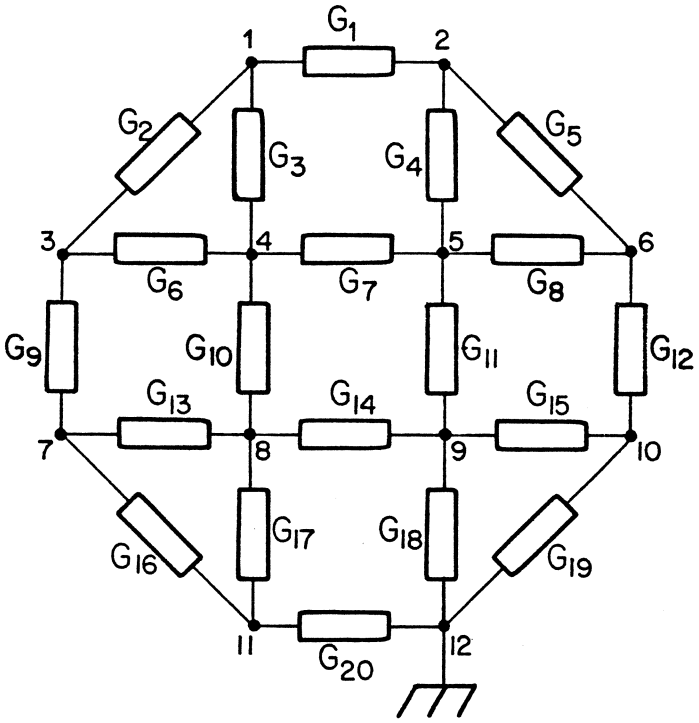
G1
1
2
G2
G3
G4
G5
3
4
5
6
G6
G7
G8
G9
G10
G11
G12
G13
G14
G15
7
8
9
10
G16
G17
G18
G19
11
12
G20

Fig. 23

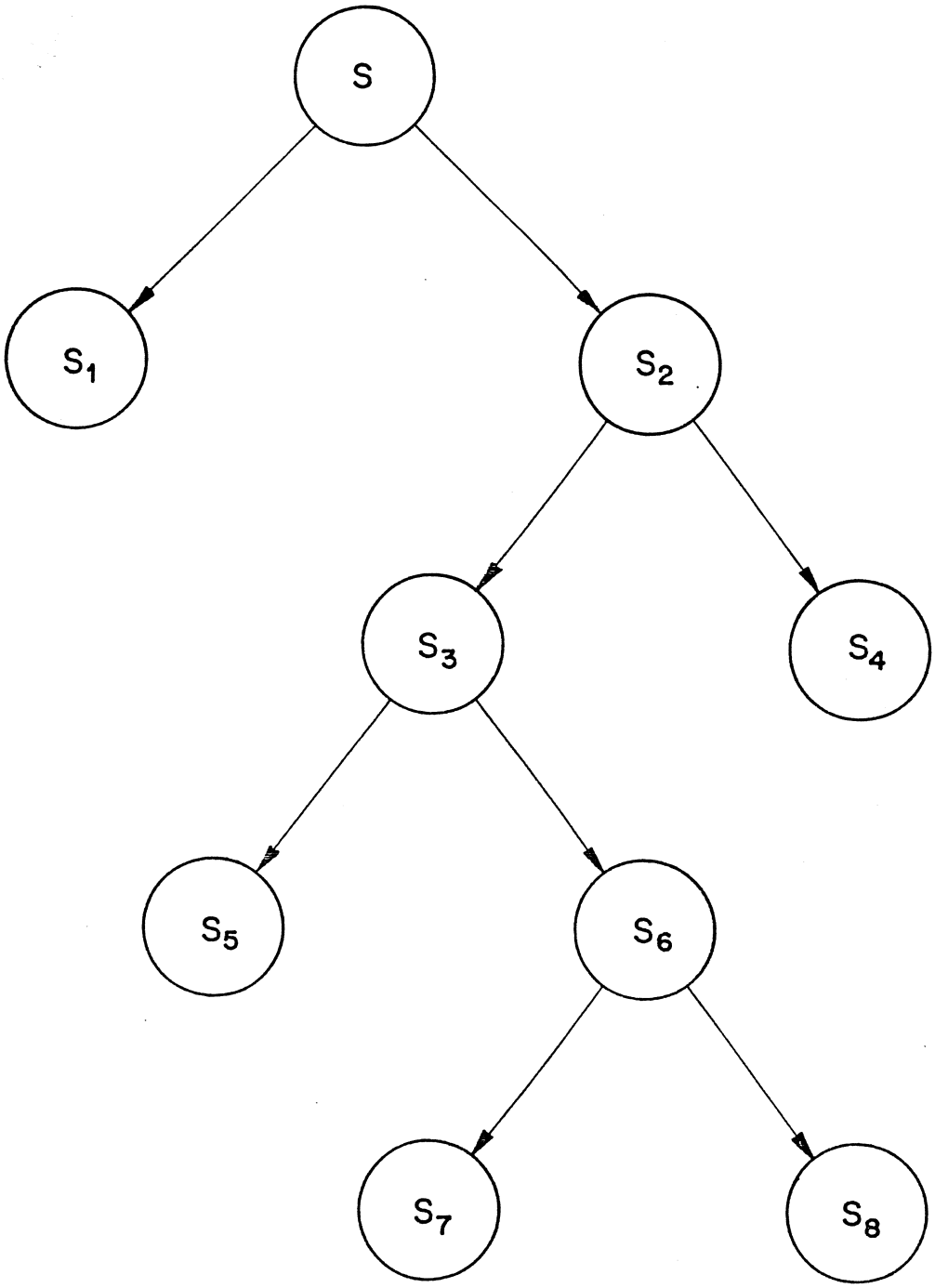

Fig. 24

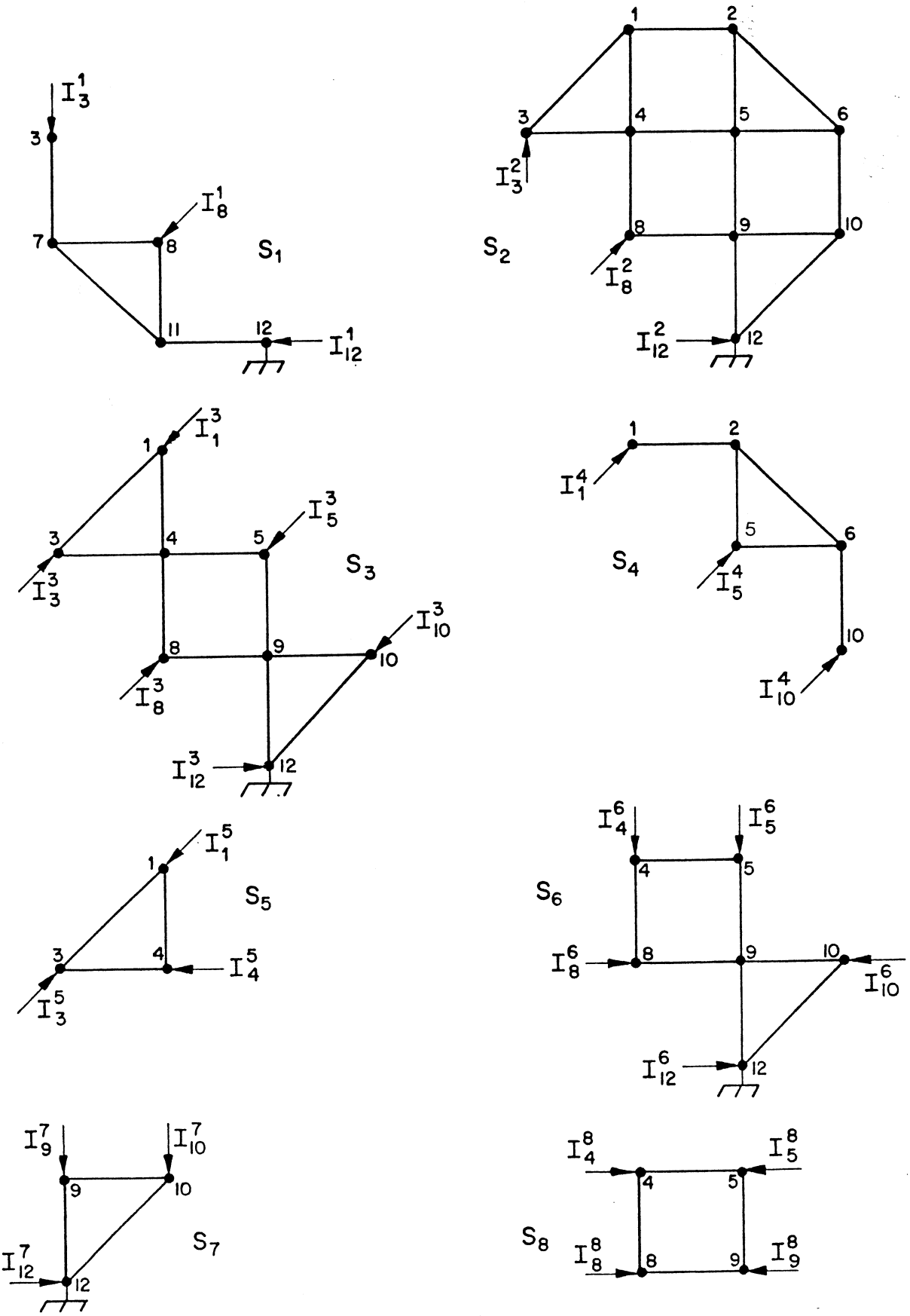
I_3^1
3
I_8^1
7
8
S_1
11
12
I_{12}^1
1
2
3
4
5
6
I_3^2
8
9
10
S_2
I_8^2
I_{12}^2
12
I_1^3
1
I_5^3
3
4
5
S_3
I_3^3
I_{10}^3
8
9
10
I_8^3
I_{12}^3
12
1
2
I_1^4
5
6
S_4
I_5^4
10
I_{10}^4
I_1^5
1
S_5
3
4
I_4^5
I_3^5
I_4^6
I_5^6
4
5
S_6
I_8^6
8
9
10
I_{10}^6
I_{12}^6
12
I_9^7
I_{10}^7
9
10
S_7
I_{12}^7
12
I_4^8
I_5^8
4
5
S_8
I_8^8
8
9
I_9^8

Fig. 25

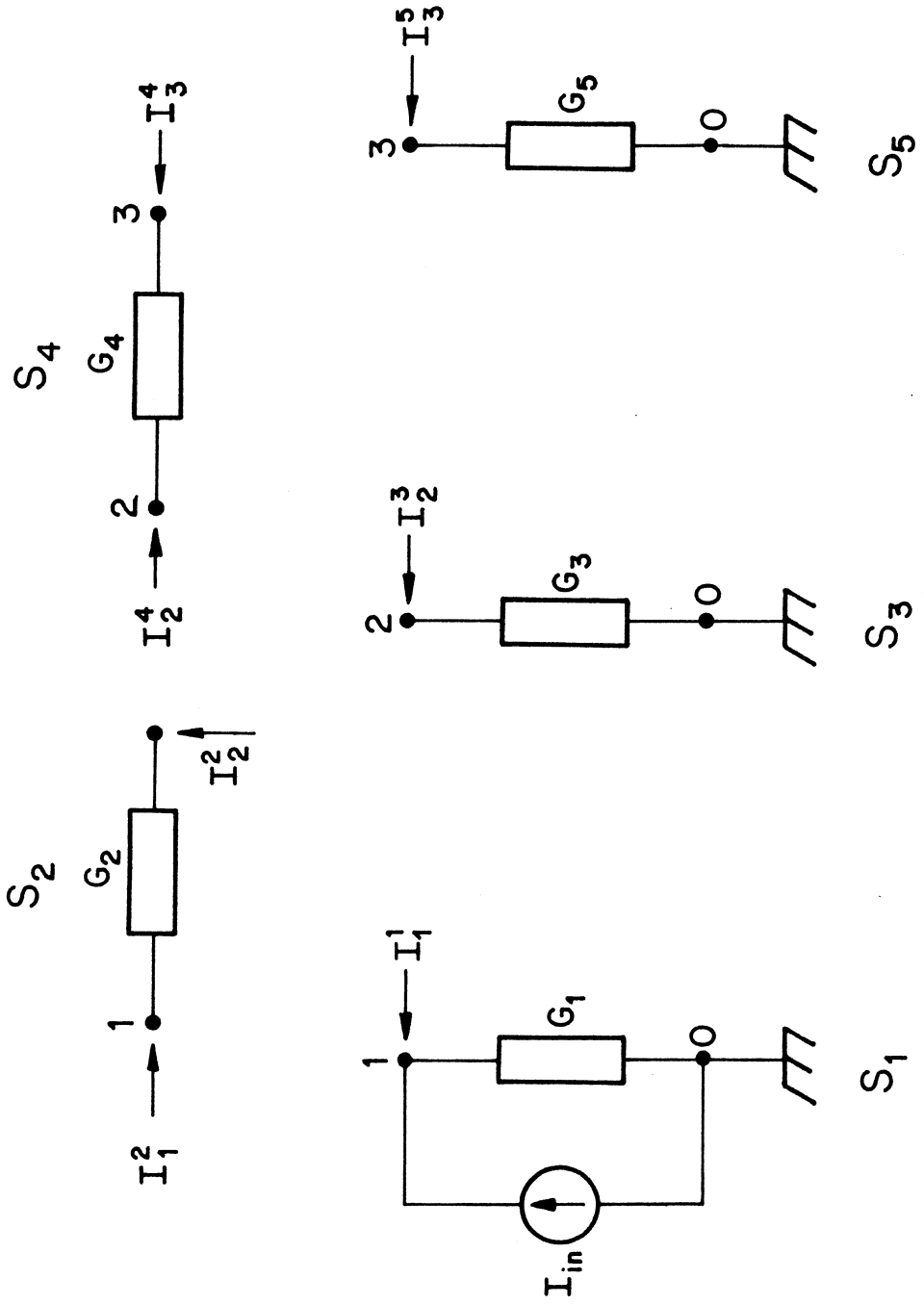

Fig. 26

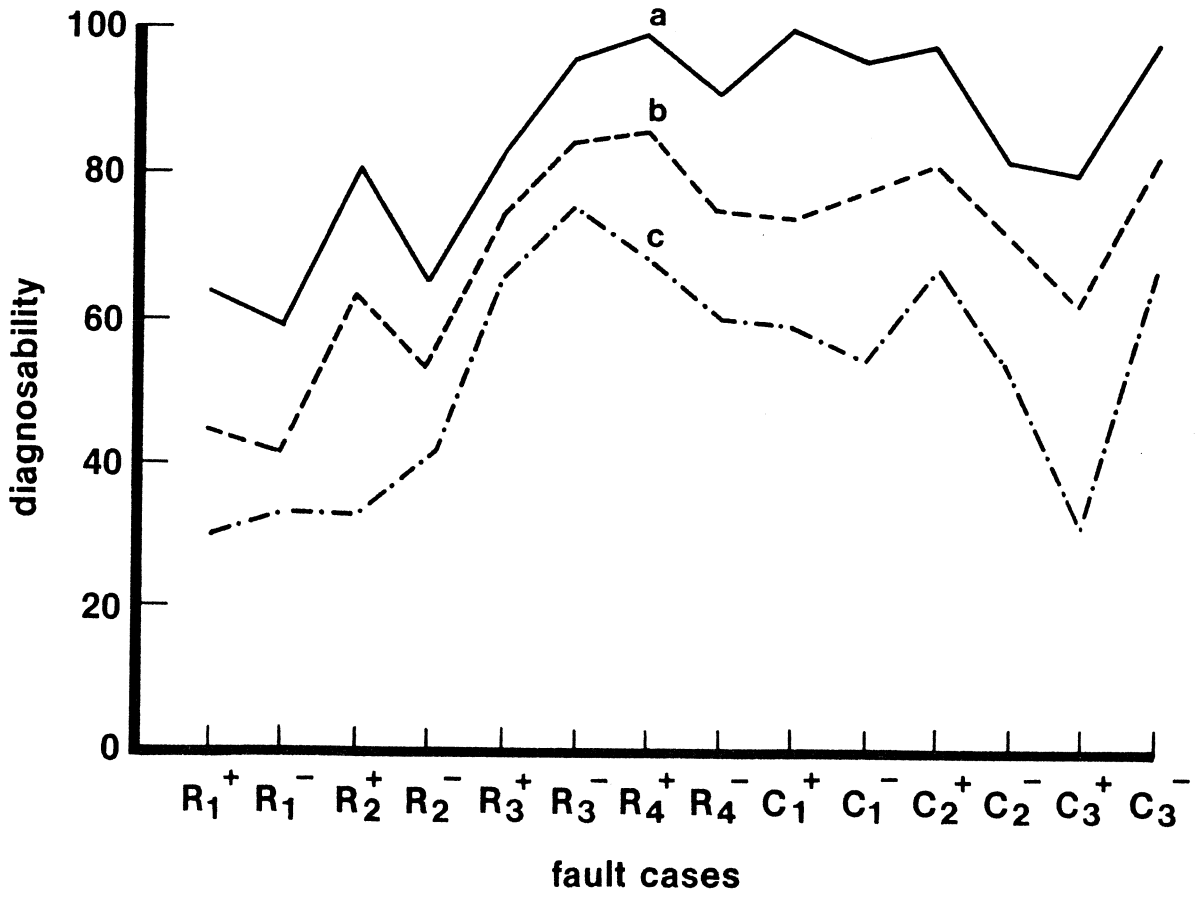
100
80
60
40
20
0
diagnosability
a
b
c
R_1^+ R_1^- R_2^+ R_2^- R_3^+ R_3^- R_4^+ R_4^- C_1^+ C_1^- C_2^+ C_2^- C_3^+ C_3^-
fault cases

Fig. 27

TABLE 2.9

FAULT ISOLATION RESULTS USING THE NEAREST-NEIGHBOR RULE CRITERION FOR THREE INDUCED FAULTS IN THE VIDEO AMPLIFIER EXAMPLE

Induced Fault	Nearest-Neighbour Rule Criterion For Different Faults																			
	1	2	3	4	5	6	7	8	9	10	11	12	13	14	15	16	17	18	19	20
Q3 BES Fault No. 4	130	29	299	0.6*	7	231	228	69	109	146	119	146	93	141	306	151	264	96	215	148
Q6 BES Fault No. 10	17	179	155	144	148	88	86	69	73	1.2*	14	1.2*	143	36	161	39	142	39	69	36
DZ1S Fault No. 14	18	129	189	139	167	120	117	70	74	35	21	35	300	1.2*	196	40	143	40	104	36

* identifies the minimum distance measure.